

NASA-CR-162,087

NASA-CR-162087  
19820025823

FINAL REPORT  
ON  
CONTRACT NO. NAS8 - 34337  
BETA EXPERIMENT  
JUNE 1982

LIBRARY COPY

DEC 20 1980

LANGLEY RESEARCH CENTER  
LIBRARY NASA, HAMPTON, VA.

Prepared by:

Applied Research, Inc.  
131 Longwood Drive  
Huntsville, AL 35804

**Applied Research, Inc.**

P. O. Box 194 • Huntsville, Alabama 35804 • (205) 533-6987



NF01677

FINAL REPORT  
ON  
CONTRACT NO. NAS8 - 34337  
BETA EXPERIMENT  
JUNE 1982

Prepared by:

Applied Research, Inc.  
131 Longwood Drive  
Huntsville, AL 35804

---

---

**Applied Research, Inc.**

P. O. Box 194 • Huntsville, Alabama 35804 • (205) 533-6987

N82-33699#

## TABLE OF CONTENTS

	Page
1. Introduction . . . . .	1
2. Task 1: Doppler Signal Generator for Coherent Focal Volume Mapping . . . . .	5
3. Task 2: Assistance for Design and Fabrication of Lens Mounts . . . . .	13
4. Task 3: System Calibration Data Analysis . . . . .	14
5. Task 4: Assistance in Flight Preparations and Ground Testing . . . . .	17
6. Task 5: Design of a Two Color Beta Measurement System . . . . .	18
7. Task 6: Evaluation of Applicability of Adaptive Filtering to Pulsed LDV Signal Processing . . . . .	54
8. Task 7: Correlation of Beta Experiment Data with LDV Data . . . . .	66
9. Task 8: Determination of $L_{eff}$ . . . . .	72
10. Task 9: Calibration Using the Spinning Wire . . . . .	83
11. Task 10: Single Aerosol Response . . . . .	150
12. Task 11: Software for Transfer to Sigma V Computer . . . . .	161
13. Task 12: Interface of HP 1000L Computer with Peripheral Devices . . . . .	162
14. Conclusion . . . . .	164

**This Page Intentionally Left Blank**

## LIST OF FIGURES

	Page
1.1     Single Particle Generator . . . . .	9
1.2     Pneumatic Control Panel . . . . .	10
1.3     Pneumatic Control Panel . . . . .	11
1.4     Particle Injector, Current Configuration . . . . .	12
5.3.1a   Two Color System Beam Splitter Combiner Design . . . . .	22
5.3.1b   Two Color System (Dichroic) Beam Splitter Combiner Design . . . . .	25
5.3.2     Two Color Beta System Off-Axis Beam Insertion Design . . . . .	26
5.3.3     Heterodyne Efficiency Contours . . . . .	48
5.3.4     Approximation of Wave Front Tilt . . . . .	49
6.1     Adaptive Noise Canceller . . . . .	59
6.2     Adaptive Linear Prediction Filter . . . . .	59
6.3     Adaptive Line Enhancer in LDV System . . . . .	60
6.4     Maximum Entropy Spectrum and Whitening Filter . . . . .	61
6.5     ALPF Simulation . . . . .	62
6.6     Circular First Moment Frequency Estimator . . . . .	63
7.1     Particle Number Histograms. . . . .	70
7.2     Particle Number Histograms . . . . .	70
7.3     Particle Number Histograms . . . . .	70
7.4     Particle Number Histograms . . . . .	70

# LIST OF FIGURES

(Continued)

	Page
7.5 Flight Distance (Meters) as a Function of Beta and Density . . .	71
8.1 Doppler Shift and Band Width Vs. Disk Speed . . . . .	78
8.2 $L_{eff}$ as a Function of Range . . . . .	79
8.3 Horizontal Beam Profile at the Waist (10-Meter Focus) . . . . .	80
8.4 Vertical Beam Profile at the Waist (10-Meter Focus) . . . . .	81
9.1 Frequency Bin 1.25 Meter Behind Focus . . . . .	90
9.2 Frequency Bin 1.0 Meter Behind Focus . . . . .	91
9.3 Frequency Bin .75 Meter Behind Focus . . . . .	92
9.4 Frequency Bin .5 Meter Behind Focus . . . . .	93
9.5 Frequency Bin .25 Meter Behind Focus . . . . .	94
9.6 Frequency Bin - Focus . . . . .	95
9.7 Frequency Bin .25 Meter in Front of Focus . . . . .	96
9.8 Frequency Bin .5 Meter in Front of Focus . . . . .	97
9.9 Frequency Bin .75 Meter in Front of Focus . . . . .	98
9.10 Frequency Bin 1.0 Meter in Front of Focus . . . . .	99
9.11 Frequency Bin 2.5 Meter Behind Focus . . . . .	100
9.12 Frequency Bin 2.0 Meter Behind Focus . . . . .	101
9.13 Frequency Bin 7.5 Meter Behind Focus . . . . .	102

# LIST OF FIGURES

(Continued)

	Page
9.14 Frequency Bin 1.0 Meter Behind Focus . . . . .	103
9.15 Frequency Bin .5 Meter Behind Focus . . . . .	104
9.16 Frequency Bin - Focus . . . . .	105
9.17 Frequency Bin .5 Meter in Front of Focus . . . . .	106
9.18 Frequency Bin 1.0 Meter in Front of Focus . . . . .	107
9.19 Frequency Bin 1.5 Meter in Front of Focus . . . . .	108
9.20 Frequency Bin 2.0 Meter in Front of Focus . . . . .	109
9.21 Longitudinal Distance (Meters) Linear Contour Plot of 10m Data . . . . .	110
9.22 Longitudinal Distance (Meters) Logarithmic Contour Plot of 10 Meter Data . . . . .	111
9.23 Longitudinal Distance (Meters) Linear Contour Plot of 20 Meter Data . . . . .	112
9.24 Longitudinal Distance (Meters) Logarithmic Contour Plot of 20 Meter Data . . . . .	113
9.25 S/ $\sigma$ Versus Area (Relative Scale) . . . . .	114
10.1 Single Particle Signals . . . . .	156

## 1. Introduction

Applied Research, Inc. is pleased to submit the enclosed final report which concludes contractual efforts on Research Study: Beta Experiment under NASA/MSFC Contract NAS8-34337. The contractual effort had a period of performance extending to July 15, 1982.

This contract included twelve (12) tasks related to the design, development, calibration and test of a focused Laser Doppler Velocimeter (LDV) system to be employed for the measurement of atmospheric backscatter (Beta) from aerosols at infrared wavelengths.

Task 1 involved the design, development, and fabrication of a Doppler signal generator which were used in mapping the coherent sensitive focal volume of a focused LDV system.

Task 2 provided technical assistance for design and fabrication of optical components that were employed in the Beta measurement system.

Task 3 provided technical assistance for the analysis of system calibration data during the flight test activity scheduled for the Beta system during July 1981. These analyses were performed to determine the acceptability of the Beta measurement system's performance and to make



recommendations on the operating parameter setting to increase system performance when needed.

Task 4 provided for support during the system integration phase into the NASA/ARC CV-990 aircraft. This support included ground testing and system calibration after the equipment was loaded into the aircraft but before the start of the flight test series.

Task 5 involved the design of a Beta measurement system which operates at 10.6  $\mu\text{m}$  and 9.1  $\mu\text{m}$  simultaneously. The technical effort included design trade-offs, hardware and software recommendations, and an assessment of the degree to which common hardware could be shared by the two wavelength systems.

Three contract modifications were attached to the NAS8-34337 contract. These modifications included seven additional technical tasks to be performed within the existing period of performance. These modifications included seven additional technical tasks to be performed within the existing period of performance. These tasks were referred to as Tasks 6, Task 7, 8, 9, 10, 11 and Tasks 12.

Task 6 involved the providing of manpower, facilities, and materials to accomplish the evaluation of the applicability of adaptive filtering to signal processing of the data from

NASA/MSFC pulsed Doppler lidar. This task specifically analyzed the applicability of adaptive filtering to Doppler lidar data from calibrated targets, aerosol targets with known velocity, and aerosol targets with turbulence.

Task 7 involved the development of software algorithms, experiments, data processing capability, and data analysis capability as required for the correlation of the Beta Measurement data with previously recorded laser Doppler system data and related aerosol density data.

Task 8 involved the design and performance of a sequence of measurements to determine  $L_{eff}$  (the effective range increment to be associated with a hard target signal), the determination of the ranges at which these measurements should be made, and the determination of the supporting data (such as frequency of Doppler shift and lidar system output power). These data were analyzed and the results documented in regular monthly reports.

Task 9 involved the design and performance of a test which utilized a wire calibration target which was spun through the lidar beam. The detected signal was digitized and processed to provide sensitivity contours which were employed in the calibration of the Beta system. The results were reported in regular monthly progress reports.

Task 10 involved the defining of a technique by which the response of the lidar to a single aerosol could be measured. This included design and fabrication of apparatus for generating and propelling single aerosols through the lidar beam. Development of software to analyze the resulting lidar data, along with documentation of the measurement results were included in this task.

Task 11 involved development of software which was required to transfer backscatter data collected during the summer 1981 flight program to the Sigma V computer. The backscatter data which existed in protocol, file structure device characteristics, signal levels, etc., at NASA/MSFC were provided GFE to Applied Research, Inc., personnel.

Task 12 involved the generation of the necessary software to interface a Hewlett-Packard 1000L computer with several peripheral devices for the purpose of transferring, processing, displaying, and storing of recorded data.

## 2. Task 1: Doppler Signal Generator for Coherent Focal Volume Mapping

ARI has designed and assisted NASA/MSFC personnel in the development and fabrication of a Doppler signal generator for use in mapping the coherent sensitive focal volume of a focused LDV system. This apparatus consists of a method of sending single aerosol particles into the focal volume region, called a single particle generator, and a spinning wire target. Figure 1.1 shows a photograph of the completed single particle generator.

The single particle generator consists of a plexiglass test chamber, a pneumatic control panel, a particle generating chamber and a particle injector. These units were constructed early in 1981, assembled and tested in September. These preliminary tests revealed problems in the design that required modification to correct.

1. The Test Chamber: The test chamber is constructed of 5/16" acrylic sheet. This was originally assembled with epoxy. However, under negative pressure the long seams proved to be too weak, resulting in leaks. This was corrected by reassembling the structure with 1/2" aluminum reinforcing members at all seams. The plexiglass is fastened to the aluminum bars with 5-32 screws and all seams are sealed with RTV. A new top was also constructed from

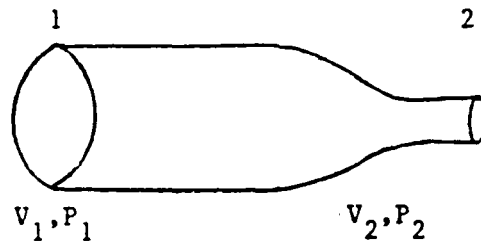
1/2" acrylic sheet. Since the top must be removable the added thickness was required for rigidity. Aluminum bars were fastened to the top to support the inside top edges of the sides. The wing nut fasteners for the top were originally secured to the sides of the chamber by epoxy. When negative pressure was applied to the chamber the sides flex enough to break the epoxy bond. This was corrected by using screws in addition to the epoxy to secure the fasteners. The flexing of the sides also caused the gasket providing the seal for the germanium window to leak. A channel was milled around the window opening and the gasket was replaced by an o-ring.

2. Pneumatic Control Panel: The pneumatic control panel was originally configured as shown in Figure 1.2. This configuration was based on the requirement for the system to operate at either positive or negative pressure. Since the system will now only operate at negative pressure and because of modifications to other parts of the system, the control panel has been reconfigured as shown in Figure 1.3. A Millipore filter has been added to the air inlet to reduce the number of ambient particles in the test chamber.

3. Particle Generating Chamber and Injector: Originally the particle injector was a commercial air brush connected by tygon tubing to the generating chamber. Although this had worked well in tests before the test chamber was

constructed, it did not function properly when placed in the negative pressure environment. The air brush was replaced by a hypodermic needle attached directly to the tubing. This arrangement worked, but not reliably. There was also a considerable build up of particles in the tubing which occasionally clogged the line. The generating chamber was moved inside the test chamber and the hypodermic needle was fitted directly through its side, giving direct access to the particles (see Figure 1-4). The generating chamber is an aluminum cylinder with a speaker in the bottom to provide sonic excitation (at about 600 Hz) to the particles. Aside from the relocation and modification mentioned above it is unchanged.

In addition to these modifications, a water manometer was built and connected in the test chamber vacuum line. The manometer permits more precise measurement of the pressure in the test chamber and thus more control over the air flow through the particle generating chamber. The exit velocity of particles from the single particle generator may be estimated from Bernoulli's equation. The following figure shows the assumed model in which the density of the fluid is taken to be constant.



$$P_1 + 1/2 \rho V_1^2 = P_2 + 1/2 \rho V_2^2$$

Because of the difference in areas at points 1 and 2,  $V_1$  is considered negligible compared to  $V_2$ . Hence

$$V^2 \equiv V_2^2 = 2 \Delta P / \rho_{\text{air}}$$

$$\rho_{\text{air}} = .081 \text{ lb / ft}^3$$

$$\Delta P = \rho_{\text{water}} g h$$

$$V^2 = 2 \frac{\rho_{\text{water}}}{\rho_{\text{air}}} g h$$

$$= 2 \left( \frac{62.4}{.081} \right) g h$$

$$= 1.51 \times 10^4 h$$

$$V = 19.6 \sqrt{h} \text{ (m/sec, with } h \text{ in inches)}$$

Under measurement conditions  $h$  was found to be about .125 inch. Hence  $V = 6.9 \text{ m/sec}$  is the expected velocity, under the above assumptions.

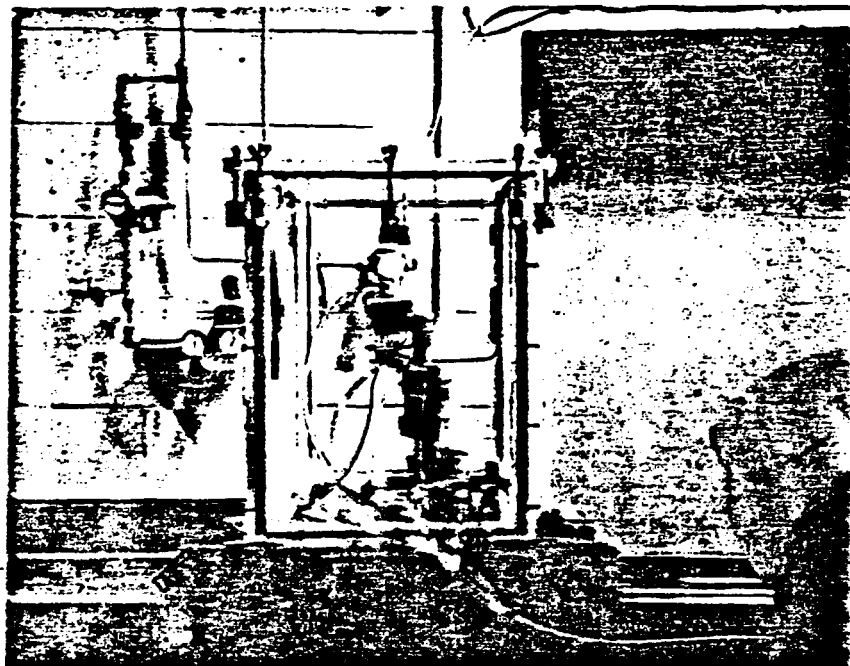
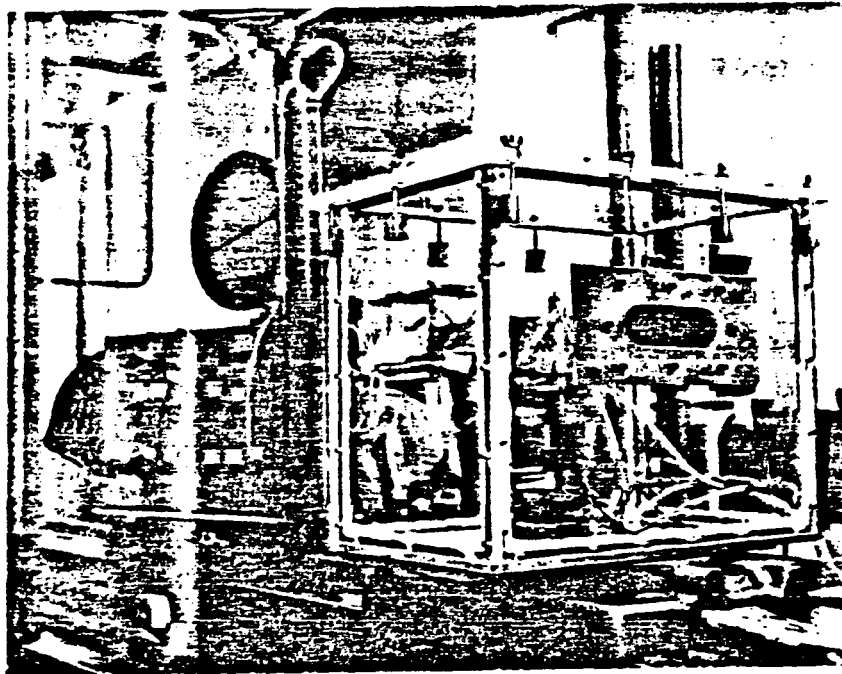


Fig. 1.1. Single Particle Generator



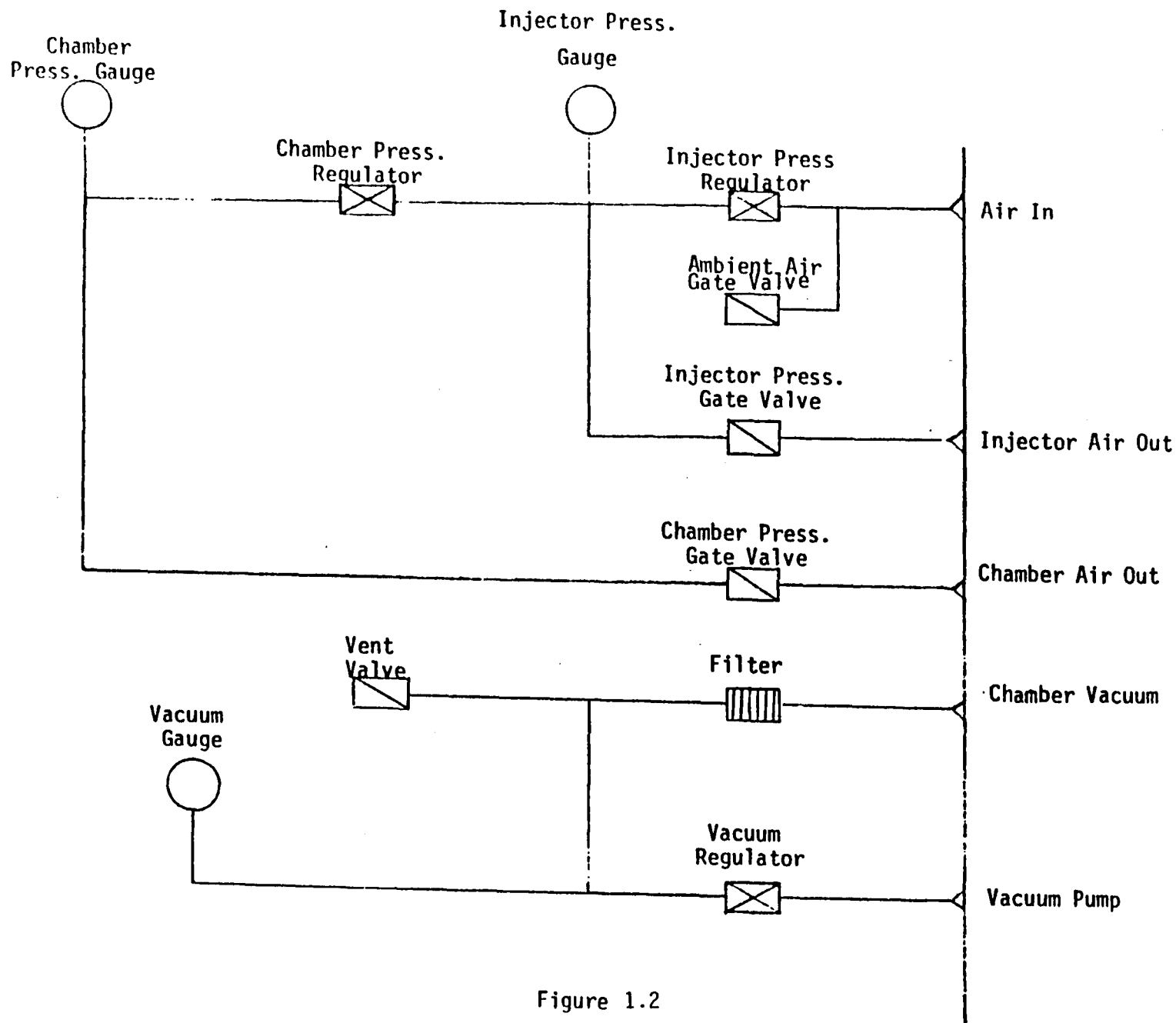


Figure 1.2

PNEUMATIC CONTROL PANEL

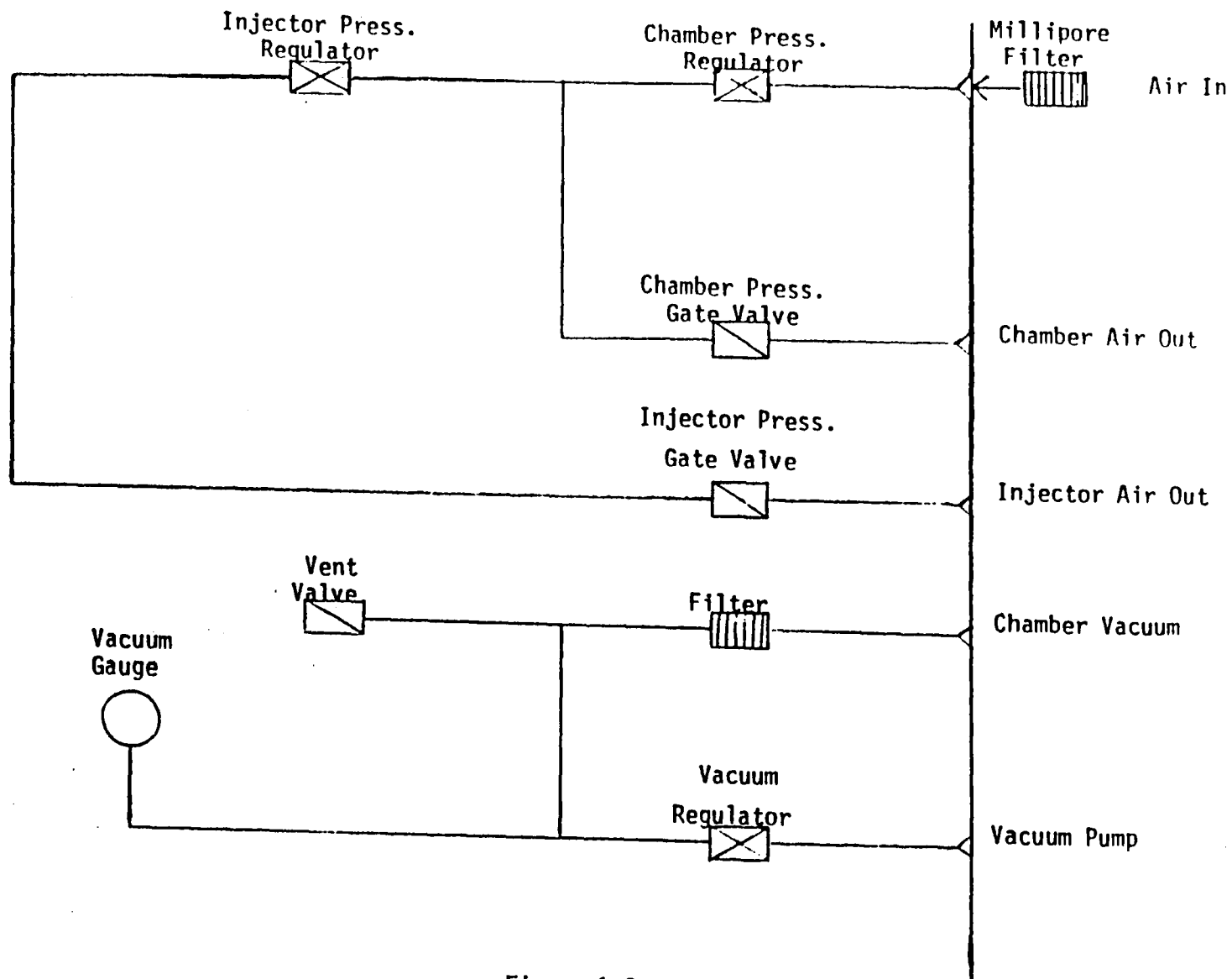


Figure 1.3

PNEUMATIC CONTROL PANEL

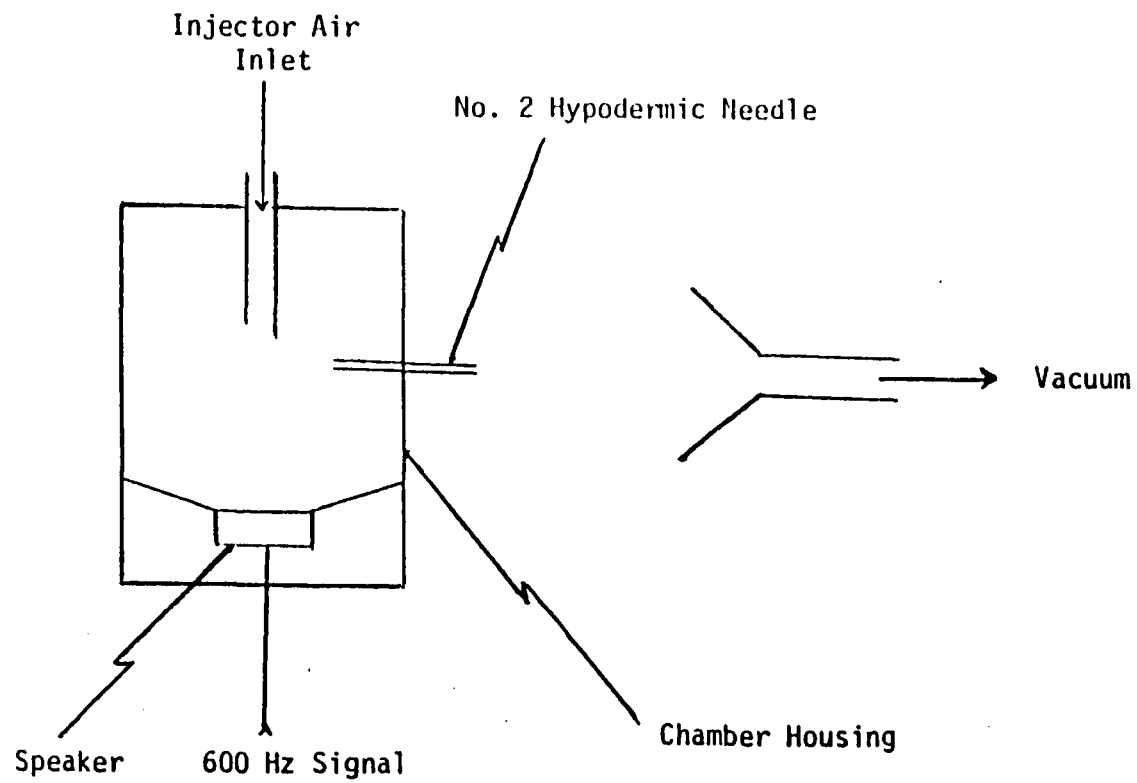


Figure 1.4  
PARTICLE INJECTOR, CURRENT CONFIGURATION

3. Task 2: Assistance for Design and Fabrication of Lens Mounts

Technical assistance in the design and fabrication of optical components was provided in the fabrication of a gimbal mirror mount for the output mirror of the telescope. Modification of the case which encloses the interferometer and laser was accomplished in order to provide improved access to controls. Optical components including lens mounts, detector mount fixture, zinc selenide (ZnSe) lens and adjustable lens mount fixtures were designed, fabricated and procured. The Beta system design has the support structures to accommodate a flexible design which uses either the Honeywell or the Hughes CO<sub>2</sub> laser.

A decision to employ the Honeywell CO<sub>2</sub> laser for the initial flight test series permitted optical support fixtures for optical elements to be fully integrated into the Beta system. The Beta system was assembled and preparation was made for calibration tests, prior to shipment, for the volume backscatter mode.

#### 4. Task 3: System Calibration Data Analysis

During July, 1981, Applied Research, Inc. personnel provided technical assistance for the analysis of system calibration data during flight test activities onboard the NASA/ARC Convair 990 aircraft. These analyses were performed to determine the acceptability of the Beta measurement system's performance and to make recommendations on the operating parameter settings to increase system performance.

To determine  $\beta$  in the volume mode, the expression  $S = \beta G$  is used. For an untruncated Gaussian beam it has been shown (T.R. Lawrence et.al, RSI, 43, 512(1972)) that  $G = \pi \eta \lambda P/B$ , where

$\eta$  = system efficiency

$\lambda$  = wavelength

$P$  = number of transmitted photons/sec

$B$  = electronic bandwidth.

For truncated beams an appropriate system response must be used. This response can be represented by the same expression, except that  $\eta$  becomes a function of focal range.

The volume mode calibration involves determining the system response  $G$  to a volume distribution of aerosols for a beam which is usually significantly truncated. In principle,  $G$  could be determined by mapping the focal volume with a single particle probe and integrating. In practice, calibration is usually accomplished by observing the backscattered signal from a plane rotating disk. For the truncated Gaussian beam, the volume signal  $S$  and disk signal  $S_D$  are related by

$$S_D = \Delta L S \text{ with } \Delta L = f^2 \lambda / R^2$$

where  $f$  is the focal length and  $R$  is the Gaussian radius. From this it follows that  $\rho = \Delta L \beta$ , where  $\rho$  is the bidirectional reflectance of the disk in inverse steradians. The length  $\Delta L$  is a range increment from which approximately 50% of the energy is returned in the volume mode for an untruncated Gaussian beam. Hence for such a beam, the efficiency factor may be calculated from the length  $\Delta L$  and the known reflectance of the disk. To calibrate a truncated beam the corresponding  $\Delta L$  must be found by measurement or by computation of truncated beam propagation characteristics. This quantity is found to vary differently with range from the untruncated  $\Delta L$ .

Volume mode calibrations of the Beta system were

accomplished using both the sandpaper and sulfur Doppler targets. The system performance from the laboratory test showed 68 dB signal-to-noise from the sandpaper target and 82 dB signal-to-noise from the sulfur target. These signal-to-noise figures indicate an overall system efficiency of approximately 10% for the Beta system operating with 6 watts transmitter power and a spectrum analyzer bandwidth of 100 KHz. These performance numbers indicate that the current Beta system will have sensitivity to measure atmospheric backscatter to approximately  $10^{-10} \text{ m}^{-1} \text{ str}^{-1}$  with a signal-to-noise of 1.

In June, 1981, the Beta system was used to observe the atmosphere at a focal range of approximately 100 ft and with line of sight winds greater than 2 m/sec. SNR's in excess of 20dB were observed with a transmitted output power of 6.2 watts.

5. Task 4: Assistance in Flight Preparations and Ground Testing

Applied Research, Inc. personnel assembled the protective cover for the Beta system which will be employed to meet air safety requirements when flying on the CV-990. The Beta system with all supporting hardware and equipment was packaged and shipped to ARC for participation in the Severe Storms Measurement System flight test program.

Work continued at Ames Research Center (ARC) to provide technical support during the system's integration phase into the NASA/ARC CV - 990 aircraft. This support included ground testing and system calibration following shipment of the system to ARC before CV - 990 flight test activities began.

ARI assisted in fitting of the equipment into an aircraft flight rack. This included the spectrum analyzer oscilloscope, chiller, stepping motor monitor panel, CRT terminal, signal processor, disc drive and laser power supplies. The stepping motor junction box was interconnected with new cable. ARI also assisted in testing the system by measuring and analyzing the return utilizing the shutter mechanism.



## 6. Task 5: DESIGN OF A TWO-COLOR BETA MEASUREMENT SYSTEM

### 1. INTRODUCTION

The recent success of NASA/MSFC's Laser Doppler Velocimeter System which is designed to measure atmospheric backscatter,  $\beta$ , at 10.6  $\mu\text{m}$  has generated an interest in determining the design of a two-color  $\beta$  measurement system. Applied Research, Inc. has undertaken an analytical system design effort, centered around existing  $\beta$ -system hardware, to result in a two-color  $\beta$  system. This effort is focused toward employing existing hardware to the maximum extent possible and does not explore the development of new signal processing electronics and/or mixing of two-color reflected signals on a common detector with two local oscillator frequencies. The results of this design study, including a ray trace analysis of a proposed two-color  $\beta$ -system design which employs the current system's beam expander, is given in the following sections of this report.

### 2. DESIGN CONSIDERATIONS

The decision to investigate two-color  $\beta$ -system designs that employ the maximum amount of existing MSFC hardware has been driven by consideration of other efforts which are more extensive and will explore multi-color

$\beta$ -system designs. The design to be derived from this study was not considered to fit inside a pre-determined small volume envelope or weight limit. This design effort considered several two-color system designs which ultimately result in two design options:

- A beam splitter combined two-color system which results in a common focal volume for the two transmitted beams. (System A)
- A two beam directing insertion mirror system which uses a common beam expander and focuses the two transmitted beams at approximately the same spatial location. (System B)

System A was analyzed for two configurations. One design which employed a 50% beam splitter as the beam combining component (for  $\lambda_1$  and  $\lambda_2$ ) on the transmit leg of the system was analyzed and found to have relatively low performance potential when compared to the other designs.

The other design which was considered employed a dichroic beam splitter as the beam combining component. This design was analyzed and found to have relatively higher potential for performance than the 50% beam splitter design. Other considerations employed a dichroic beam splitter in the return leg to separate reflected signals ( $\lambda_1'$  and  $\lambda_2'$ ) such that they could be combined with separate LOs and heterodyned on separate detectors. These designs are more fully discussed in Section 3.1, Design Analysis of the Beam Splitter Combined Two-Color  $\beta$ -Systems.

The second design, Two-Beam Directing Insertion Mirror System, System B was analyzed and found to have a very good system performance potential relative to the existing single-color  $\beta$ -systems. This second design was chosen for further system design analysis because it can potentially employ the existing  $\beta$ -system's interferometer, laser transmitter, beam expander, detector, and signal processing. This design will require the use of an additional signal processor (or time-sharing with the current signal processor), laser of wavelength  $\lambda_2$ , detector, interferometer and a

folding/beam directing flat mirror for beam insertion of the second color onto the existing beam expanding secondary. This system's design will be such that the spatial relationship of the two focal volumes will be known for various focal ranges and such that statistical correlation of  $S(\pi)$  may be made for the two-colors whether employed in the single particle mode or the volume mode.

The System B design obviously employs more hardware and thus has larger volume and weight characteristics than the System A design. However, from the design analysis which predicts system performance, it is indicated that the System B design will provide greater sensitivity (fewer system losses) assuming that all other system characteristics such as laser power, optical efficiency, heterodyne efficiency are held constant.

### 3. DESIGN ANALYSIS

Several two-color  $\beta$ -system designs were analyzed to determine their performance characteristics. All the designs were found to reduce to two basic two-color  $\beta$ -system designs which will be analyzed in Sections 3.1 and 3.2.

A  $\beta$ -system which employs a beam splitter for combining the two transmitter output signals is analyzed in Section 3.1. A  $\beta$ -system which employs two folding insertion mirrors is analyzed in Section 3.2. As a system design trade-off between the two potential designs, a ray trace analysis which incorporates the effects of off-axis insertion of one of the input beams, is performed. The results of this analysis indicate that the signal to noise loss due to off-axis insertion of the second color is

less expensive, in terms of s/n loss, than the 50% beam splitter combining system which has 3 db of losses on the transmit leg and approximately 3 db of losses on the receiving leg of the system.

The dichroic beam splitter version of the System A has potential for an improved s/n performance over the 50% beam splitter version. Initial discussions<sup>(3)</sup> with vendors of such beam splitters indicate that as great as 80% transmission of 10.6  $\mu\text{m}$  radiation can be achieved while at the same time reflecting as much as 80% of the 9.1  $\mu\text{m}$  radiation. This performance will improve the System A design performance significantly both in the transmit leg and in the receiver leg, through use of separate L.O.'s. The transmitter and receiver leg loss are each reduced to less than 1 db.

### 3.1 DESIGN ANALYSIS OF THE BEAM SPLITTER COMBINED TWO-COLOR

Two options are presented with respect to beam splitter choices for this design. The first option employs conventional beam splitters, while the second option utilizes dichroic beam splitters, at critical points, in order to enhance the transmittance and reflectance at  $\lambda_1$  and  $\lambda_2$  as desired.

#### 3.1.1 CONVENTIONAL BEAM SPLITTERS

Fig. 5.3.1a gives the optical configuration for the beam splitter combined two-color  $\beta$ -system. This system combines the radiation from two  $\text{CO}_2$  Lasers ( $\lambda_1$  and  $\lambda_2$ ) and passes the combined beam through a single interferometer. The output beam from Laser 1 is reflected off mirror  $M_1$  and onto beam splitter  $S_1$ . The radiation from Laser 2 is reflected on beam splitter  $S_1$  such that the output powers of the two lasers are combined at  $S_1$  and are of approximately equal power. The requirement

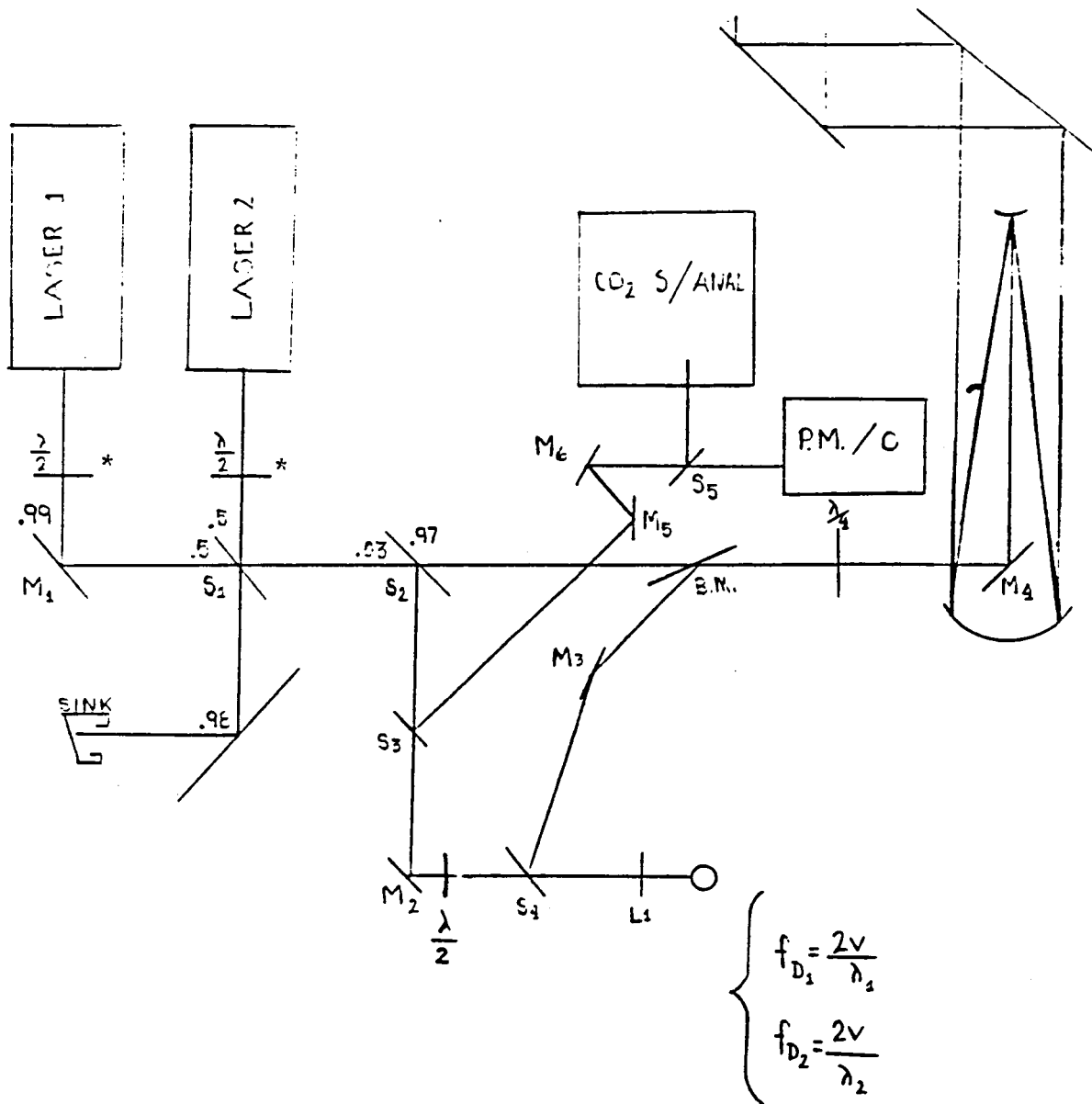


FIGURE 5.3.1a

# TWO COLOR SYSTEM BEAM SPLITTER COMBINER DESIGN

\*Necessary for vertically polarized lasers.

to have equal power components of  $\lambda_1$  and  $\lambda_2$  in the combined transmitted beam results in approximately 3 db of output power loss from each of the laser transmitters. The radiation that is reflected by  $S_1$  must be dumped from Laser 1 and the radiation from Laser 2 that is transmitted by  $S_1$  must be dumped from the system. Fig. 5.3.1a shows this radiation being dumped into a radiation sink. The remainder of the system is exactly as the  $\beta$ -system which flew on the Ames Research Center's Convair 990 as part of MSFC Summer 1981 test program. (Reference Fig. 2, "Design and Calibration of a Coherent Lidar for Measurement of Atmospheric Backscatter", SPIE Conference, San Diego, CA. May 1981.) A positive attribute of this system is that the two colors are focused in the same spatial volume. This permits comparison of single particle signal returns for single particle measurement operations and a direct comparison of backscatter for the volume mode operation (without applying statistics to the signals).

This system may be operated in one of two possible modes for handling the signal processing of the reflected returns. The reflected radiation  $\lambda_1$  and  $\lambda_2$  may be heterodyned with the combined beams local oscillator signal which will result in the use of one detector and signal processor. The Doppler returns when mixed with the combined  $\lambda_1$  and  $\lambda_2$  L. O. radiation can be sufficiently separated such that the signal processing of the separate colors will be possible. However, the L.O. radiation of  $\lambda_1$  will appear as noise for the processing of  $\lambda_2$  (reflected returns for  $\lambda_2$ ) radiation against the L.O. and vice-versa for  $\lambda_1$  and  $\lambda_2$ . This effect will tend to reduce the operating efficiency of this design further, maybe as much as 3 db.

This  $\alpha$ -system design suffers from a system efficiency point of view in that the inherent losses for each color may be as much as 6 db, 3 db on the transmit leg and 3 db on the receiver leg.

### 3.1.2 DICHROIC BEAM SPLITTERS

A dichroic beam splitter can be designed<sup>(3)</sup> which will permit high reflectance at  $\lambda_2$  and high transmittance at  $\lambda_1$ , or vice-versa. In Fig.5.3.1b such a splitter is utilized to effect separate mixing of  $\lambda_1$  and  $\lambda_2$  on separate detectors.

Transmit beams from Laser 1 and Laser 2 are combined at  $S_2$ , a dichroic splitter with strong transmittance at  $\lambda_1$  and strong reflectance at  $\lambda_2$ . Local oscillator signals from Laser 1 and Laser 2 are not mixed, as in Fig.5.3.1a, but are combined separately with returned signals at  $S_4$  and  $S_5$ , which are dichroic splitters with high reflectance for  $\lambda_1$  and  $\lambda_2$  respectively. It is only necessary to obtain enough L.O. upon transmittance to maintain shot noise limited operation. Also, the effect of strong reflectance of the  $\lambda_1$  L.O. onto  $S_5$  will be minimized since  $S_5$  has strong  $\lambda_1$  transmittance. This system offers about 2 db less power loss in transmit and receive legs than the previously discussed option.

### 3.2 DESIGN ANALYSIS OF THE $\beta$ -SYSTEM EMPLOYING TWO BEAMS WITH FOCUSING AT SEPARATE POINTS

The schematic design of the two-beam system is shown in Fig. 5.3.2. This design has inherently good optical efficiency in that it avoids the

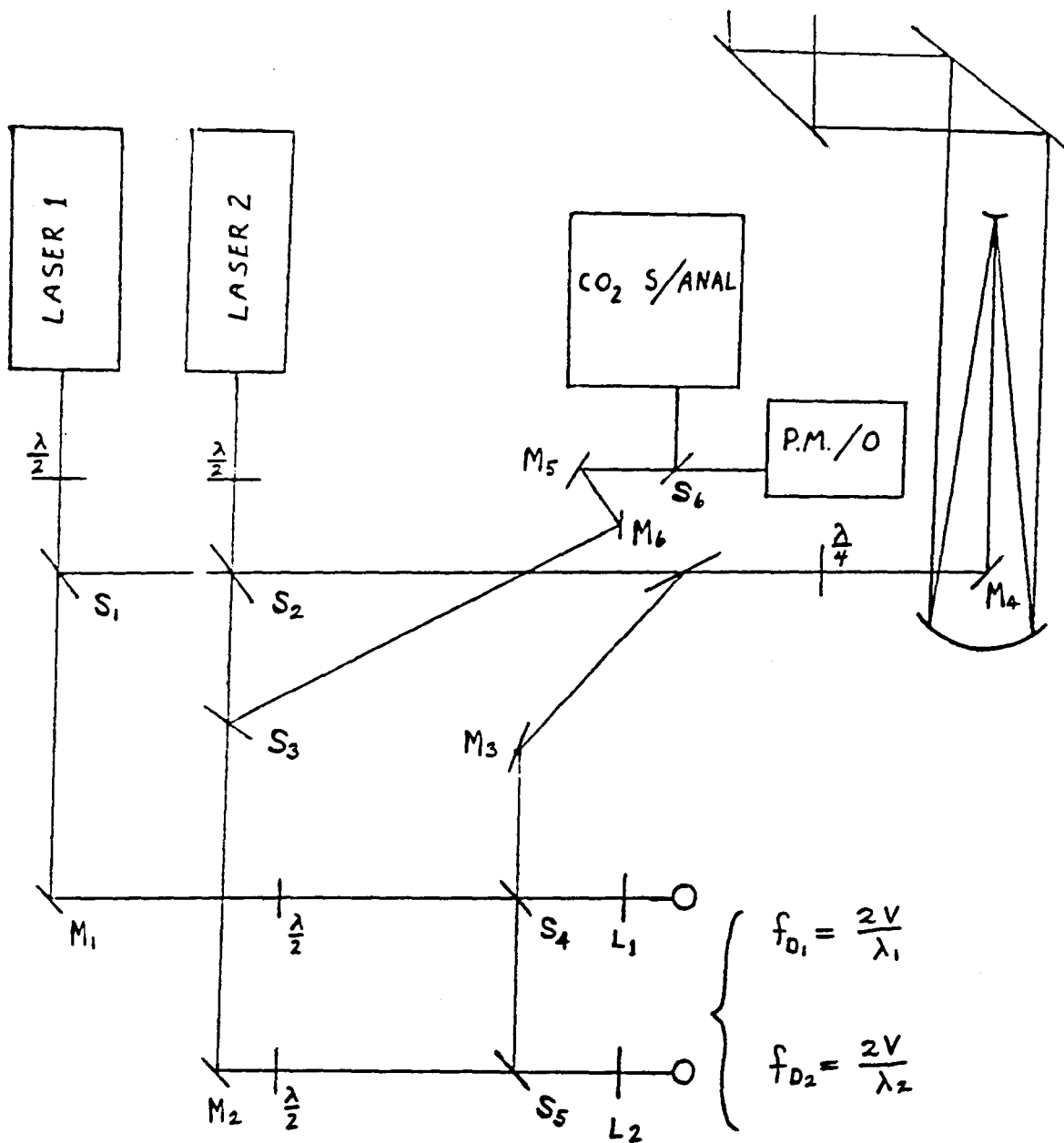


FIGURE 5.3.1b TWO COLOR SYSTEM (DICHROIC)  
BEAM SPLITTER COMBINER DESIGN



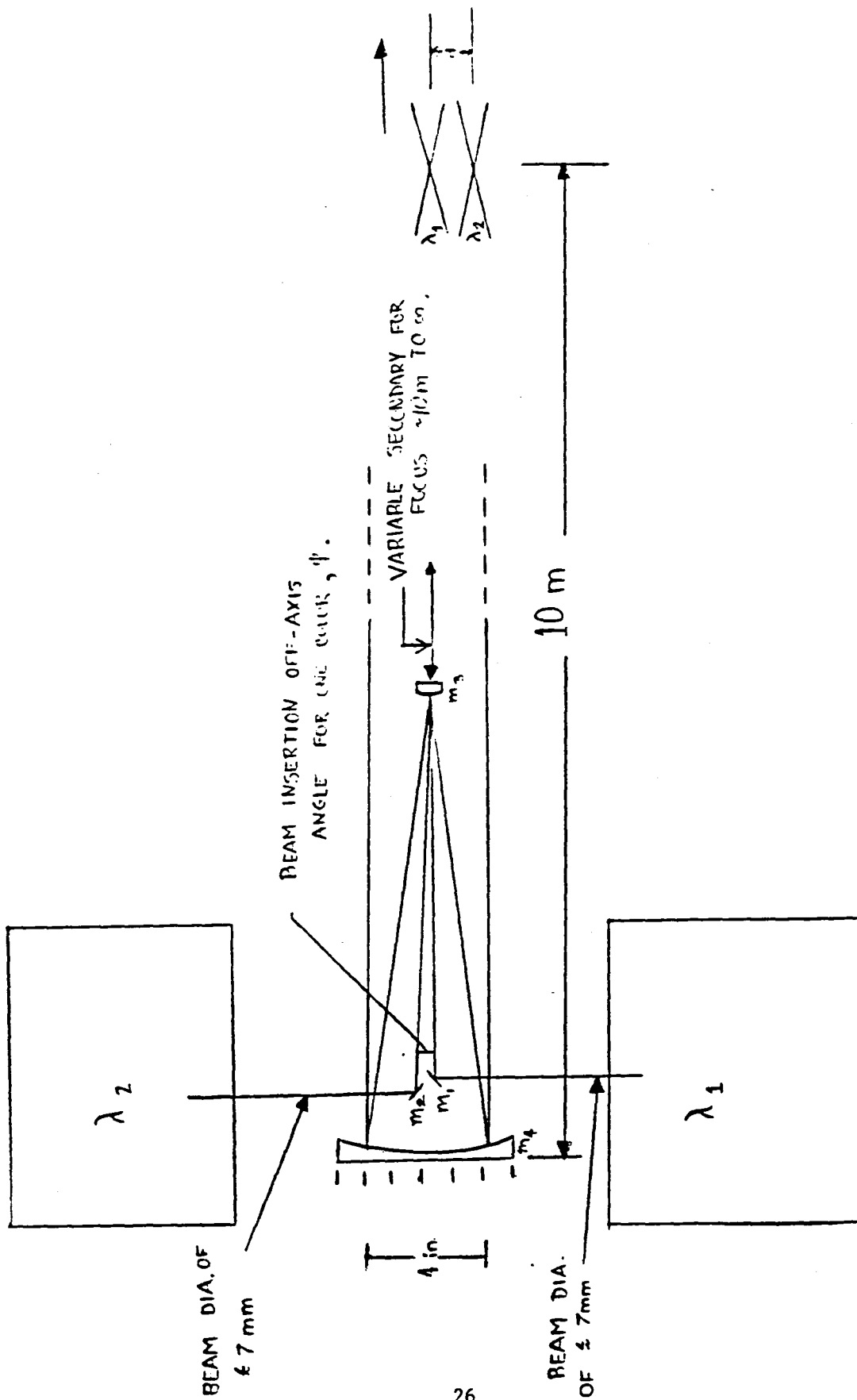


FIGURE 5.3.2  
TWO COLOR BETA SYSTEM OFF-AXIS BEAM INSERTION DESIGN

previously discussed system's 3 db output power loss on the transmitter optical leg and avoids the  $\sim 3$  db signal loss in the receiver optical leg of the system. However, the potential for heterodyne efficiency degradation due to off-axis insertion of the  $\lambda_2$  beam must be investigated to insure that the design's overall system efficiency is preserved. The following is a design analysis of the two beam directing insertion mirror system which considers the proposed optical design and employs the existing  $\beta$ -system optical beam expanding telescope. Operating ranges of 10 meters and 30 meters have been considered in this analysis. It should be noted that focussing of this system at longer ranges tends to reduce the effect of off-axis beam insertion.

As depicted in Fig.5.3.2 this optical design results in the two colors being focused at approximately the same range but in slightly separated spatial volumes.

A detailed discussion of this system's optical design and ray trace analysis is as follows.

One of the two flat mirrors,  $M_1$  and  $M_2$ , shown in Fig.5.3.2, is located above the optic axis (out of the paper), with  $\lambda_1$  parallel to the axis. The second  $\lambda_2$  beam is located in the same plane (parallel to the paper) but displaced as shown. The plane of the two laser beams striking the secondary (small) mirror,  $M_3$ , is perpendicular to the plane of bilateral symmetry of the beam expander. The angle between the two beams is made as small as practicable to minimize aberation of the  $\lambda_2$  beam.

The center of the  $\lambda_2$  beam at the flat mirror is 1.3 cm from the plane of bilateral symmetry through the optic axis (perpendicular to the paper). The mirror is then adjusted so that both beams have spatially identical images on the large focusing mirror,  $M_4$  (called the primary). These images are approximately 4 inches in diameter, as shown in Fig. 5.3.2. Note that the flat mirrors appear to obscure the beams coming from the secondary (see figure) but in fact do not, since the primary is completely off axis, in a direction out of the paper.

The center of the  $\lambda_1$  beam strikes the secondary slightly above the optic axis (out of the paper). The center of the  $\lambda_2$  beam strikes the secondary at the same distance above the optic axis and at a point that is displaced slightly in a perpendicular direction (toward the top of the paper). The amount of this lateral displacement of the point on the secondary is, however, less than 0.1 mm, and can easily be ignored in ray-tracing calculations. To see this, note that if the central ray of  $\lambda_2$  struck the secondary at the same point as that of  $\lambda_1$ , it would be displaced at the primary by about 1.4 mm from the central ray of  $\lambda_1$ .

The Gaussian focal point (aberrations ignored) of the off-axis beam will be in the focal plane of the on-axis beam, and can be obtained by a simple geometrical construction. It is displaced to the opposite side of the optic axis from the plane mirror, and the displacement distance for the 10 meter focus is 0.3 inches.

By comparison of the wavefront shift at different points on the secondary in Tab. 5.3.9 and Tab. 5.3.10, we see that the two beams should have essentially the same characteristics. A second beam

added to the Lidar system, as described in this section, should give results almost as good as the original beam. Indeed, the differences between the two would be inconsequential.

### 3.2.1 ABERRATIONS OF THE TWO-BEAM SYSTEM

The geometrical theory of aberrations is given by many authors. The authoritative source Born and Wolf <sup>1</sup> (B & W) was used for the calculations reported here. The important performance characteristics of an optical system may be more adequately analyzed for the purpose of this design effort using the Born & Wolf approach. Most of the pertinent material is contained in Chapter V, pp 203-232. References to pages numbered 100 + are to pages in B and W. There are five third-order aberrations of a monochromatic system: Spherical aberration, astigmatism, curvature of field, distortion, and coma. Associated with these are five coefficients - B, C, D, E, and F, respectively - which can be calculated from the Gaussian variables (object distances, radii of curvature, image distances, etc.).

For a two mirror system like the beam expander considered here, the object distances are defined to be  $S_1$  and  $S_2$ ; image distances,  $S_1'$  and  $S_2'$ ; and radii of curvature,  $r_1$  and  $r_2$ . With the proper choice of signs for radii of curvature, (both positive) and indices of refraction ( $n_0 = 1$ ,  $n_1 = -1$ ,  $n_2 = 1$ ), one gets the following related quantities (p. 224):

$$\begin{aligned} h_1 &= -1 \\ h_2 &= -S_2/S_1' \\ k_1 &= 0 \\ k_2 &= d_1/h_2 \end{aligned}$$

where  $d_1$  is the distance between the primary and secondary mirrors.  
Four other quantities involved in the calculation of the aberration coefficients are

$$K_1 = \frac{1}{r_1} - \frac{1}{s_1}$$

$$K_2 = \frac{1}{s_2} - \frac{1}{r_2}$$

Eq. (15), p. 223

and  $b_1 = -1 = b_2$ . The values of  $b_1$  and  $b_2$ , the deformation coefficients for the mirrors, represent the fact that the mirrors are paraboloidal.

It is convenient to define three more sets of intermediate variables

$$\alpha_i = \frac{1}{2} h_i^4 b_i (n_i - n_{i-1}) / r_i^3$$

$$\beta_i = h_i^2 k_i K_i$$

$$\gamma_i = \frac{1}{2} (1/n_i s_i' - 1/n_{i-1} s_i').$$

The equations for the aberration coefficients (Eq. (24), p. 225) then become

$$B = \sum_i [ \alpha_i + h_i^4 K_i \gamma_i ]$$

$$C = \sum_i [ \alpha_i k_i^2 + (1 + \beta_i)^2 \gamma_i ]$$

$$D = \sum_i [ \alpha_i k_i^2 + \beta_i (2 + \beta_i) \gamma_i ]$$

$$E = \sum_i [ \alpha_i k_i^3 + k_i (1 + \beta_i) (2 + \beta_i) \gamma_i ]$$

$$F = \sum_i [ \alpha_i k_i + h_i^2 K_i (1 + \beta_i) \gamma_i ]$$

The aberrations themselves are calculated using the so-called Seidel variables (pp. 208). For the purposes of this design analysis these are

$$y_0 = Y_0 / D_0$$

where  $Y_0$  is the lateral displacement of the object point from the optic axis and  $D_0$  is the object distance to the first mirror, and

$$\xi_2 = (x_2 + D_2 p_2) / M'$$

$$\eta_2 = (Y_2 + D_2 q_2) / M'$$

where  $(x_2, Y_2)$  is the lateral position of the image point,  $(-D_2)$  is the image distance from the second mirror, and  $M'$  is the lateral magnification between the two mirror planes. The ray components  $p_2$  and  $q_2$  are direction cosines at the image plane (p. 134) with respect to the x and y axes, respectively, where the optic axis is the z axis.

The displacement of the wavefront (fourth-order correction) and displacement of the image point (third-order correction) are then calculated. Let  $x_1 - x_1^*$  and  $Y_1 - Y_1^*$  be the corrections to the position of the image point in the image plane (p.205).

Define  $\rho$  and  $\theta$  by

$$\xi_2 = \rho \sin\theta \quad (\text{p. 213})$$

$$\eta_2 = \rho \cos\theta.$$

and define the displacement of the wavefront due to the aberrations as  $\phi^{(4)}$ . Then with

$$x_1 - x_1^* = \frac{D_2}{M'} \Delta^{(3)} x$$

$$Y_1 - Y_1^* = \frac{D_2}{M'} \Delta^{(3)} y$$

one finds (Eq. (7-8), p. 213)

$$\Delta^{(4)} = \frac{1}{2} B \rho^4 - C y_0^2 \rho^2 \cos^2 \theta - \frac{1}{2} D y_0^2 \rho^2 + E y_0^3 \rho \cos \theta$$

$$+ F y_0 \rho^3 \cos \theta$$

$$\Delta^{(3)} X = B \rho^3 \sin \theta - 2 F y_0 \rho^2 \sin \theta \cos \theta + D y_0^2 \rho \sin \theta$$

$$\Delta^{(3)} y = B \rho^3 \cos \theta - F y_0 \rho^2 (1 + 2 \cos^2 \theta) + (2C + D) y_0^2 \rho \cos \theta - E y_0^3$$

thus, there exists a complete method of calculating the aberrations once the Gaussian parameters are known.

### 3.2.2 BASIC PARAMETERS OF THE TWO-BEAM SYSTEM

The basic parameters needed for geometrical calculations are for the radii of curvature of the two mirrors and the distance between them. The basic data were given directly from the blueprint <sup>2)</sup> supplied by the original manufacturer of the beam expander. The most accurate data are the original distance between mirrors (for parallel beams) and the magnification which are respectively 32.670 and 14.987 inches. [Note: Henceforth, unless otherwise noted, all lengths are in inches. To avoid any round-off errors, more than the actual number of significant figures are given for some numbers.] The focal lengths are then determined to be

$$f_p \text{ (primary)} = 35.006$$

$$f_s \text{ (secondary)} = 2.3357$$

Most of the remaining parameters depend on the location of the image plane. The design effort considered examples where the image planes are 10 meters and 30 meters from the primary mirror. These are actually the focal planes of the two-mirror system.

### 3.2.3 ABERRATIONS IN THE FOCUS OF THE INITIAL LASER BEAMS

There are two basic problems to consider: (1) The aberrations in focussing the original beams and (2) the aberrations in the returning beams. The first case is considered in this section. The distances of the image plane (focal plane) from the primary (large) mirror are 10 meters (393.7 inches) and 30 meters (1811.1 inches).

The quantities needed for calculating the aberration coefficients (Section 3.2.1) are given in Tab. 5.3.1.



TABLE 5.3.1

Quantities Needed for Calculating Aberration Coefficients

for 10 - meter and 30 - meter Focus .

Quantity <sup>a)</sup>	10 Meters <sup>b)</sup>	30 Meters
$r_1$	4.6715	4.6715
$r_2$	70.012	70.012
$d_1$	36.087	33.740
$s_1$	$-\infty$	$-\infty$
$s'_1$	2.3357	2.3357
$s_2$	38.423	36.076
$s'_2$	393.7	1181.1
$M'$	16.46	15.44

a) See Section 3.2.1.

b) All lengths in inches.

-----

From these quantities one can determine the related quantities  $h_1$ ,  $k_i$ ,  $K_i$ ,  $\alpha_i$ ,  $\beta_i$  and the aberration coefficients (see Section 3.2.1). For the coefficients one gets the results in Tab. 5.3.2.

TABLE 5.3.2  
Aberration Coefficients for Focus  
of Initial Laser Beams

Coefficient <sup>a)</sup>	10 Meters	30 Meters
B	-0.069152	-0.019091
C	-0.73171	-0.49090
D	-0.53193	-0.29112
E	1.3227	0.79201
F	0.15127	0.041664

a) See Section 3.2.1. The dimensions of the different coefficients are not uniform. Numbers given are in units of (inches)<sup>n</sup> where n is an integer.

-----

Rays to the image point can be identified in terms of points on the primary mirror from which they were reflected. This is the easiest way to determine the ray components  $p_2$  and  $q_2$ , which are the direction cosines (Gaussian approximation) of the rays at the image plane. To encompass the beam, we pick points around the 4 inch spot made by the beam on the primary. Let the y - z plane be the plane of bilateral symmetry of the beam expander. We then label rays in terms of x and y positions on the primary mirror as follows:

	<u>X Position</u>	<u>Y Position</u>
Ray 1	5.80 inches	0
Ray 2	3.80 inches	2.00 inches
Ray 3	1.80 inches	0

These labels will be used in the calculations to follow.

The Seidel variables are calculated from the equations in Section 3.2.1. The angles of the rays are small enough that sines may be replaced by tangents to 3 significant figures. The image points for the  $\lambda_1$  beam are, of course, on the optic axis. For the  $\lambda_2$  beam, it is sufficient to find one ray through the image plane to locate the image point in the Gaussian approximation. The lateral magnification  $M'$  between the two mirror planes depends on  $d_1$ . Its values are given in Tab. 5.3.1. This means, of course, that the extent of the beam striking the primary varies slightly with image distance, by less than 7%. This variation has not been taken into account in choosing Rays 1 - 3, but fixed points on the primary have been used to define the rays, for simplicity.

For the  $\lambda_1$  beam, we see that  $y_0 = 0$ , so only B is involved in the aberrations (spherical aberration). For the  $\lambda_2$  beam,  $y_0$  is the tangent of the angle made by a ray in the initial beam with the plane of bilateral symmetry of the beam expander. This involves the location of the flat mirror, which is taken as 3.00 inches forward of the primary, with the beam center striking the flat mirror at 1.3 cm from the symmetry plane.

This gives

$$y_0 = 1.31 \times 10^{-2}.$$

and for the positions of the Gaussian focal points of the beam,

$$(X_1^*, Y_1^*) = (0, -0.314) \text{ for 10 meters.}$$

$$= (0, -1.00) \text{ for 30 meters.}$$

Using these values, the Seidel variables  $\xi_2$ ,  $\eta_2$ ,  $\rho$ ,  $\sin \theta$ , and  $\cos \theta$ , and from them the wavefront shifts  $\phi^{(4)}$  and displacements  $(X_1 - X_1^*, Y_1 - Y_1^*)$  can be calculated. The results for the  $\lambda_1$  beam is given in Tab.5.3.3-5.3.4; those for the  $\lambda_2$  beam are in Tab.5.3.5-5.3.6.

TABLE 5.3.3  
Seidel Variables and Aberration  
Results for On-Axis Beam; 10 - Meter Focus.

Quantity	Ray 1	Ray 2	Ray 3
$\xi_2$	0.352 <sup>a)</sup>	0.231	0.109
$\eta_2$	0	0.122	0
$c^{(4)}$	6.7 $\mu\text{m}$	2.0 $\mu\text{m}$	0.1 $\mu\text{m}$
$X_2 - X_2^*$	- 0.072	-0.026	-0.002
$Y_2 - Y_2^*$	0	-0.014	0

a) All lengths in inches except as noted.

TABLE 5.3.4

## Seidel Variables and Aberration

Results for On-Axis Beam, 30 - Meter Focus.

Quantity	Ray 1	Ray 2	Ray 3
$\xi_2$	0.376	0.246	0.117
$\eta_2^{(4)}$	0	0.130	0
$c$	2.4 $\mu\text{m}$	0.7 $\mu\text{m}$	0.03 $\mu\text{m}$
$x_2 - x_2^*$	-0.078	-0.028	-0.002
$y_2 - y_2^*$	0	-0.015	0

TABLE 5.3.5

## Seidel Variables and Aberration

Results for Off-Axis Beam; 10 - Meter Focus

Quantity	Ray 1	Ray 2	Ray 3
$\xi_2$	0.352	0.231	0.109
$\eta_2$	0	0.122	0
$c^{(4)}$	6.7 $\mu\text{m}$	2.6 $\mu\text{m}$	0.008 $\mu\text{m}$
$x_2 - x_2^*$	- 0.072	- 0.029	- 0.002
$y_2 - y_2^*$	- 0.006	- 0.018	- 0.001

TABLE 5.3.6

## Seidel Variables and Aberration

Results for Off-Axis Beam; 30 - Meter Focus

Quantity	Ray 1	Ray 2	Ray 3
$\xi_2$	0.376	0.246	0.117
$\eta_2$	0	0.130	0
(4)			
$\zeta$	2.5 $\mu\text{m}$	1.0 $\mu\text{m}$	0.03 $\mu\text{m}$
$x_2 - x_2^*$	-0.079	-0.031	-0.003
$y_2 - y_2^*$	-0.006	-0.022	-0.001



The numbers in Tab. 5.3.3-5.3.6 can be used to define the spot size of the focus in each case, as well as the wavefront variation for rays coming to different points on this spot. By comparing Tab. 5.3.3 with Tab. 5.3.5 and Tab. 5.3.4 with Tab. 5.3.6, it can be seen that the difference brought about by having the  $\lambda_2$  beam offset from the symmetry plane is indeed slight. In regard to focussing properties, the two-beam  $\delta$ -system should perform essentially as well as the one-beam system.

#### 3.2.4 ABERRATIONS IN THE RETURNING BEAMS

The question of the effect on waves reflected from the aerosol particles in the focus of a beam will now be considered. Again the cases of  $\lambda_1$  and  $\lambda_2$  beams at 10 and 30 meters are treated. The roles of primary and secondary mirrors are now reversed. Quantities corresponding to those in Tab. 5.3.1 are given in Table 5.3.7.

TABLE 5.3.7

Quantities Needed for Calculating  
Aberration Coefficients for Returning Beams

Quantity	10 Meters	30 Meters
$r_1$	70.012	70.012
$r_2$	4.6715	4.6715
$d_1$	36.087	33.740
$s_1$	393.7	1181.1
$s_1'$	38.423	36.076
$s_2$	2.3357	2.3357
$s_2'$	$-\infty$	$\infty$
$M'$	0.06075	0.06477

The related quantities are calculated as before, and we arrive at the aberration coefficients given in Tab. 5.3.8

TABLE 5.3.8  
Aberration Coefficients for Returning Beams

Coefficient	10 Meters	30 Meters
B	$9.4423 \times 10^{-7}$	$3.3522 \times 10^{-7}$
C	$-1.269 \times 10^{-3}$	$-4.21 \times 10^{-4}$
D	$-2.0105 \times 10^{-1}$	$-2.0020 \times 10^{-1}$
E	$-7.5126 \times 10^1$	$-6.6612 \times 10^{-1}$
F	$1.61 \times 10^{-6}$	$1.7 \times 10^{-7}$

The parameter,  $\phi^{(4)}$ , the wavefront displacement at different points on the secondary mirror is calculated from

$$\xi_2 = X_2' / M'$$

$$\eta_2 = Y_2' / M'$$

where  $(X_2', Y_2')$  is the point at which a ray leaves the secondary. For simplicity Ray  $n'$  is defined as the reverse of ray  $n$ . Results are given in Tab. 5.3.9 and Tab. 5.3.10.

TABLE 5.3.9

Seidel Variables and Aberration  
Results for Returning Beam on Axis

Quantity		Ray 1'	Ray 2'	Ray 3'
10 meters	$\xi_2$	5.80	3.80	1.80
	$\eta_2$	0	2.00	0
	$\zeta^{(4)}$	-6.8 $\mu\text{m}$	-2.0 $\mu\text{m}$	-0.06 $\mu\text{m}$
30 meters	$\xi_2$	5.80	3.80	1.80
	$\eta_2$	0	2.00	0
	$\zeta^{(4)}$	-2.4 $\mu\text{m}$	-0.7 $\mu\text{m}$	-0.02 $\mu\text{m}$

TABLE 5.3.10

Seidel Variables and Aberration  
Results for Returning Beams Off-Axis

	Quantity	Ray 1'	Ray 2'	Ray 3'
-10 meters	$\xi_2$	5.80	3.80	1.80
	$\tau_{12}$	-1.51	2.47	-1.51
	$c^{(4)}$	-7.7 $\mu\text{m}$	-2.5 $\mu\text{m}$	-0.2 $\mu\text{m}$
30 meters	$\xi_2$	5.80	3.80	1.80
	$\tau_{12}$	-0.442	2.44	-0.442
	$c^{(4)}$	-2.4 $\mu\text{m}$	-0.08 $\mu\text{m}$	-0.02 $\mu\text{m}$

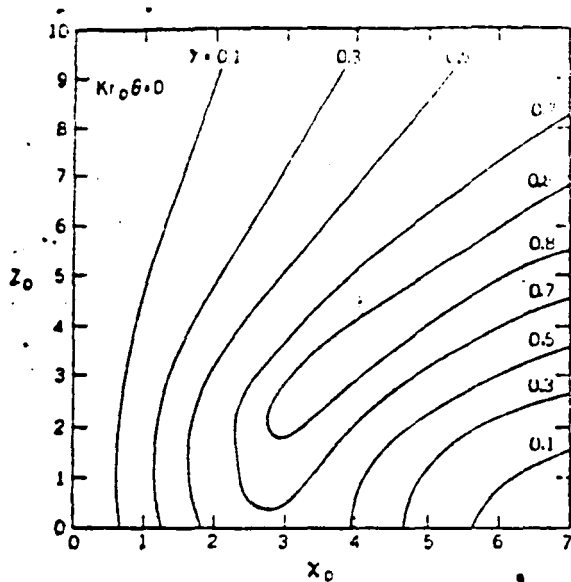
### 3.3 HETERODYNE EFFICIENCIES FOR THE ON-AXIS AND OFF-AXIS REFLECTED RADIATION:

The heterodyne efficiencies associated with radiation backscattered into the system from  $\lambda_1$  and  $\lambda_2$  focal volumes can be calculated using the information contained in Table IX and X and Fig.5.3.3. Fig. 5.3.3 is taken directly from "Heterodyne detection: phase front alignment, beam spot size, and detector uniformity", Steven C. Cohen, August, 1975/ Vol. 14, No. 8/ Applied Optics, page 1957. The assumptions for use of the Figure 5.3.3 in calculating the heterodyning efficiency are as follows:

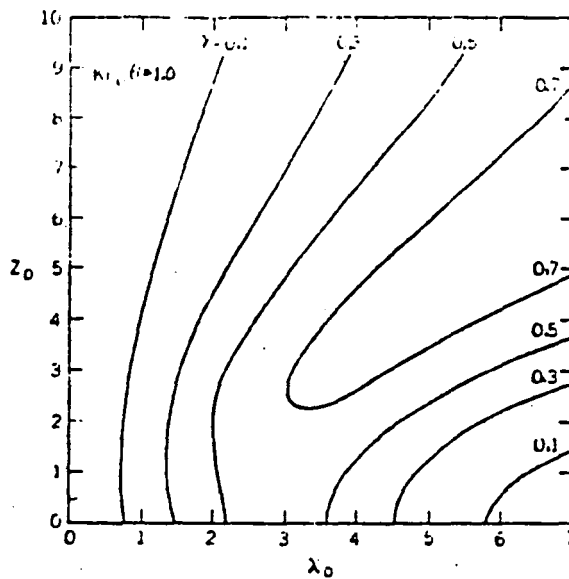
- The local oscillator is assumed to have a Gaussian beam profile.
- The returns signal beam profile is assumed to be an Airy Disk.
- The Airy Received signal parameter  $X_0$  is given by  $\frac{\pi r_0}{\lambda F}$  where  $r_0$  (beam radius on the detector) = .05 mm,  $\lambda$  equal the wavelength of the transmitted radiation, and  $F$  equal the F/No. for the focusing lens placed immediately in front of the detector.  $X_0$  is assumed equal to  $\sim 3$ .
- The Gaussian local oscillator parameter  $Z_0$  is given by  $\frac{r_0}{w}$  where  $w = \frac{1}{e}$  radius of L. O. beam. It is assumed that  $Z_0$  equals 1.

For a phase front tilt of  $\lambda$  over the detector the heterodyne detector parameter,  $\gamma$ , is found to be  $\sim 0.1$ . Note that,

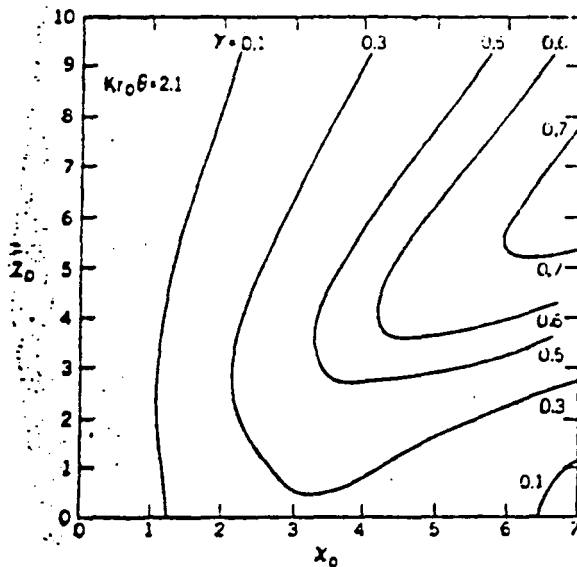
$$Kr_0\theta = K \frac{\lambda}{2} = \frac{2\lambda}{\lambda} \frac{\lambda}{2} = \pi \text{ and from Fig.5.3.3(d) with } Z_0 = 1 \text{ and}$$



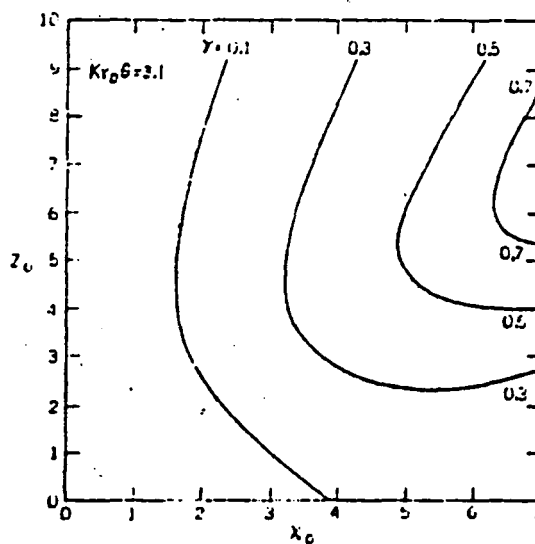
(a)



(b)



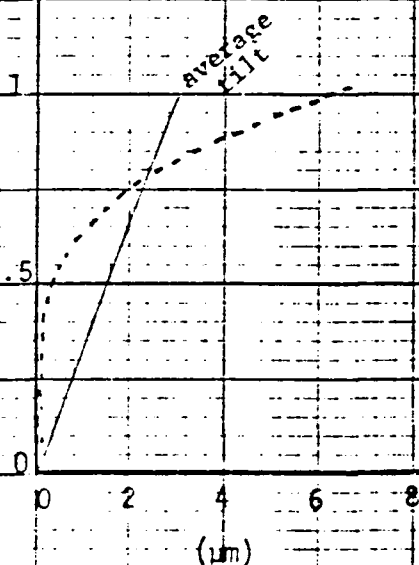
(c)



(d)

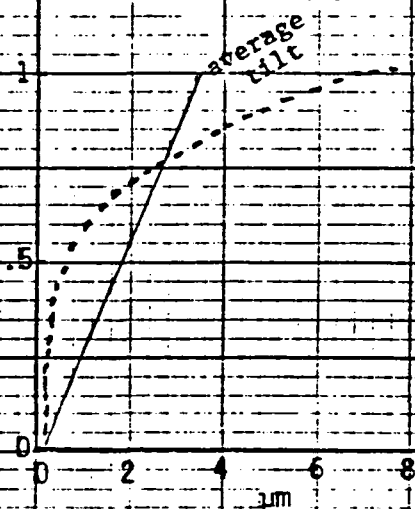
FIGURE 5.3.3 HETERODYNE EFFICIENCY CONTOURS  
Contours of equal valued heterodyne detection parameter  $\gamma$  as a function of Airy received signal parameter  $X_0$  and Gaussian local oscillator parameter  $Z_0$  : (a)  $Kr_0\theta = 0$ ; (b)  $Kr_0\theta = 1$ ; (c)  $Kr_0\theta = 2.1$ ; (d)  $Kr_0\theta = 3.1$ .

$$X = (6.8) y^4 + .06$$



X, Phase Shift  
(a)

$$X = (7.5) y^4 + .2$$



X, Phase Shift  
(b)

FIGURE 5.3.4

Approximation of Wave Front Tilt



$X_0 = 3$  it can be seen that  $\gamma \approx 0.1$ . Similarly, for a wave front tilt of  $\frac{\lambda}{2}$  the  $\gamma$  is found to be  $\sim 0.6$ . Using the information from Fig. 3.3 and the phase shifts calculated for the proposed  $\beta$ -system in Tables IX and X the relative heterodyne detection parameter can be calculated.

From Table IX it can be seen that the phase shift for the two extreme rays, Ray 1' and Ray 3' (for the existing  $\beta$ -system) for returning beams on axis when the system is focused at 10 meters is approximately  $6.7 \mu\text{m}$ . It is also understood that this tilt takes on a shape that is given by Fig. 5.3.4(a). This fourth power relationship permits a conservative approximation of the wavefront tilt at the secondary to be estimated at  $\sim 1.5 \mu\text{m}$ . This is further supported by the assumed Gaussian beam shape on the local oscillator beam and the Airy disk beam shape on the reflected beam. An observation of Fig. 5.3.3 indicates that the heterodyne detection parameter,  $\gamma$ , is approximately equal to 0.7.

This performance tends to increase as the existing system is focused at longer ranges and approaches  $\gamma = 0.75$  for a focus at 30 meters. From Table X it can be seen that the phase shift for the two extreme rays, Ray 1' and Ray 3' (for the proposed  $\beta$ -system) for returning beams off-axis when the system is focused at 10 meters is approximately  $7.5 \mu\text{m}$ . Again the tilt takes on a shape that is given by Fig. 5.3.4 b).

This fourth power relationship permits a conservative approximation of the wavefront tilt at the secondary to be estimated at  $2.0 \mu\text{m}$ . This estimate is also supported by the assumed beam shapes

of the local oscillator and the reflected/collected beam. An observation of Fig.5.3.3 is that the heterodyne detection parameter,  $\gamma$ , is approximately equal to 0.65.

This performance tends to increase as the proposed system is focused at longer ranges and also approaches the  $\gamma = 0.75$  for a focus at 30 meters.

#### 4. SUMMARY

Currently completed analyses of the two basic two-color  $\beta$ -system designs which have been investigated, indicate that the two beam directing insertion mirror design will have the higher system performance efficiency, considering all other things equal. The study has resulted in a ray trace analysis which indicates that the existing system has a beam expanding telescope which couples with the Laser Doppler System to give relatively good heterodyne performance even when focused to 10 meters.

The ray trace analysis indicates that the system can accommodate off-axis beam insertion without the serious penalty of substantially lower heterodyne efficiency. Relative performance between the on-axis beam and the off-axis beam may be undetectably small when measured in the field.

The beam splitter combined two color  $\beta$ -system design has several desirable attributes in that it requires only one detector, interferometer, and signal processor thus potentially becoming a smaller and lighter instrument package. This design may potentially be the more desirable, of the two investigated designs, if performance efficiency for the system becomes less important and/or if simultaneous measurement of single particle signal events from  $\lambda_1$  and  $\lambda_2$  becomes more important. Further investigation and analysis of the data taken with the existing  $\beta$ -system will provide insight into the correct system design to choose for the two-color  $\beta$ -system.

1. Max Born and Emil Wolf, Principles of Optics, 4th. ed. (Pergamon Press, New York, 1970).
2. Blueprint supplied with Optronics International, Inc., beam expander, 15XC10150-VF.
3. T. Kordos, Broomer Laboratories, Inc. Plainview, N. Y., Personal Communication.

7. Task 6: Evaluation of Applicability of Adaptive  
Filtering to Pulsed LDV Signal Processing

Adaptive filtering is appropriate for signals whose statistical properties are not known a priori, or whose properties change with time. In either case, adaptive processing constructs a Wiener filter matched to the particular signal. If the signal is stationary (not statistically changing with time), the Wiener filter is achieved and does not change with time. If the signal has non-stationary statistics, to be useful, the adaptive process must occur rapidly enough to "track" the changing signal properties. Since LDV signals are non-stationary narrow band random processes, it is appropriate to consider whether adaptive filtering can provide enhanced spectral estimation for LDV signals. While adaptive filtering applied to signal channel time series is reasonably well developed as "off-the-shelf" processing, applications to the spectral domain or to multi-channel data are not well developed. These latter applications would require significant research and development.

Adaptive filtering has many forms,<sup>1,2</sup> each suited to specific signal processing problems. Forms originally considered for LDV applications were the Adaptive Noise Canceller (ANC) and the Adaptive Line Enhancer (ALE) implemented as an Adaptive Linear Predictive Filter (ALPF).

The ANC form is shown in Figure 6.1. This form requires two inputs: signal plus noise  $d(k)$  and a correlated noise source  $x(k)$  used as a reference channel. The reference channel noise is filtered and subtracted from the signal plus noise channel to improve the signal-to-noise ratio (SNR). Since a correlated noise source is not available for LDV processing, the ANC form is not appropriate.

The ALE in the form of the ALPF is shown in Figure 6.2. There is a signal channel input to this filter, whose weight  $w_j$  are adjusted so that the  $e(k)$  output is a minimum (in the least mean square sense). The output  $x(k)$  is then the approximation to the signal without noise. This filter would be incorporated into an LDV system, as shown in Figure 6.3, between the preamp and the final processor, if an additional processor is desired. In this way, the ALE is entirely independent of the additional processor and may be removed, if desired, in the case of search and track failures. The purpose of the ALE is to improve the SNR into the processor, and it can be considered an add-on device. Uncertain at present are the convergence time (possibly too long) and tracking performance for a narrow band random process (aerosol signal).

Details on the ALPF:

The filter coefficients  $w_j$ , shown in Figure 6.2, which give minimum mean-square error for the  $e(k)$  are determined by values of the auto-correlation function of the input signal at various time lags.<sup>1</sup> These values of  $w_j$  constitute the "Weiner filter". For a narrow band random process, this is a matched filter around the signal. As the signal changes, the filter must "adapt". To accomplish this, a "least mean-square" algorithm has been devised which continually seeks the "least mean-square" error.<sup>1</sup> This is a method of tracking the Weiner filter without calculating the auto-correlation lags. Important about this process is the time necessary for convergence for a narrow band random process, which has yet to be evaluated.<sup>3</sup>

Linear predictive filtering, itself, gives an estimate of the spectrum of the signal, called the "maximum entropy spectrum". Details of this are given elsewhere,<sup>2</sup> but, in summary, the spectrum is determined by the filter weight values. Figure 6.4 shows the relation between the maximum entropy spectrum  $Q(w)$  and the transfer function of the "whitening filter  $H(w)$  which converts the signal  $x(k)$  in to white noise  $e(k)$ . This method would be used only if the ALPF were the final stage of processing.

## Improvement in LDV Processing Offered by ALPF:

Analytical formulae for evaluating the improvement in SNR offered by the ALPF in an LDV system are not available. However, evaluation of this effect can be accomplished by simulated narrow band random process data processed by an ALPF. The improvement on stationary data is shown in Figure 6.5. This figure<sup>3</sup> shows the velocity error to be expected in estimation of the mean frequency, as a function of SNR. The Cramer-Rao bound<sup>7</sup> represents a theoretical upper limit on the possibility of improving the velocity error at a given SNR. The pulse pair (PP) curve is the theoretical response for the processing of 1024 points. This figure applies to a spectral width of 1 m/sec. Clearly about 12 dB of improvement above the PP curve is indicated. Thus it is reasonable to attempt to achieve this SNR improvement, although the processing techniques which would bridge this gap have not been identified. Also shown in this graph is the result for a linear predictive filter (LPF) as a final processor. A nominal improvement of about 3 dB is seen, but the performance is worse at the extremes of the curve. Improvement offered by a poly-pulse-pair processor as a final processor are not shown, but simulation has shown it to be very similar to the linear predictive filter curve.<sup>3</sup> Results for an ALPF followed by a pulse-pair processor or a poly-pulse-pair processor are not available. These results could be generated straightforwardly from existing



subroutines.

#### Application of ALPF to Previously Recorded Data:

An ALPF can be applied to previously recorded time series data in a straightforward manner. Power spectral data contain less information and are not amenable to conventional adaptive techniques. Attempts to apply adaptive processing schemes would require extending these to spectrum-based schemes, or to multichannel input adaptive filters. These are not "off-the-shelf" processing techniques, and would require development.<sup>4,5</sup>

Steps to improve mean frequency estimation based on power spectral data can be recommended. Noise spectrum averaging, from cases when no signal is present, provides a basis for appropriately weighting each channel. This correlation should be made. Then a circular mean estimation,<sup>6</sup> indicated in Figure 6.6, should be applied as an unbiased estimator (in contrast to peak or linear mean frequency methods). In low SNR data, a plot of the circular mean frequency would dramatically indicate whether signal were present or not, since a noise frequency estimate would be found at any point around the circle, while a real signal would be consistently found in some angular interval. This would seem to be the best method of indicating the presence of real signal power spectrum data, since it is not biased by the noise spectrum.

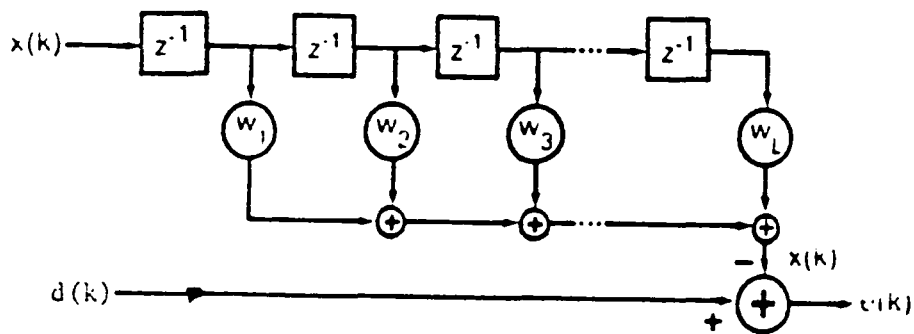


Figure 6.1  
ADAPTIVE NOISE CANCELLER

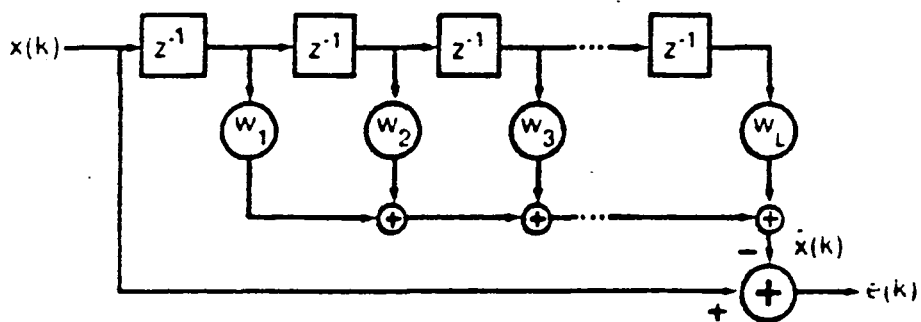


Figure 6.2  
ADAPTIVE LINEAR PREDICTION FILTER

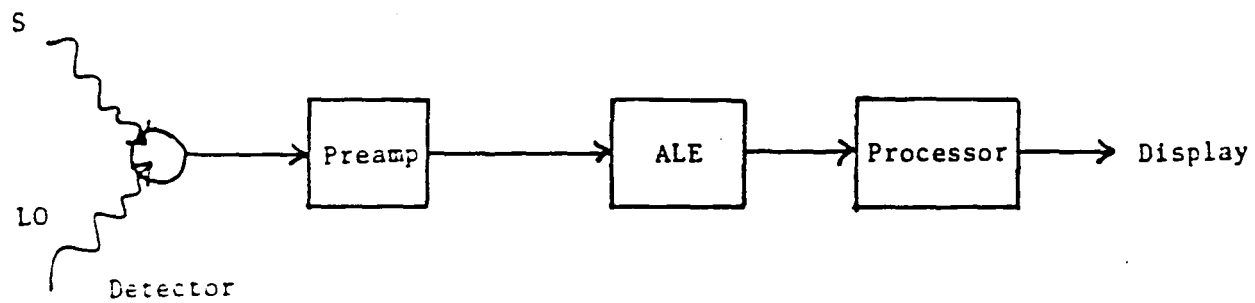
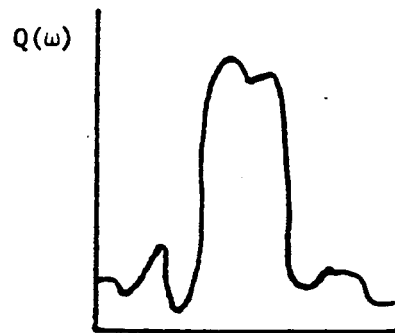
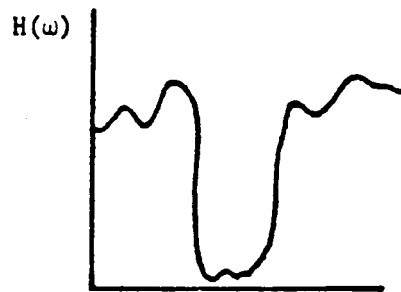
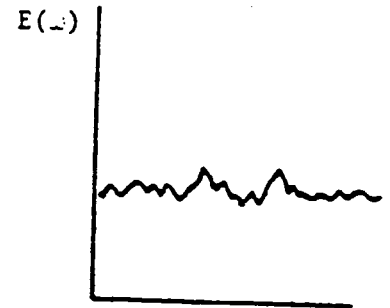
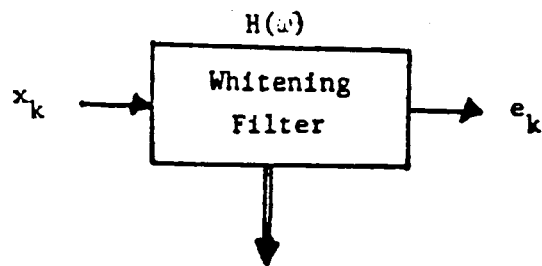


Figure 6.3

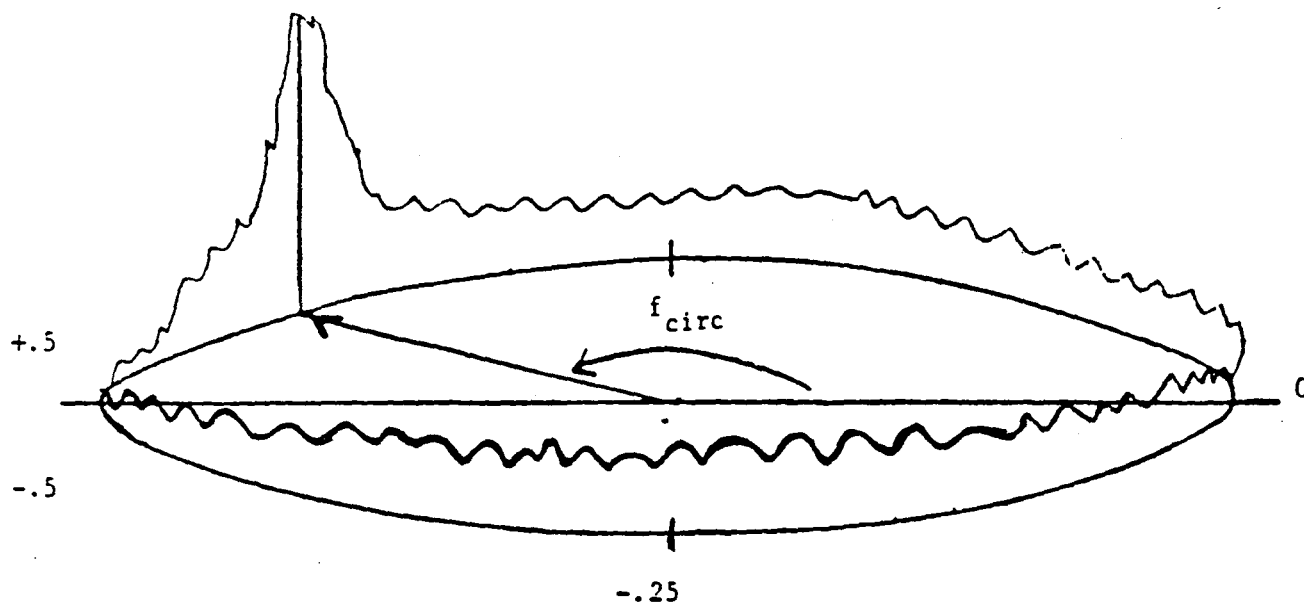
ADAPTIVE LINE ENHANCER IN LDV SYSTEM



$$Q(\omega) = |H(\omega)|^{-2}$$

Figure 6.4  
MAXIMUM ENTROPY SPECTRUM AND WHITENING FILTER

**This Page Intentionally Left Blank**



$$f_{\text{circ}} = \frac{1}{2\pi} \arctan \left[ \frac{\sum_{n=0}^{N-1} S_n \sin(2\pi n/N)}{\sum_{n=0}^{N-1} S_n \cos(2\pi n/N)} \right]$$

Figure 6.6

CIRCULAR FIRST MOMENT FREQUENCY ESTIMATOR

## Summary:

A potential gain of 10 to 12 dB in SNR beyond the response of pulse pair processing is theoretically indicated, but the processing techniques for realizing this gain have not been established. Therefore, it is reasonable to seek techniques, or combinations of techniques, which will approach this theoretical limit. Results have been presented which indicate that Adaptive Linear Predictive Filtering will contribute 3 dB of this gain, an improvement very similar to that offered by poly-pulse-pair processing. Combinations of processing techniques, such as ALPF and poly-pulse-pair processing, have not been evaluated. This could be accomplished with existing subroutines.

Previously recorded power spectral data is not amenable to "off-the-shelf" ALPF processing, but would require some extension of existing techniques to the spectral domain, or to multichannel input data. However, noise threshold compensation measures and, in particular, the use of the circular first moment frequency estimates should give a good indication of the presence of signal.

#### REFERENCES

1. Bernard Widrow, et. al., "Adaptive Noise Cancelling: Principles and Applications", Proc. IEEE, 63, No. 12, p. 1962, Dec. 1975.
2. R. Jeffrey Keeler and Lloyd J. Griffiths, "Acoustic Doppler Extraction by Adaptive Linear Filtering", J. Acoustic Soc. Am., 61, No. 5, p. 1218, May 1977.
3. R. J. Keeler, private communication.
4. Mauro Dentino, et. al., "Adaptive Filtering in the Frequency Domain", Proc. IEEE, 66, No. 12, p. 1658, Dec. 1978.
5. E. E. Ferrara, Jr. and Bernard Widrow, "Multichannel Adaptive Filtering for Signal Enhancement", IEEE Transactions on Acoustics, Speech, and Signal Processing, 29, No. 3, p.766, June 1981.
6. Dale Sirmans and Bill Bumgarner, "Numerical Comparison of Five Mean Frequency Estimators," Journal of Applied Meteorology, 14, p. 991, Sept. 1975.
7. J. P. Toomey, "High Resolution Frequency Measurement by Linear Prediction", IEEE Trans. AES, AES-16, No. 4, p. 517, July 1980.



## 8. Task 7: Correlation of Beta Experiment Data With LDV Data

Software algorithms were developed to provide data processing capability to determine the backscatter coefficient from single particle measurements. These algorithms are capable of providing a correlation of beta measurement data with laser doppler data recorded in a different (volume) mode. Part of this work is also described in chapter 11.

Single particle  $\beta$  predictions were made using data obtained an extreme focus of 40 meters. Figures 7.1, 7.2, 7.3, and 7.4 show signal histograms of the data used to derive each prediction. The data used in the three figures was very sparse containing only 329, 705 and 192 single particle respectively. The correlation between predictions and this volume mode data ( $f = 40\text{m}$ ) is not straightforward since these particles would be relatively large and the density of these large particles is also very low.

Several assumptions were made in order to make these predictions. They are: 1) The noise level is constant at -59 dB. 2) The signal threshold was set at a S/N of approximately 7.5 dB. 3) The maximum signal bin is at -41 dB and the correspondence between signal bin and signal is linear. Based on these values and other assumed system

parameters the beta inversion algorithms produced these results:

- 1) Density of particles - 1 particle/m<sup>3</sup>
- 2) Average cross-section (backscatter) - 33μ<sup>2</sup>
- 3) Smallest cross-section seen - 11μ<sup>2</sup>(this is due to focus of 40 meters)
- 4) Beta = 2.2 X 10<sup>-12</sup> meter<sup>-1</sup> for Figure 7.1  
= 4.7 X 10<sup>-12</sup> meter<sup>-1</sup> for Figure 7.2  
= 1.2 X 10<sup>-12</sup> meter<sup>-1</sup> for Figure 7.3

This system is currently being calibrated, however, these calculations are for an uncalibrated system. This fact plus the very small number of particles processed required that the predicted beta values be interpreted with caution. An additional case with a significant number of particles is contained in Figure 7.4. The time for this case is in error as shown, and the exact time is not available. Indications are that this case corresponds to a particle density of about 1000/m<sup>3</sup>.

The flight distances required to measure beta in the single particle mode are analyzed as follows: Since

$$\beta = D \bar{\sigma} / 4 \pi$$

and  $D = N / AL$

where  $D$  = total number of relevant particles/unit volume

$\bar{\sigma}$  = average backscatter cross-section

$A$  = LDV effective area

$N$  = number of particles required for beta inversion

$L$  = flight distance/data set,

we see

$$L = N \bar{\sigma} / 4 \pi \beta A$$

$$\text{or } \log L = - \log \beta + \log (N \bar{\sigma} / 4 \pi A).$$

This shows that the flight distance is dependent on  $\beta$  as well as on the system and distribution dependent parameters  $A$  and  $\bar{\sigma}$ , and on the algorithm parameter  $N$ . Since  $A$  and  $\bar{\sigma}$  are averages over the backscatter probability distribution to be sampled, this distribution (or a set of expected distributions) must be known to predict  $L$ , independent of the prescribed  $\beta$  value. The accompanying Figure 7.5 shows  $L$  as a function of  $\beta$  for three different focal ranges, 10, 20, 30m, and three different backscatter probability distributions: exponential,  $e^{-B\sigma}$  with  $B = .15$  and power law,  $1/\sigma^B$  with  $B = 1.7$  and  $2.4$ . These distributions are not unreasonable, but do give a difference in flight distances

of almost an order of magnitude. Because they are different distributions, the densities for each case are different as shown. Here,  $N$  was assumed to be  $10^4$ , the  $1/e^2$  intensity radius was 5.5 cm and no beam truncation was assumed.

Clearly, the smaller the parameter  $N \bar{\sigma}/A$ , the smaller the flight distance for a given  $\beta$ . For several reasons, the actual situation will be better than presented by these graphs:

1. The  $1/e^2$  radius is 4.6 cm giving a larger  $A$ .
2. The actual beam is truncated, giving a larger  $A$ .
3.  $N$  could be decreased as knowledge of the actual backscatter distribution increases.

The actual backscatter distribution, itself, might give smaller ratios of  $\bar{\sigma}/A$  than represented here.

Transit to Avg. 35000', laser p-20.  
 20:07:46-20:07:47  
 PEAK - 00020  
 SUM - 329  
 AVERAGE VOLUME BETA - 148.399

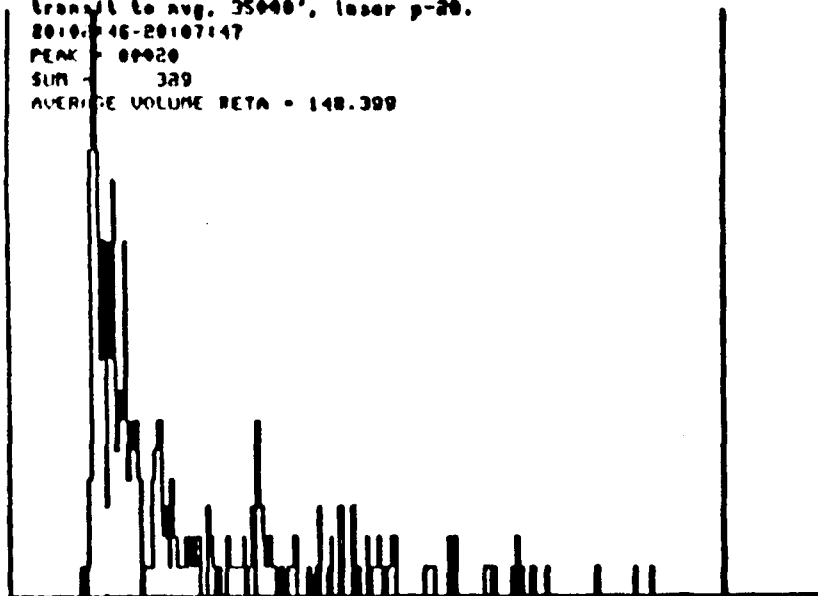


Figure 7.1

TRANSIT TO MUOC, 35000', laser p-20.  
 20:15:59-20:16:01  
 PEAK - 00048  
 SUM - 705  
 AVERAGE VOLUME BETA - 144.986

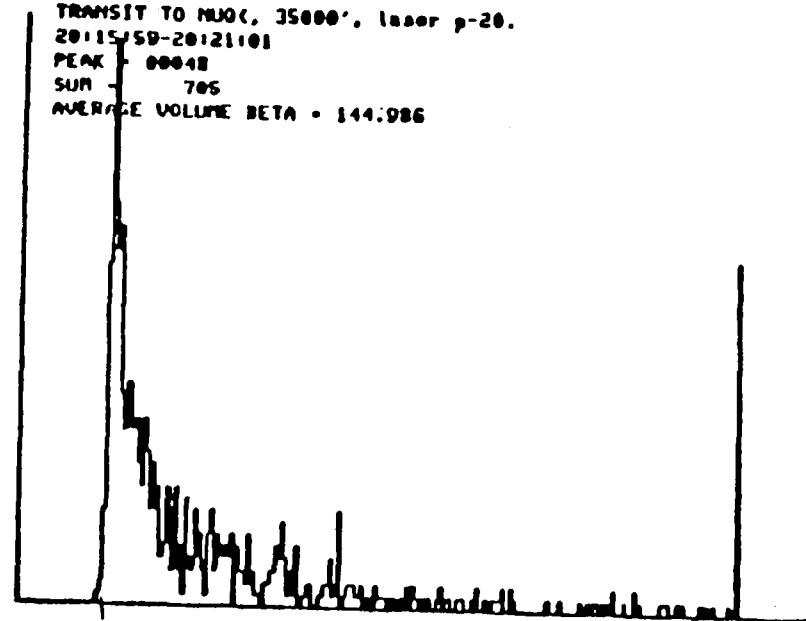


Figure 7.2

TRANSIT TO MUOC, 35000', laser p-20.  
 20:21:01-20:26:02  
 PEAK - 00019  
 SUM - 192  
 AVERAGE VOLUME BETA - 172.897

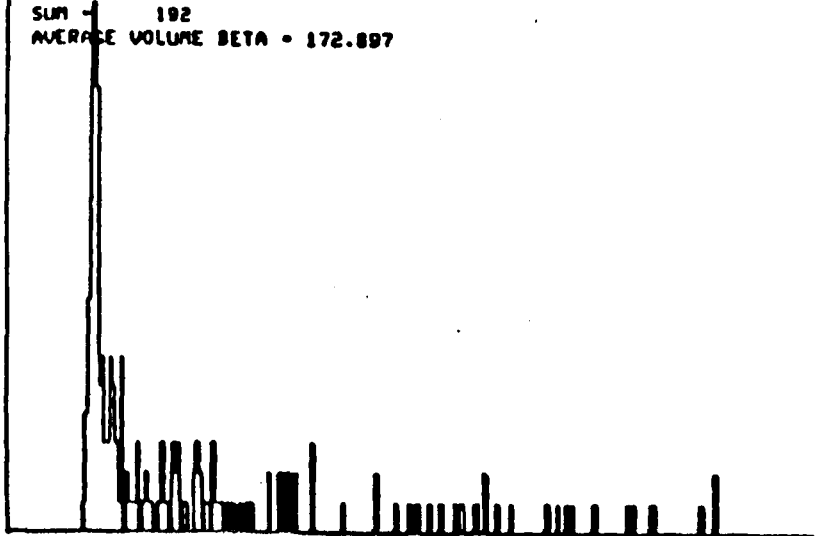


Figure 7.3

turret data 04  
 21:10:00-22:54:41  
 PEAK - 10460  
 SUM - 442321  
 AVERAGE VOLUME BETA - 22.6931

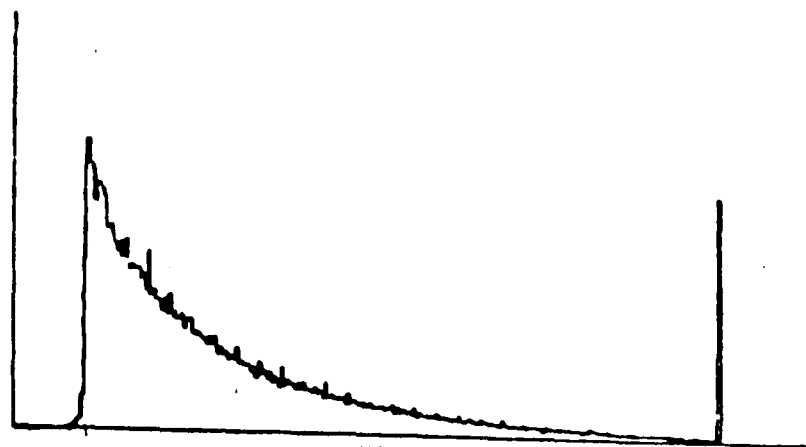
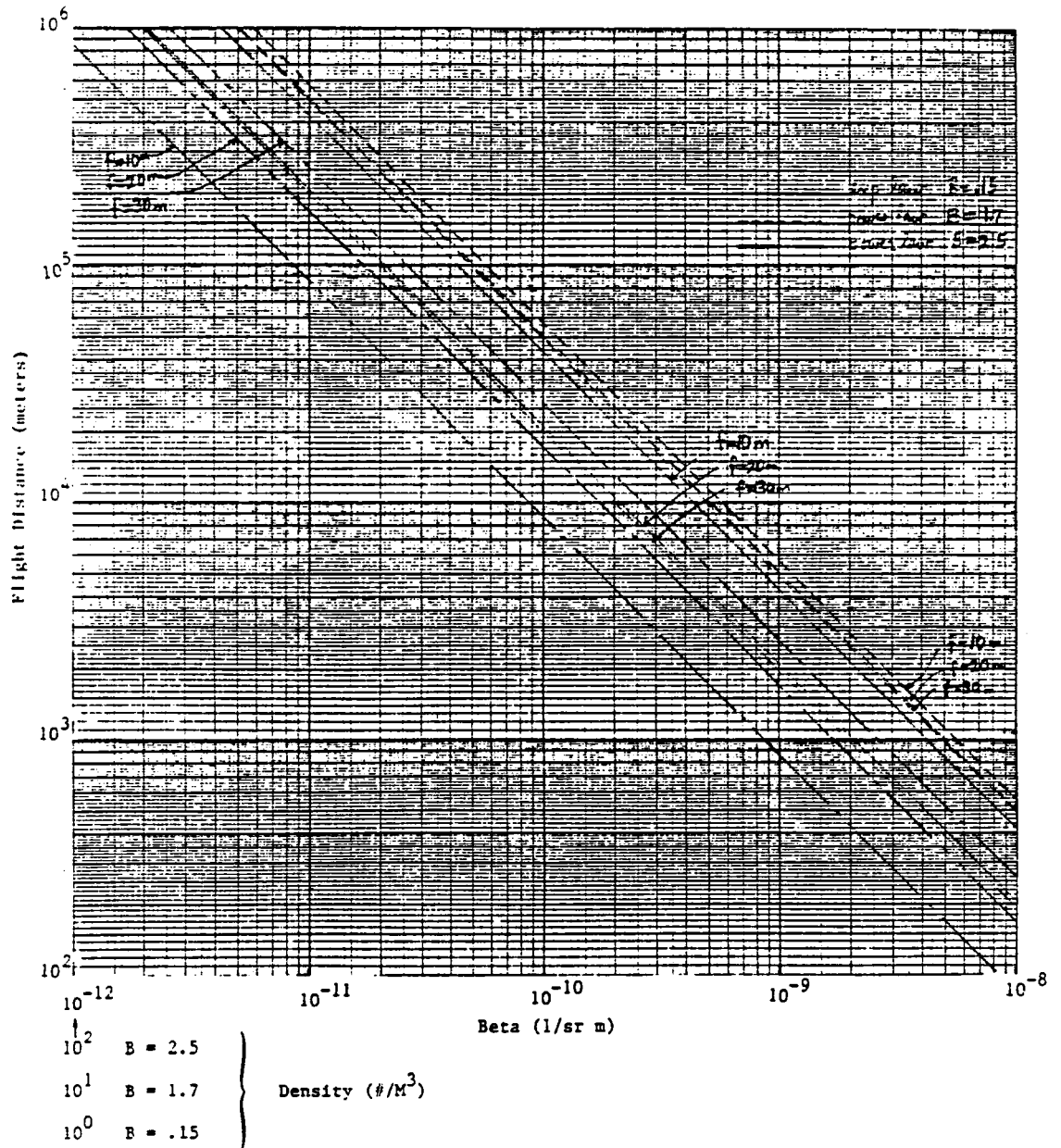


Figure 7.4

PARTICLE NUMBER HISTOGRAMS

Figure 7.5

FLIGHT DISTANCE (METERS) AS A FUNCTION  
OF BETA AND DENSITY



9. Task 8: Determination of  $L_{eff}$

The concept of  $L_{eff}$  arises when the return from a plane at the waist is used to infer the return from a volume distribution. A return from the waist plane can be written

$$S_w = \rho \int_{\text{waist}} F(x,y) dx dy$$

where  $\rho$  is the reflectance in inverse steradians and  $F(x,y)$  represents the transverse beam profile. A volume return is written

$$S_v = \beta \int F(x,y,z) dx dy dz$$

and used to define  $L_{eff}$  as

$$S_v = \beta L_{eff} \int_{\text{waist}} F(x,y) dx dy$$

Then if we ask what  $\beta$  value is implied by a measurement at the waist, we equate  $S_w$  and  $S_v$  and find

$$\rho = \beta L_{eff}$$

But we see that

$$L_{eff} = \int F(x,y,z) dx dy dz / \int_{waist} F(x,y) dx dy$$

so that  $L_{eff}$  is really a geometric mean length determined only by the beam profile.

An exact measurement of  $L_{eff}$  can be accomplished by making measurements in many planes and integrating. Let

$$S_m = \rho \sum_p \int_{plane\ p} F(x,y) dx dy$$

where closely spaced planes, separated by  $\Delta z$ , from signal beginning to signal end are chosen. Then,

$$S_m = \frac{\rho}{\Delta z} \sum_p \int_{plane\ p} F(x,y) dx dy \Delta z$$

$$\rightarrow \frac{\rho}{\Delta z} \int F(x,y,z) dx dy dz$$

So

$$L_{eff} = \Delta z S_m / S_w$$

and does not depend on the reflectivity of the target used for the measurement, or upon laser power. It does depend on correct optical alignment which is assumed.



For the precise calibration of the system, the return from twenty-one planes separated by equal distances and centering on the waist should be measured. These planes should extend to points on either side of the waist such that the contribution from neglected planes determines the acceptable error. That is, if 1 percent error is acceptable, then measurement may be stopped when the next plane contributes less than 1 percent of the value of the integral  $S_m$ . The sum of these returns divided by the waist return times the plane separation increment gives  $L_{eff}$ . This set of measurements should be made at the operating focal range. A less precise value can be obtained by taking at least two sets of measurements at less than the operating focal range and extrapolating to the operating range. One can only guess at the precision of such a procedure since the real beam profile and its range variation are unknown.

Experiments were made in January to determine  $L_{eff}$  for the NASA Beta System Laser Doppler Velocimeter (LDV). The effort was conducted using the system focused at 60 and 100 meters. In December, measurements were made at these ranges but analyses indicated that additional data were needed. First the December measurements at 60 meters were made using a 10 inch aluminum wheel with 1-inch sulphur band on the periphery. These measurements were made out to distances approximately equal to two times the theoretical  $L_{eff}$ . The  $1/e^2$  beam size expanded to about one inch in diameter at

these distances and the beam consequently was larger than the sulphur band. Measurements were, therefore, made at 60m using the sand paper disk.

Also in December, measurements were made using the vacuum chamber tunnel at 100 meters focus. Since the tunnel was only 100 meters in length, the laser beam was folded using mirrors to provide easy access to the beam at distances beyond the waist. Position of the mirrors in the tunnel did not provide enough distance beyond the waist for a good estimate of  $L_{eff}$ . Consequently, these measurements were repeated in January.

Two characteristics of the spectrum analyzer were used to determine the sand paper wheel speed which was used during these measurements. A rotation speed sufficient to give Doppler shift greater than 300 KHz dead band, yet slow enough to keep the doppler band width well within the capability of the 300 KHz filter on the spectrum analyzer was essential. The shaded area in Figure 8.1 defines these limits. The Doppler bandwidth increases as the beam spread increases at larger distances from the waist. Consequently, to identify the presence of possible frequency truncation, measurements were compared using both the 100 and 300 KHz bandwidth filters. Differences between the signal levels measured in these bands were taken as indication of frequency truncation. A difference in signal level of two

dB was considered to be significant and data showing greater than this difference were not used in calculation of  $L_{eff}$ . Slight differences in the signal levels were observed at 60 meters indicating only a minor level of frequency truncation. However, significantly differences were observed in the signal levels at distances approximately equal to  $L_{eff}$  at 100 meters focus. Consequently, frequency truncation limited the distances to which measurements could be made at 100 m focal range. This resulted in an increased uncertainty in the calculated values of  $L_{eff}$ .

An additional comment should be made about the data analyses. Generally, signal levels taken at the end points exhibited about 18 dB attenuation from values measured at the waist. An exception to this occurred at the 100 meter focus. For this focus, signal levels were attenuated only 9 dB at the end points. The distance from the waist at which data could be taken was thus limited by the beam spread which resulted in a broader Doppler spectrum. The measured data was extended over a larger range for estimation of  $L_{eff}$ , using a least square linear curve fit on the signal levels measured dB. This procedure resulted in a very good fit to the data as indicated by the variance and correlation coefficients obtained from analyses of the measured and curve fit data. The data was extended to approximately 40 dB attenuation levels using this procedure. Since the data experienced slightly faster than an exponential fall off,

this methodology results in an overestimation of  $L_{eff}$  . Results for the three ranges 30, 60, and 100 meters are depicted in Figure 8.2. These results are compared to theoretical values of  $L_{eff}$  untruncated obtained for a system with an aperture of .046 m. The majority of the difference between the curves shown in this figure can be explained in terms of over estimation of values by the procedure used to calculate  $L_{eff}$  and that the real beam is truncated. A curve for  $L_{eff}$  truncated will occur between the two curves shown in the figure. As a result, the curves define boundaries for excursions within which the true values of  $L_{eff}$  truncated will fall. These curves define the value of  $L_{eff}$  to about 20 percent in the worst case at 100 meters .

In addition to developing the curve for  $L_{eff}$  as a function of range, the beam profile was mapped for vertical and horizontal slices using 0.1 mm pin hole. Figures 8.3 and 8.4 show the beam profiles at the waist for a 10 meter focus. These figures do not show any unusual features. However, the data given in Table 8.1 show evidence of astigmatism.

Passive mapping of the beam profile was also made at 30 meters focal distance similarly to the 10 m data. No unusual features other than the presence of astigmatism were found in this data.

Figure 8.1

DOPPLER SHIFT AND BAND WIDTH VS. DISK SPEED

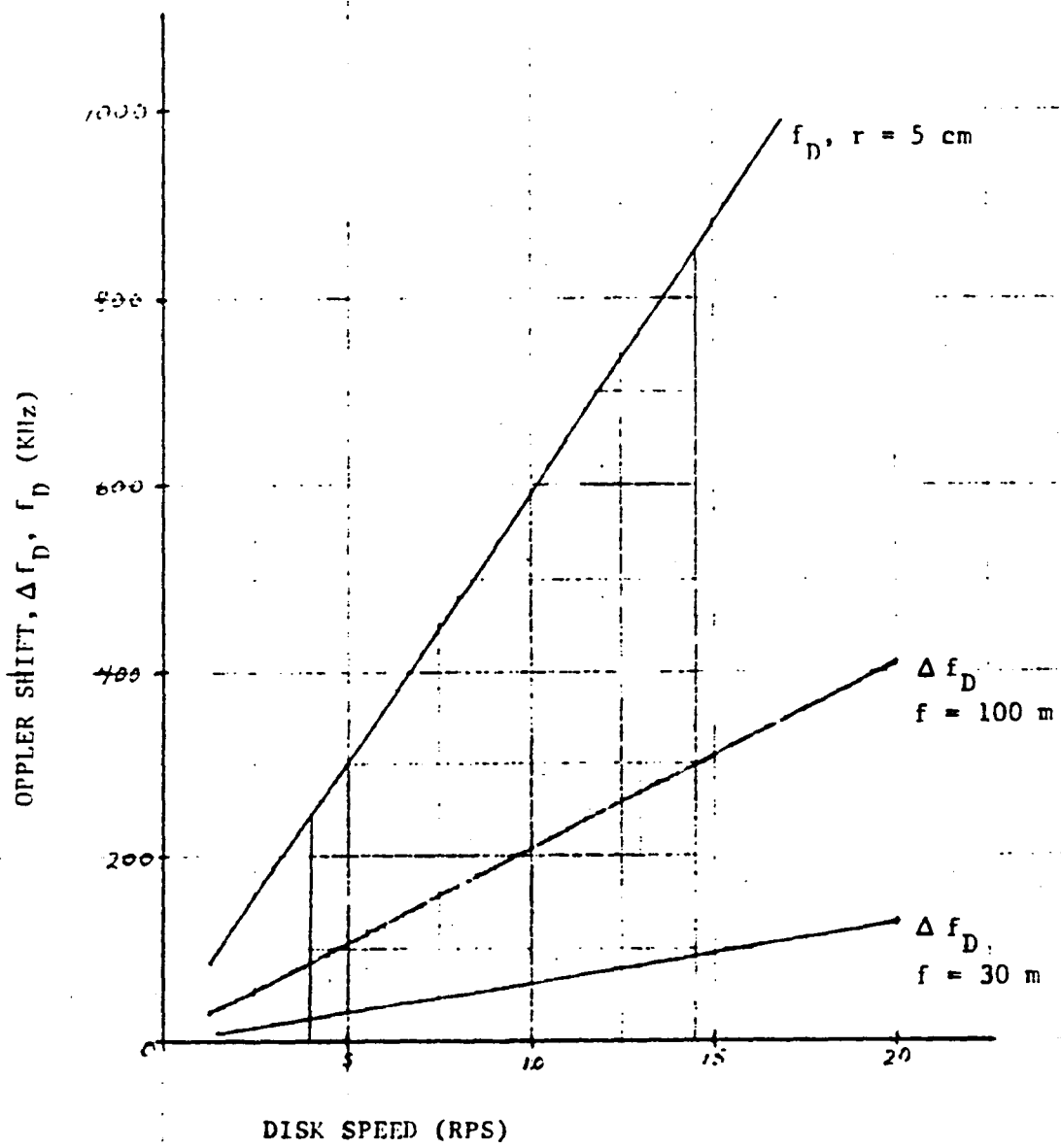


Figure 8.2  
 $L_{\text{eff}}$  as a Function of Range

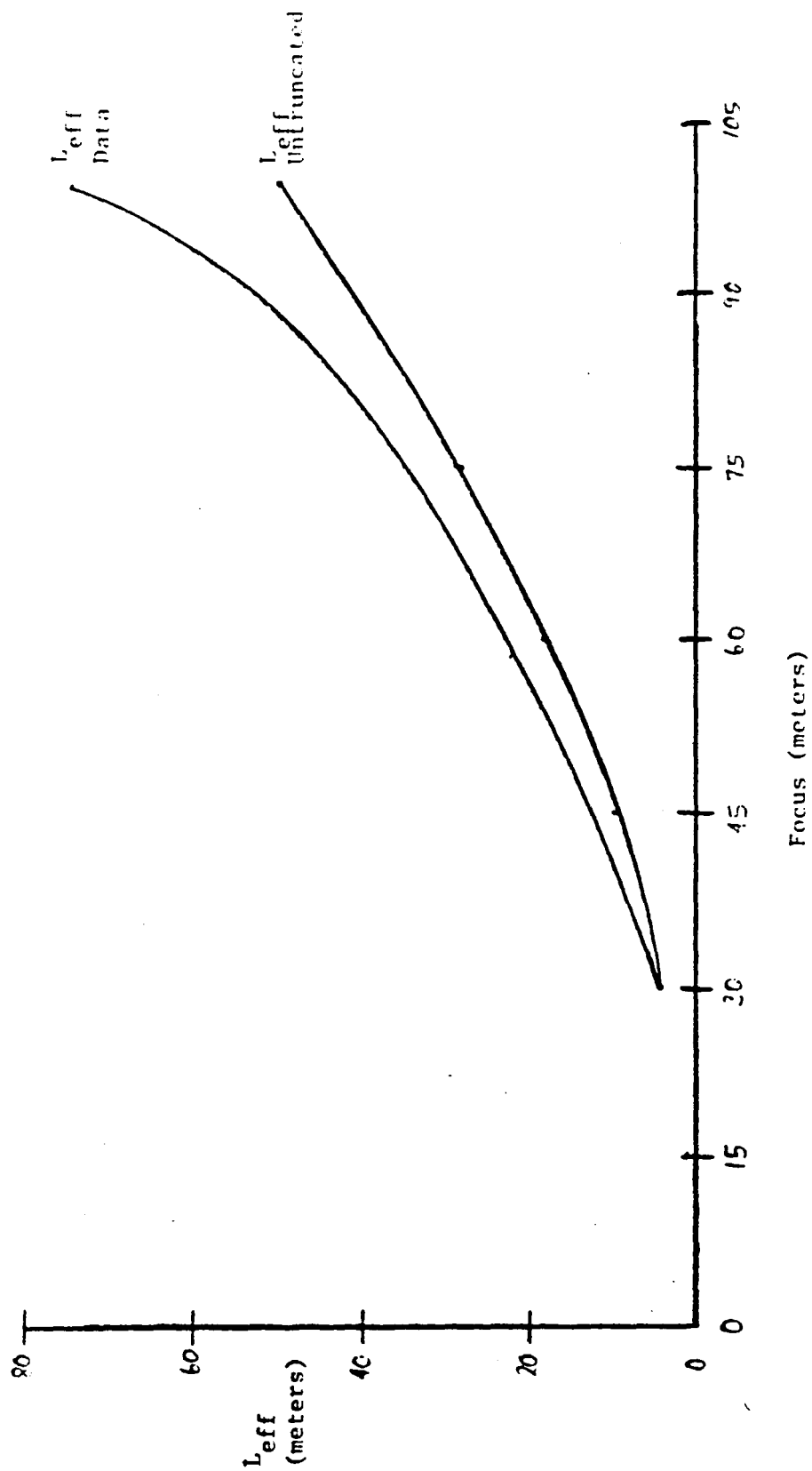


Figure 8.3

Horizontal Beam Profile at the Waist  
(10 Meter Focus)

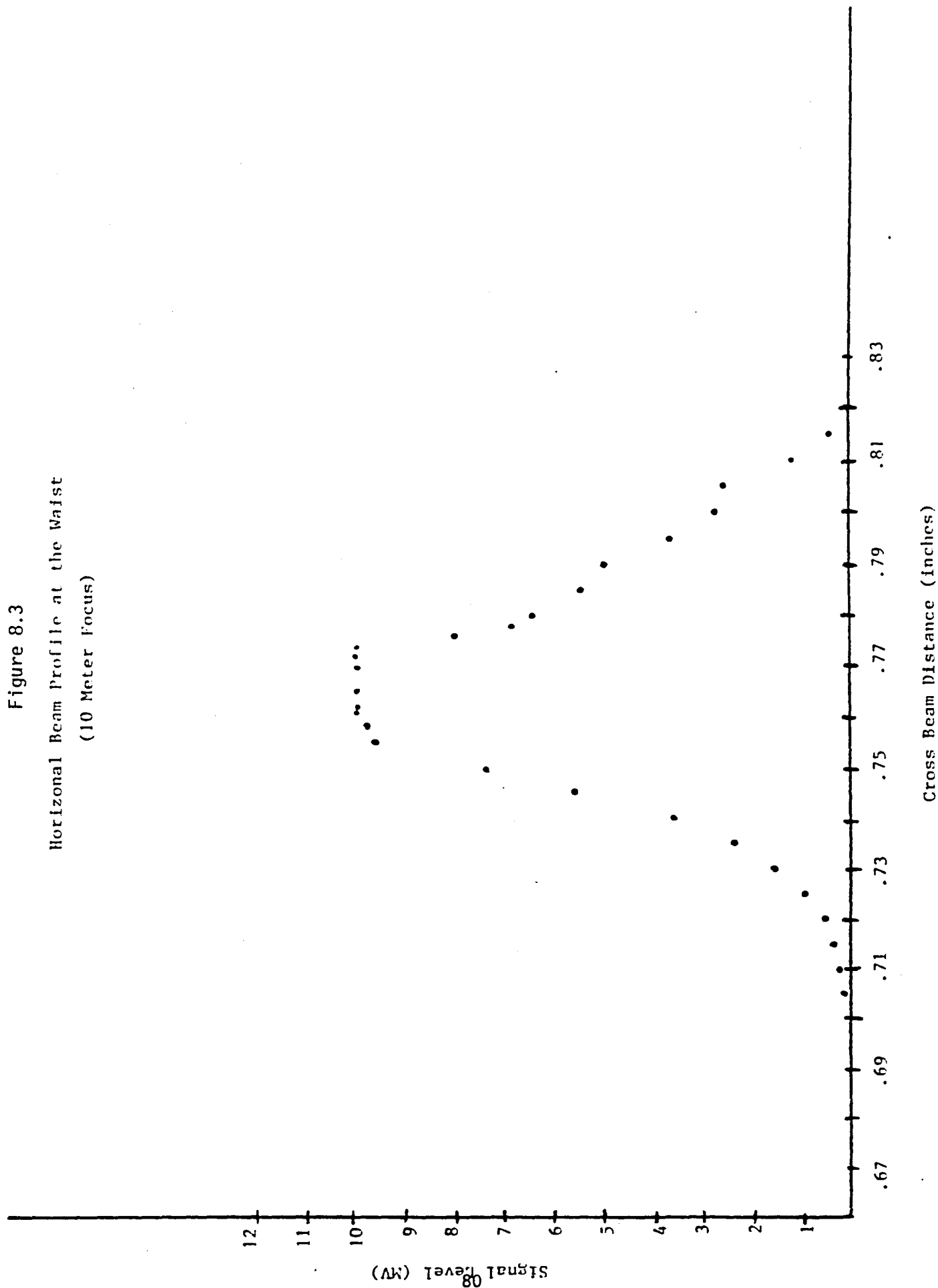


Figure 8.4

Vertical Beam Profile at the Waist

(10 Meter Focus)

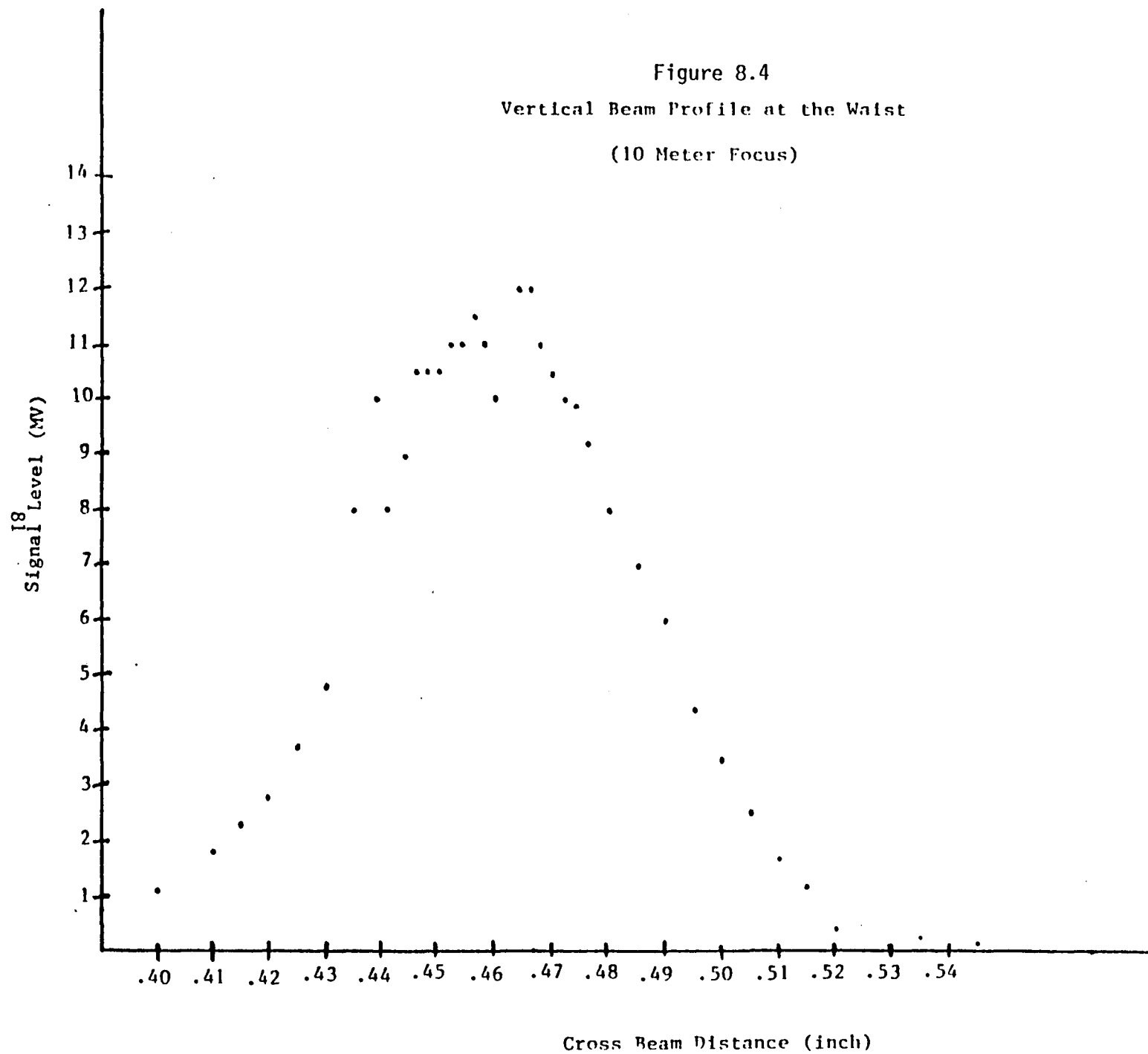




Table 8.1

Beam Width for Distances from Waist at 10 Focus m

Showing the Effects of Astigmatism

Position*	Vertical (inch)	Horizontal (inch)
16	.265	.287
17	.120	.195
18	.255	.150
19	.330	.185

\* Waist = 16 feet on the optical bench.  
The height of the beam is smallest at 17 feet a foot earlier than the narrowest width of the beam at 18 feet.

#### 10. Task 9: Calibration Using the Spinning Wire

Data for the determination of beta in the single particle mode will consist of histograms of peak signal values. Such peak signal values will occur as the particle crosses the vertical central plane of the focal volume parallel to the beam. In calibrating the focal volume, sensitivity contours within this plane must be determined. These contours are approximately elliptical figures, each defined by a constant value of the backscatter signal to cross-section ratio,  $s/\sigma$ . Therefore, mapping the intensity contours of this region by probing with a constant  $\sigma$  probe provides a determination of the sensitivity contours.

This mapping is accomplished with a rotating wire, and therefore, only specifies the  $s/\sigma$  ratio up to a constant factor, since we do not claim to know  $\sigma$  for the wire. (The wire is assumed to have the same "effective  $\sigma$ " for each measured signal value). In order to understand the beam profile, contour plots can be made by taking data on transverse beam cross-sections. Then a subset of the same data can be used to obtain contour plots in the plane of interest.

## Calibration Procedure:

The following procedure is recommended as a first try at recording data adequate for contour plotting. It is very likely that attempts to process this data will require revisions in this procedure.

- 1) The spinning wire should be configured so that the plane of rotation is parallel to the beam, intersecting the beam above the axis of rotation.
- 2) The rotation plane should be moved through the beam in at least nine equal discrete steps with the fifth step being the beam misplane. Care should be taken to avoid backlash error. Steps 1 and 9 should be near signal-loss positions.
- 3) Data should be recorded at each step as the wire passes through the vertical position, covering an angle of not more than about 30 degrees. This data should include the speed of rotation of the wire.
- 4) A single test case should be obtained, consisting of many spectra from the same wire position to investigate the effects of noise. If significant noise is found, several samples from each wire position will have to be averaged for the entire data set.

- 5) If possible, the same rotation speed of the wire should be used for each data set to avoid data processing problems.
- 6) A set of data files for each cross section should be recorded from beam waist to signal loss in each direction, utilizing at least 9 cross-sections as an initial trial.
- 7) Recording of data in files indicating X and Z coordinates where X stands for wire position and Z for beam cross-section, from 1 to 9 would be very helpful in processing.
- 8) Initial trial should be at 20 meters. Two subsequent calibrations should be made at other ranges to be determined.
- 9) Software to process these data will have to register these data with respect to the beam axis, may have to average and interpolate data values, and will have to make contour plots. These plots will be used (integrated) to determine an area versus  $s/\sigma$  graph for input into the single particle processing algorithm. The location of this curve along the  $s/\sigma$  will have to be determined by absolute calibration methods involving the single particle generator.

## Calibration Results:

Ten sets of data were taken at a focus of 10 to 20 meters, respectively. The ten sets corresponded in both cases to from 1.0 meters in front of focus to 1.25 meters behind focus in steps of .25 meters. Backscatter signal was tabulated as a function of time as a wire (spinning on a wheel) penetrated the central focal area. Five time sets were taken at each position to minimize noise. The Fourier transform of each time set was calculated and then averaged to obtain one Fourier transform for each position in front of or behind the focus. Each Fourier transform then contains the information of backscattered signal versus height in the beam. This is true because each frequency of the Fourier transform corresponds to a distinct point in the laser beam focal volume (at this range).

The method briefly described above is contained in Intergraph Corporation report 81-006 entitled, "Measurement System Design Study - Final Report (11 Jan. 1982)".

Figures 9.1-9.10 show the Fourier transform at each longitudinal position for the 10 meter focus data and Figures 9.11-9.20 show the corresponding transforms for the 20 meter focus data. In the figures shown, a 9 point data smoothing was employed to produce smoother plots. This data

smoothing did not appreciably change the features of the Fourier transforms, however, made data handling somewhat easier.

Using 300 frequency bins about the center of each Fourier transform data set (i.e., each of the 10 range positions), contour plots of signal as a function of longitudinal position and vertical position (i.e., frequency bin) were calculated. Figure 9.21 is a linear contour plot of the 10 meter focus data while Figure 9.22 is a logarithmic contour plot of the same data. Figures 9.23 and 9.24 are contour plots of the 20 meter focus data.

The 20 meter data is not ideal since the Fourier transform at some longitudinal positions is not complete. For this reason, the contour plots become unrealistic as the contour values decrease.

Using these contour plots, area as a function of  $s/\sigma$  can be tabulated. This is done by integrating the area within a contour of a particular value. Figure 9.25 shows a plot of area versus  $s/\sigma$  for the 10 meter and 20 meter focus data. The 20 meter data is more limited than the 10 meter data because of the previously mentioned problem. Also it should be noted that the data in both the 10 or 20 meter cases can be extended if data is taken from signal acquisition to signal loss along the longitudinal axis. The  $s/\sigma$  scale on

the horizontal axis is arbitrary as shown, the relative shape and spacing of the curves being the only important characteristics. Data from the single particle aerosol generator (see ARI Monthly Progress Report Number 9) is needed in order to establish absolutely the position on the  $s/\sigma$  axis where the "areas" begin. Noise is assumed to be a constant factor in Figure 9.25.

#### Calibration Software:

The software necessary for transferring these data to the Sigma 5 computer for analysis was developed.

Two software routines were written for this project, and their documentation appear after the figures at the end of this task description. They are

- A routine to collect wire wheel data and transfer to Sigma V.
- A routine to simulate the remote terminal.

The wire wheel routine reads data sampled by the Biomation Digitizer in sets of 2048 data points from one pass of the wire through the beam. Up to 20 such sets can be collected before being sent to the Sigma V. The data is sent in ASCII format and as much may be placed in Sigma V file as desired.

This software has been developed to facilitate data processing.

The remote terminal routine will allow communication to Sigma V from the test site. This routine will provide an easy means to verify the data transfer, process the data and determine the status of the Sigma in the case of transfer difficulty. Both routines have been successfully checked out using test cases.

Additional software has been written to accomplish contour plotting of the focal volume profile from the wire wheel data. Following the previously mentioned documentation is a listing of a program which reads the data from a Sigma 5 file and plot the contours. Following this listing is a contour plot of a test case sphere made with the contour plot subroutine, using data generated by a separate program.



10 METER FOCUS

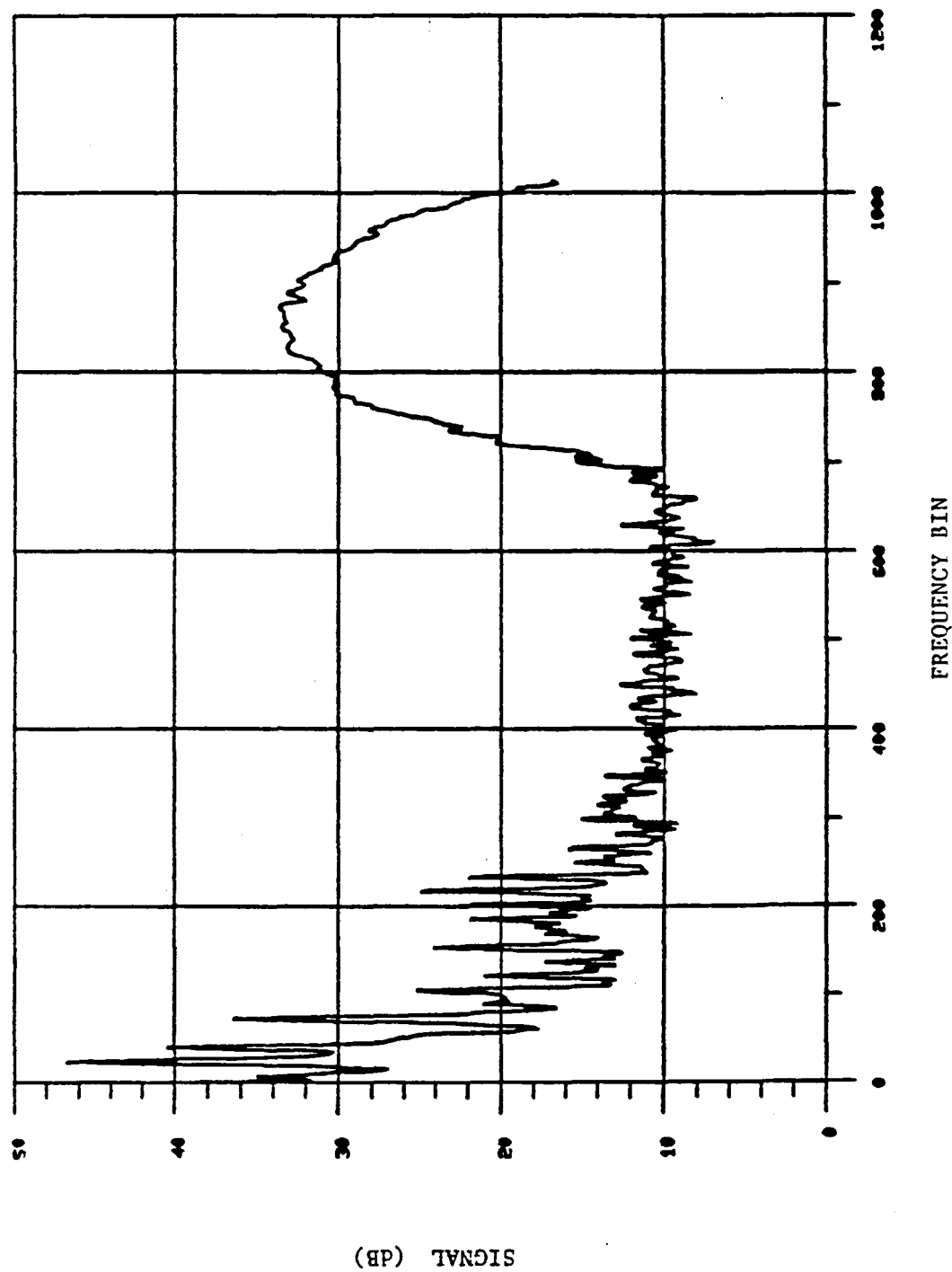
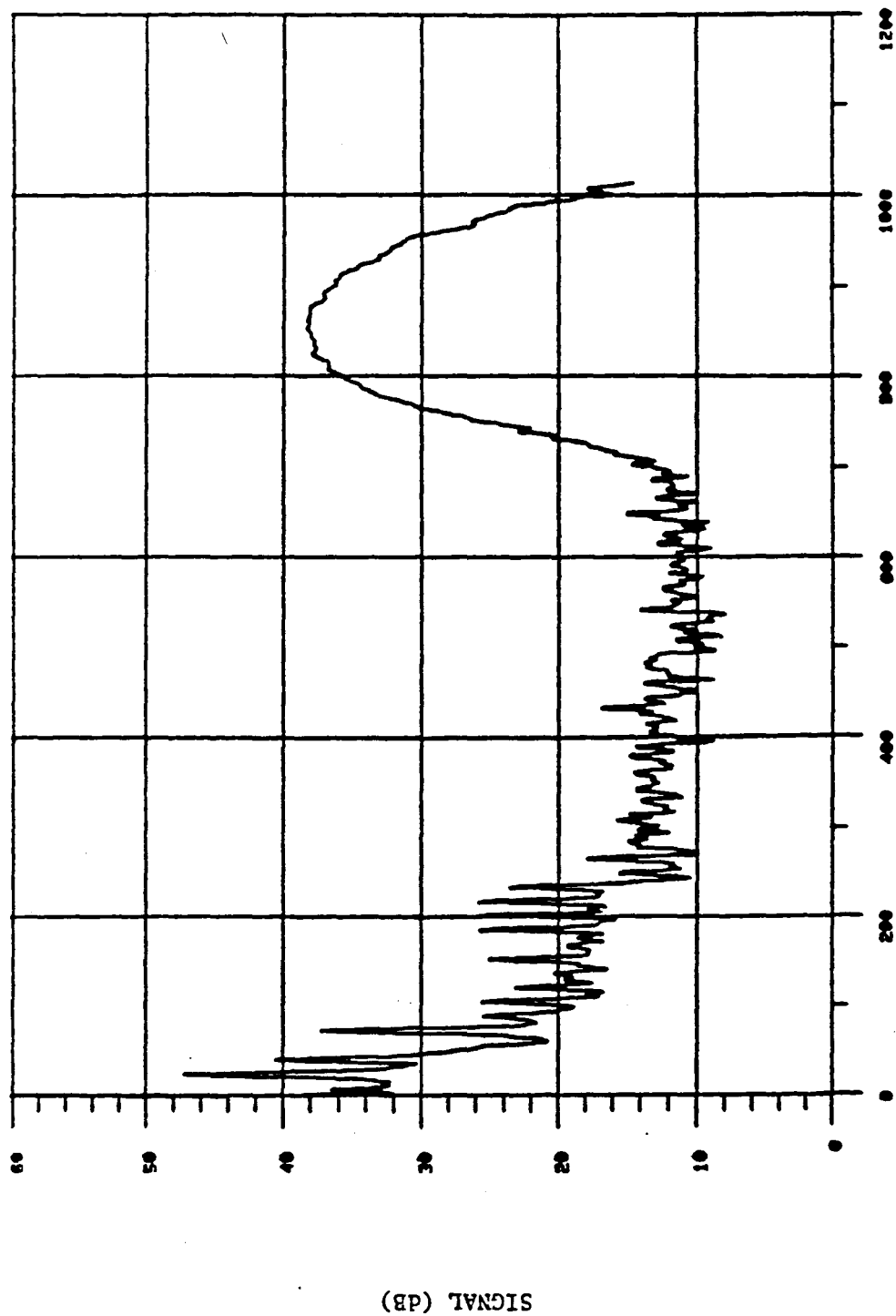


Fig. 9.1. 1.25 METER BEHIND FOCUS

10 METER FOCUS



FREQUENCY BIN

Fig. 9.2. 1.0 METER BEHIND FOCUS

# 10 METER FOCUS

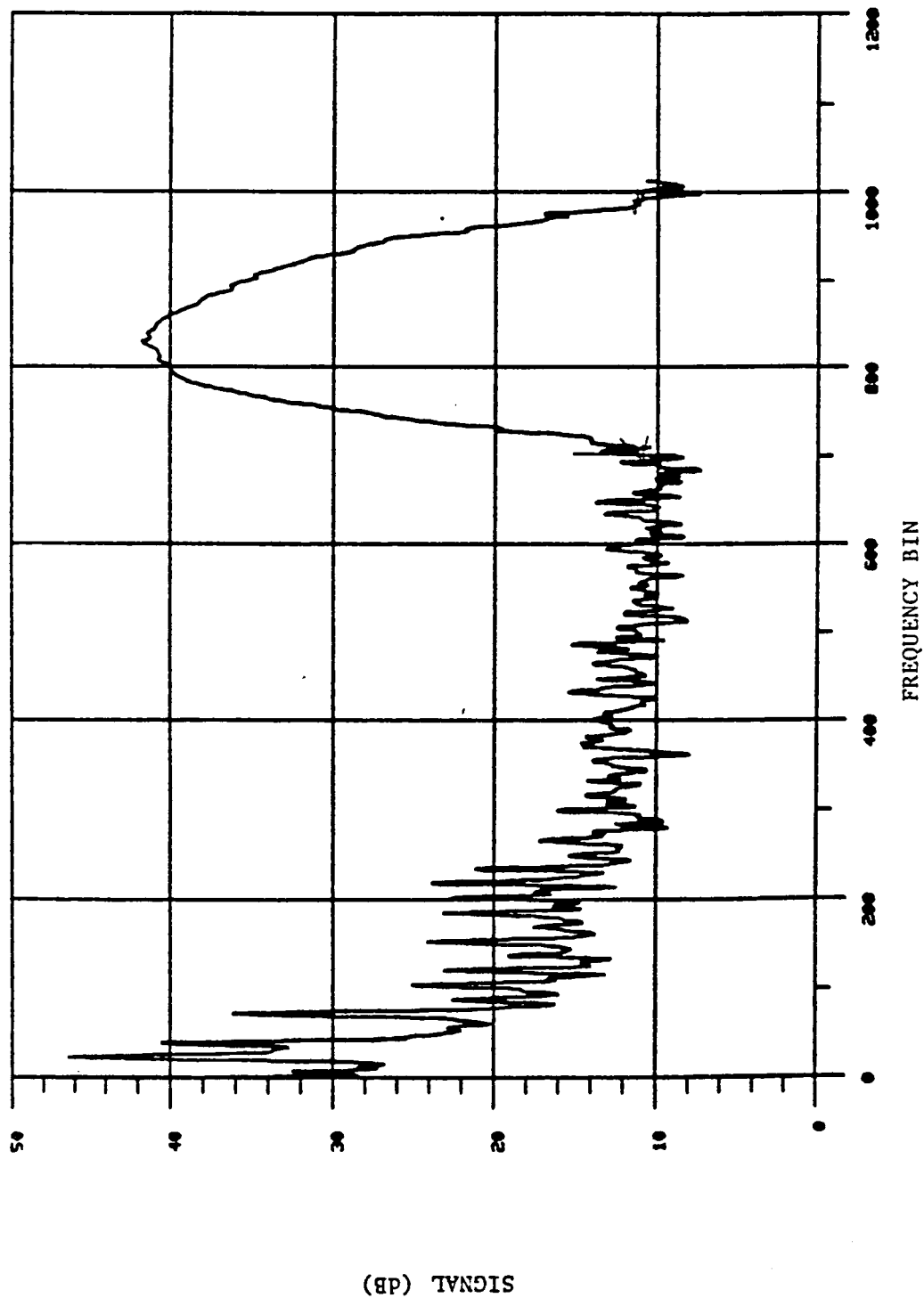


Fig. 9.3. .75 METER BEHIND FOCUS

10 METER FOCUS

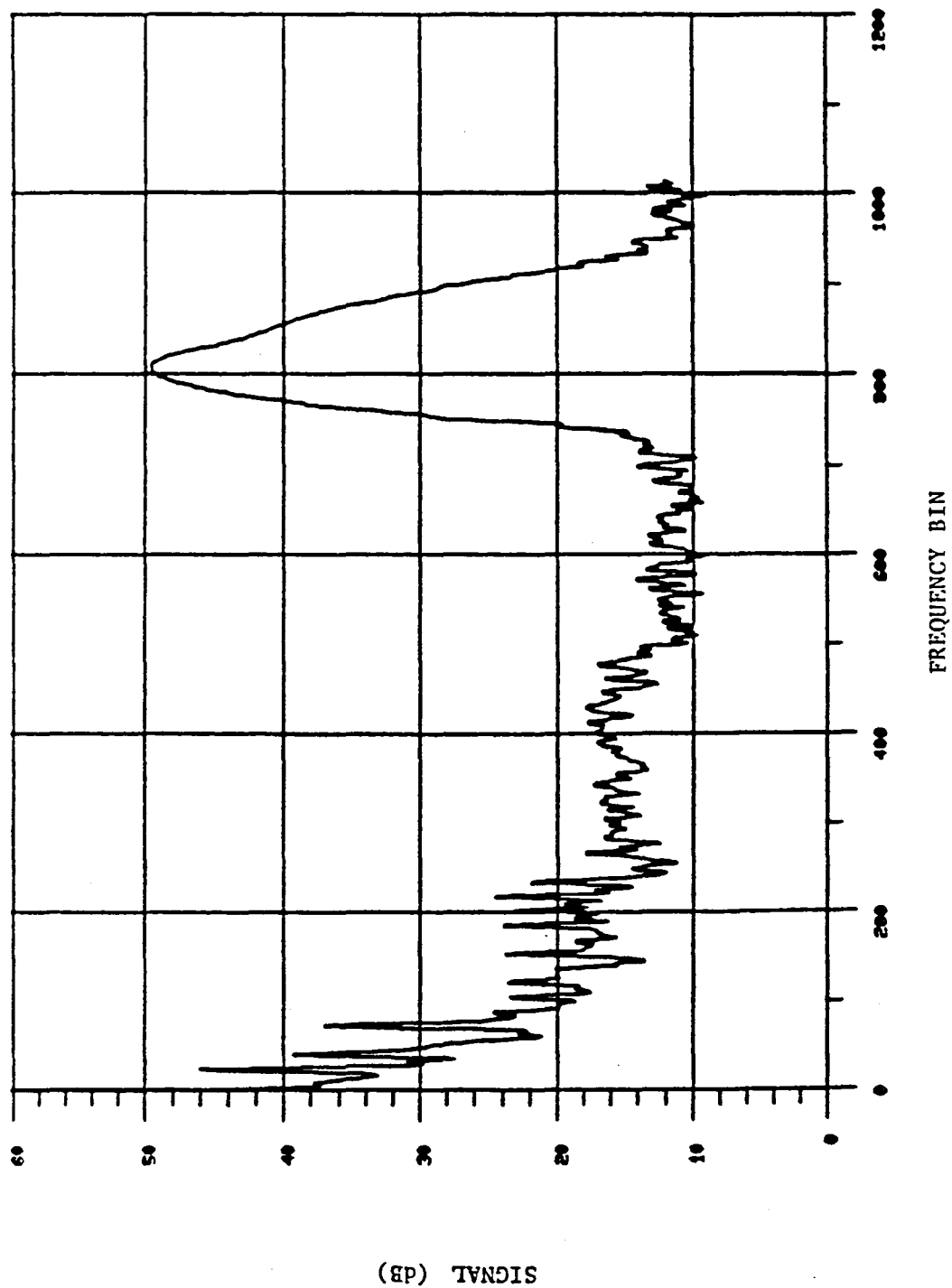


Fig. 9.4. .5 METER BEHIND FOCUS

# 10 METER FOCUS

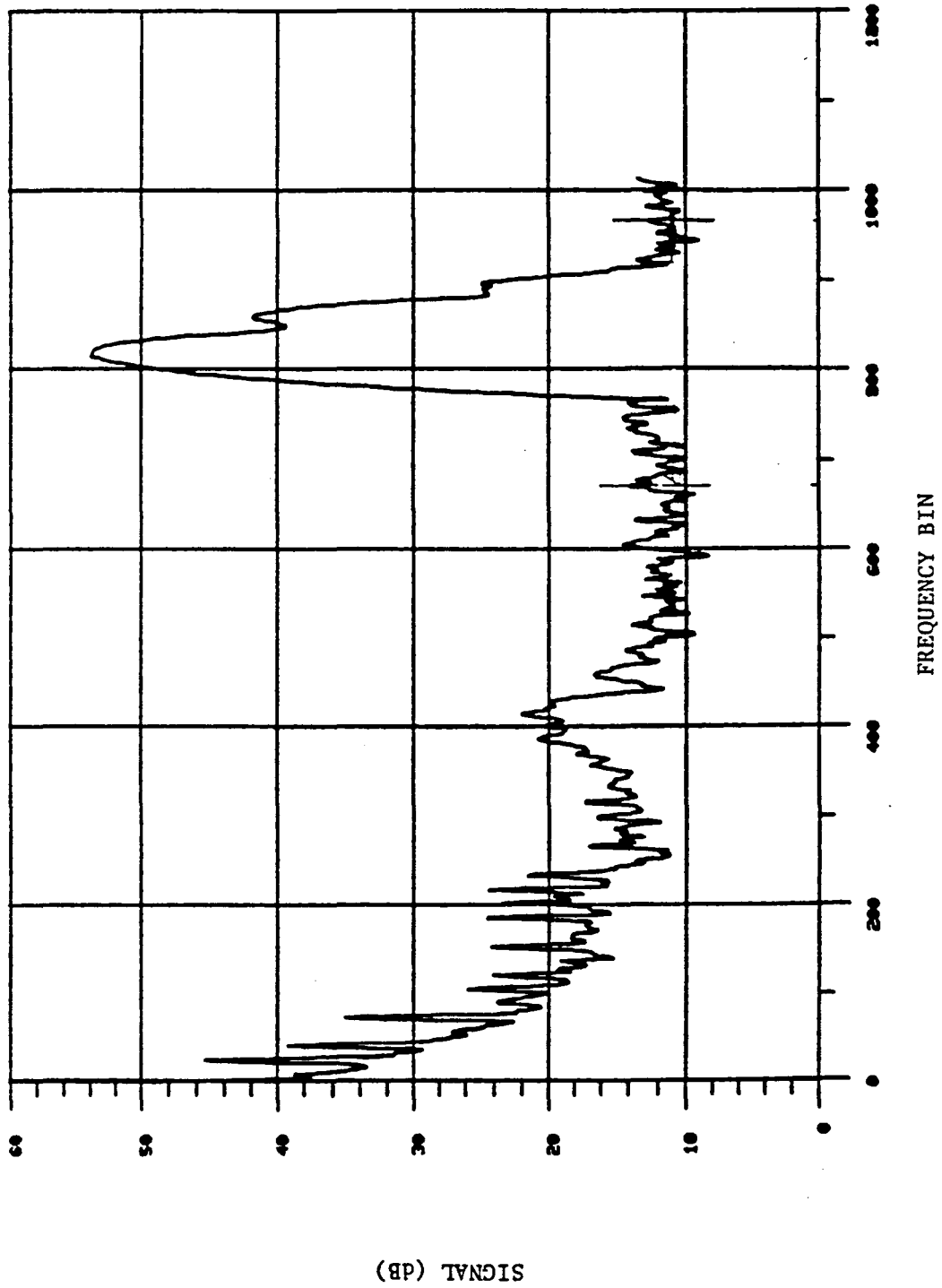


Fig. 9.5. .25 METER BEHIND FOCUS

10 METER FOCUS

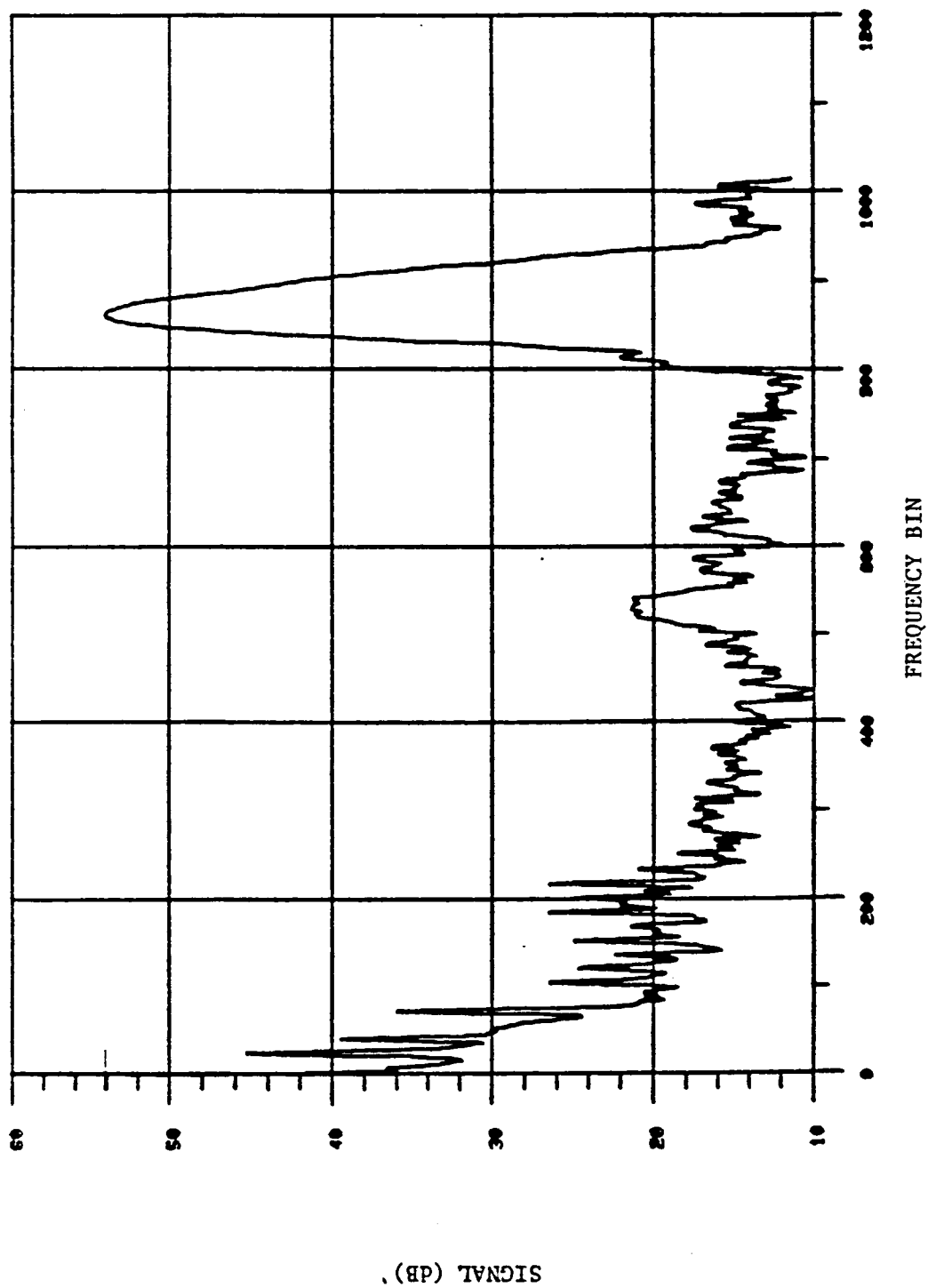


Fig. 9.6. FOCUS

10 METER FOCUS

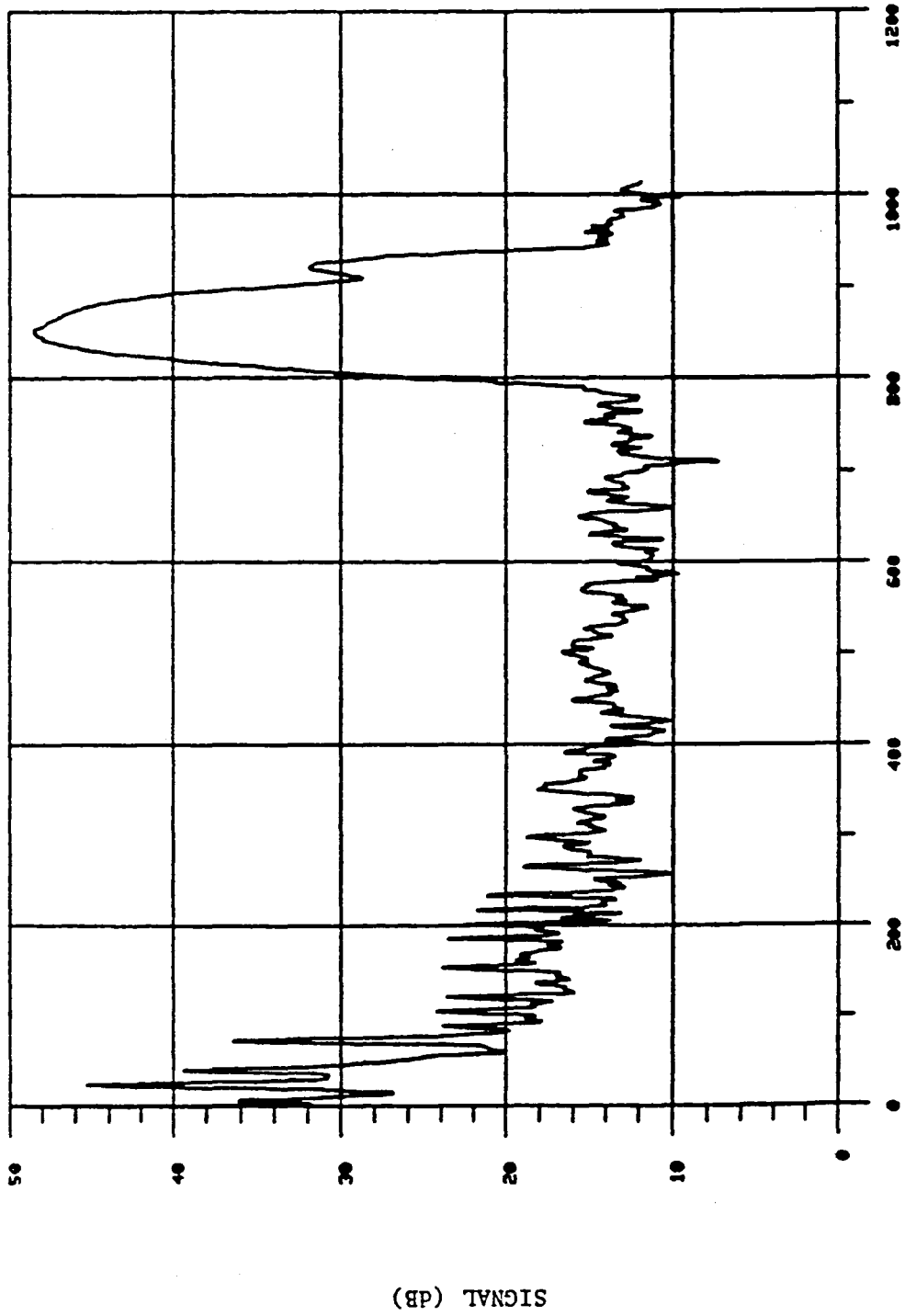


Fig. 9.7. .25 METER IN FRONT OF FOCUS

10 METER FOCUS

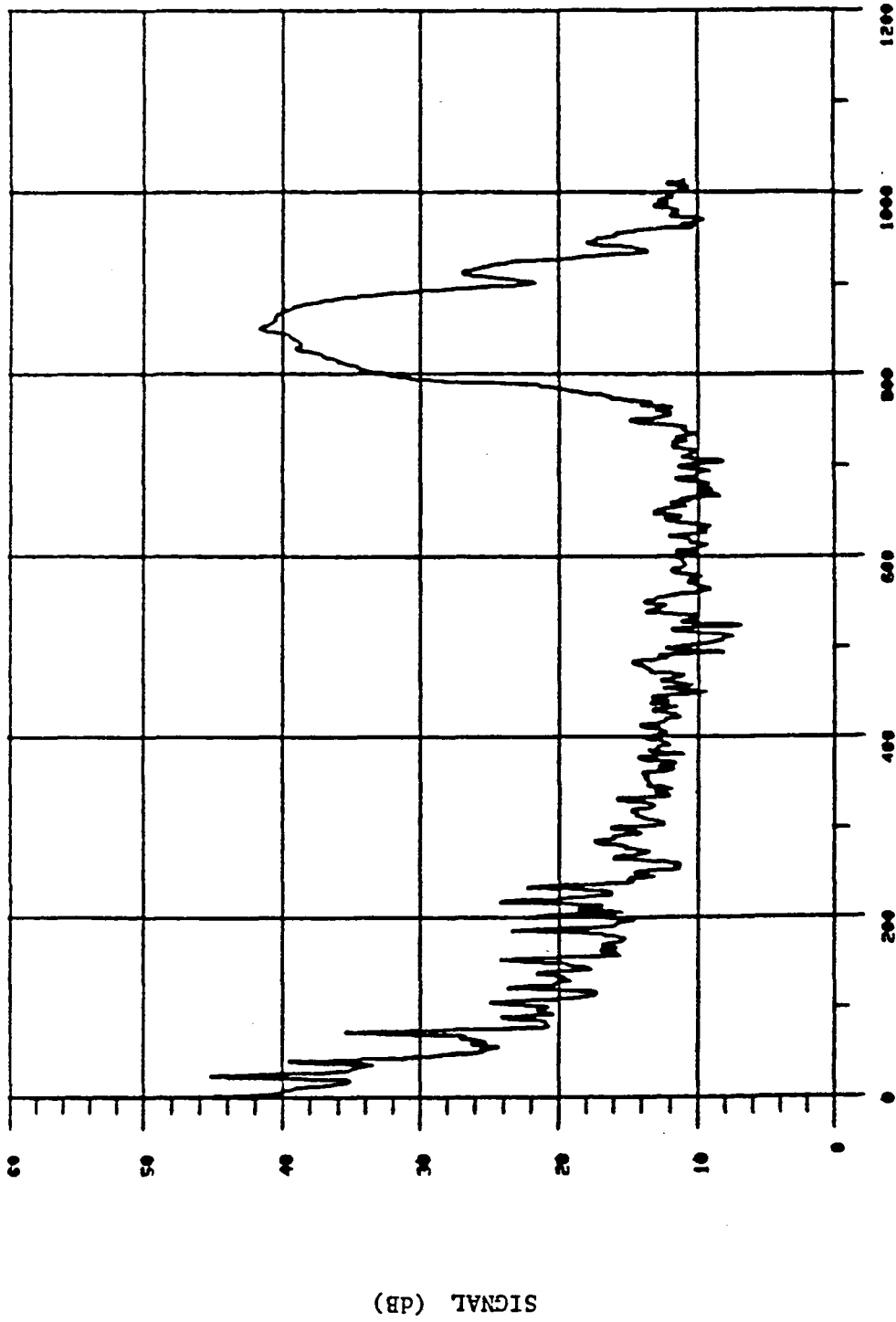


Fig. 9.8. .5 METER IN FRONT OF FOCUS



# 10 METER FOCUS

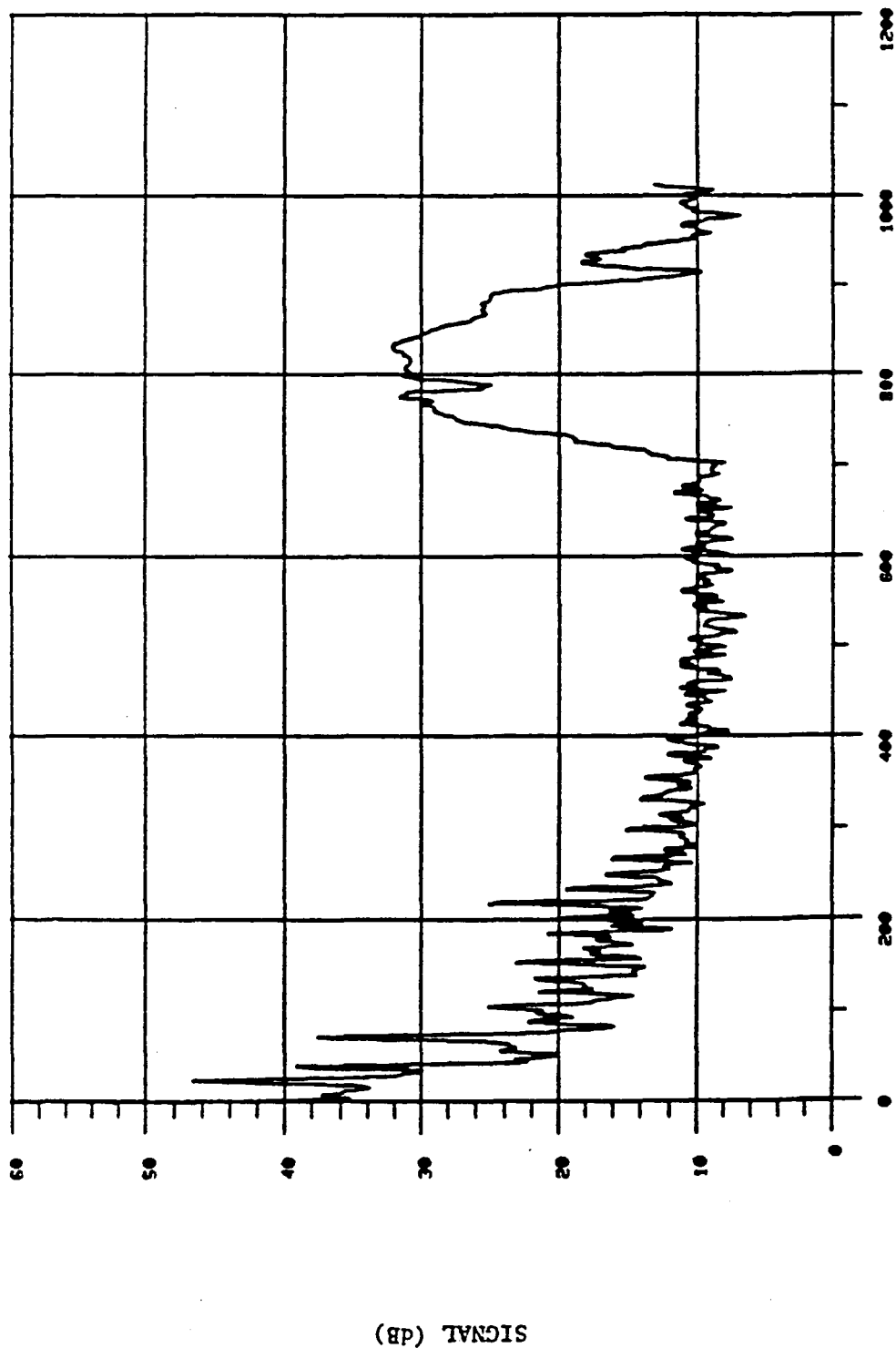


Fig. 9.9. .75 METER IN FRONT OF FOCUS

# 10 METER FOCUS

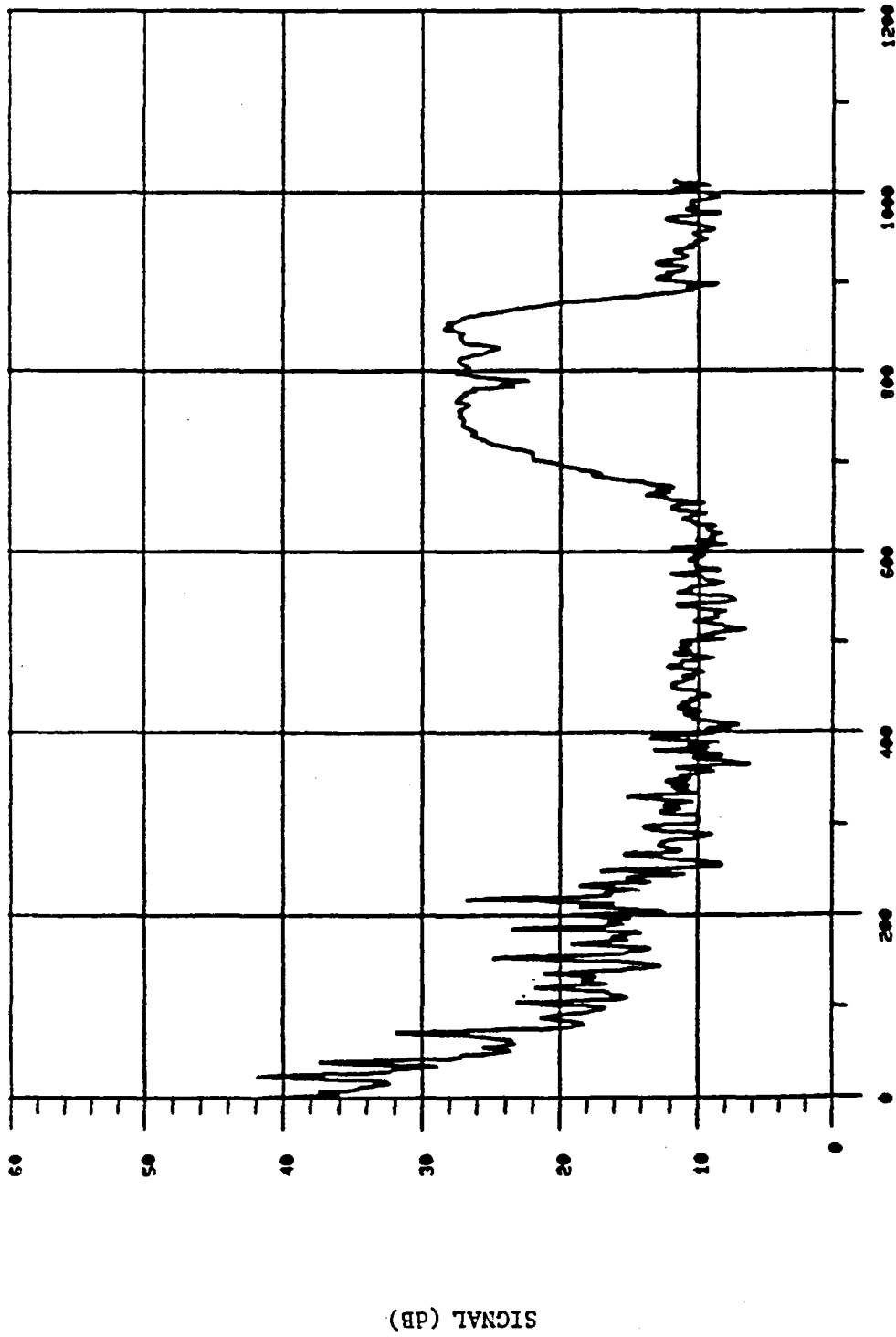


Fig. 9.10. 1.0 METER IN FRONT OF FOCUS

20 METER FOCUS

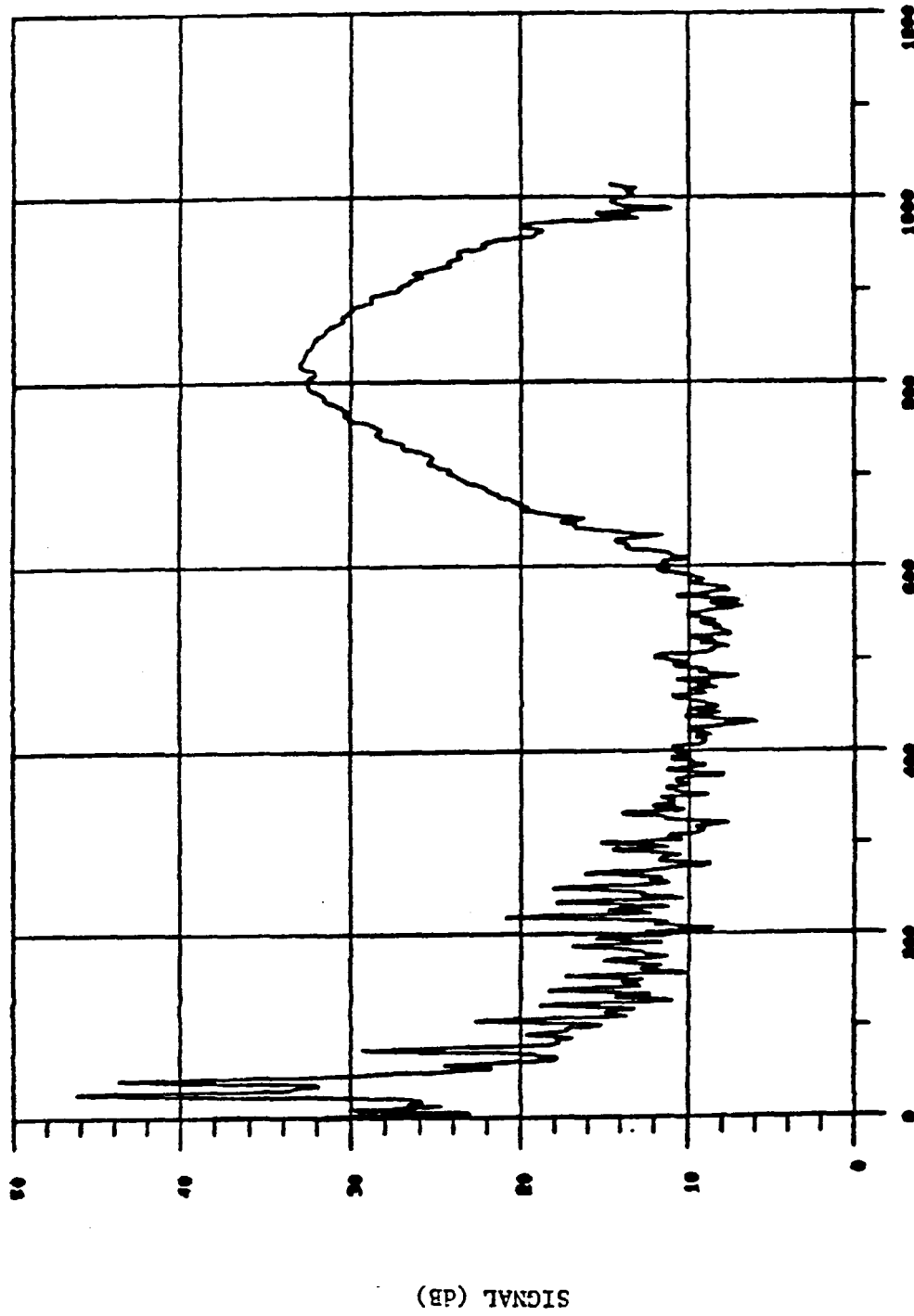
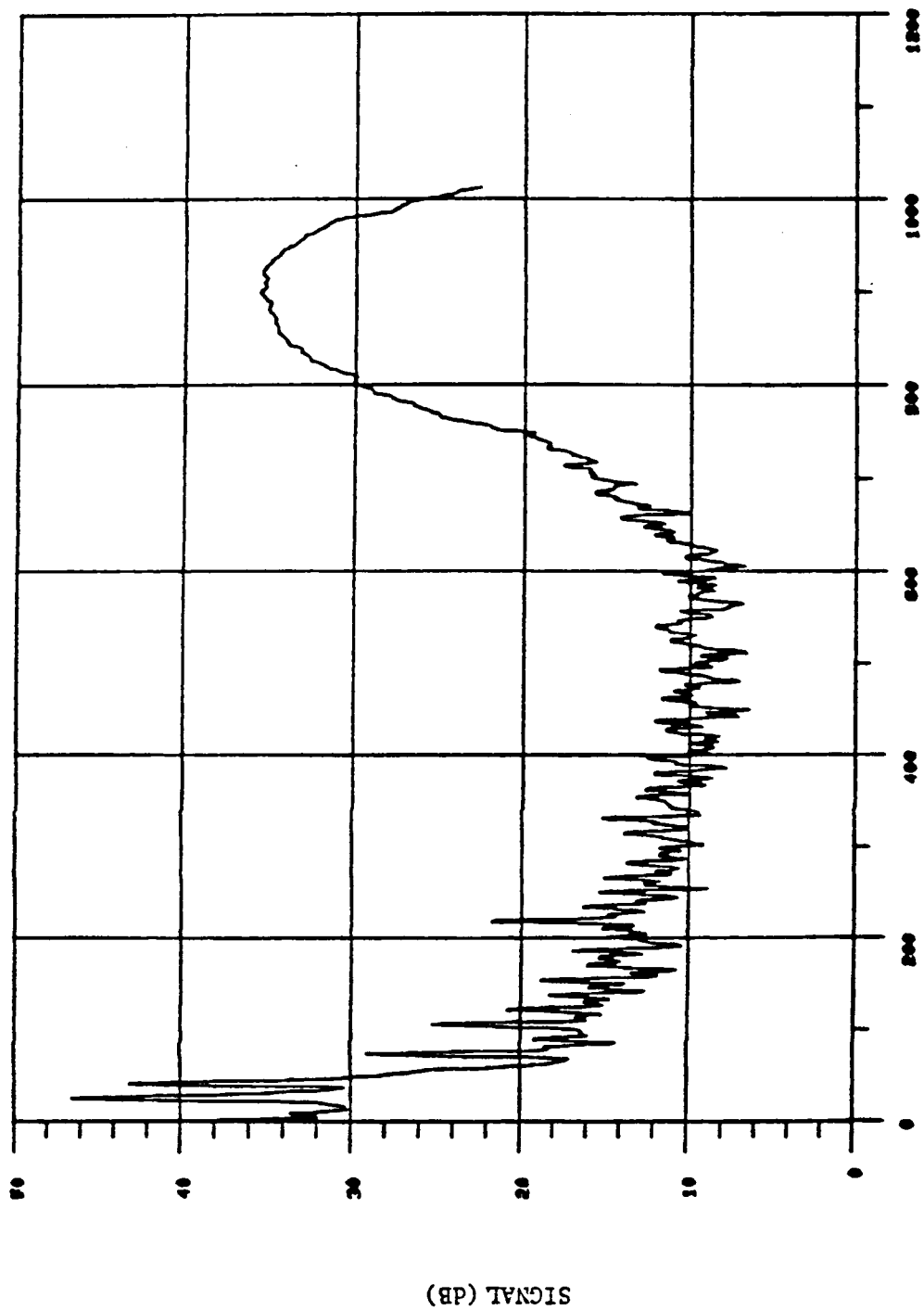


Fig. 9.11. 2.5 METER BEHIND FOCUS

# 20 METER FOCUS



FREQUENCY BIN

Fig. 9.12. 2.0 METER BEHIND FOCUS

20 METER FOCUS

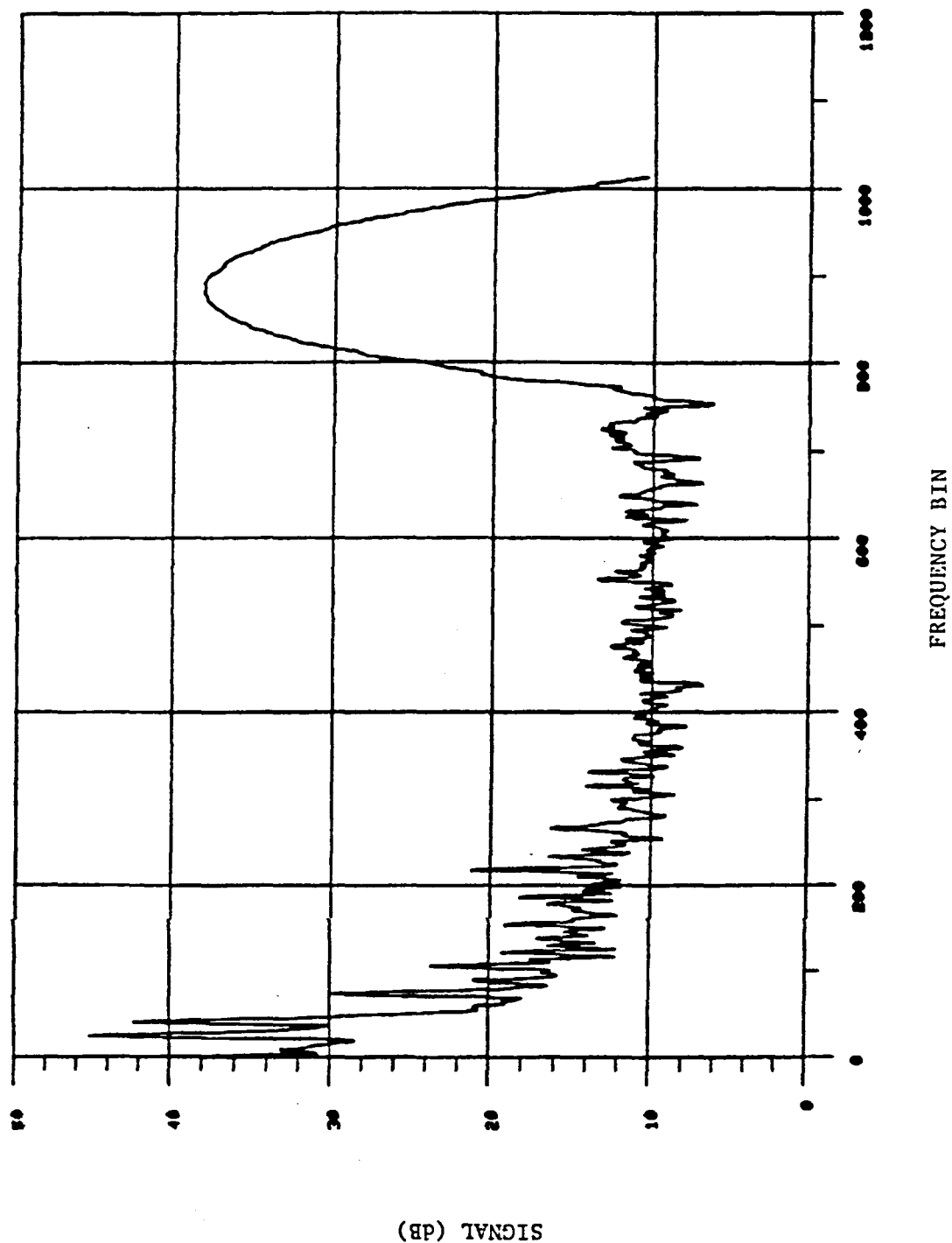


Fig. 9.13 1.5 METER BEHIND FOCUS

20 METER FOCUS

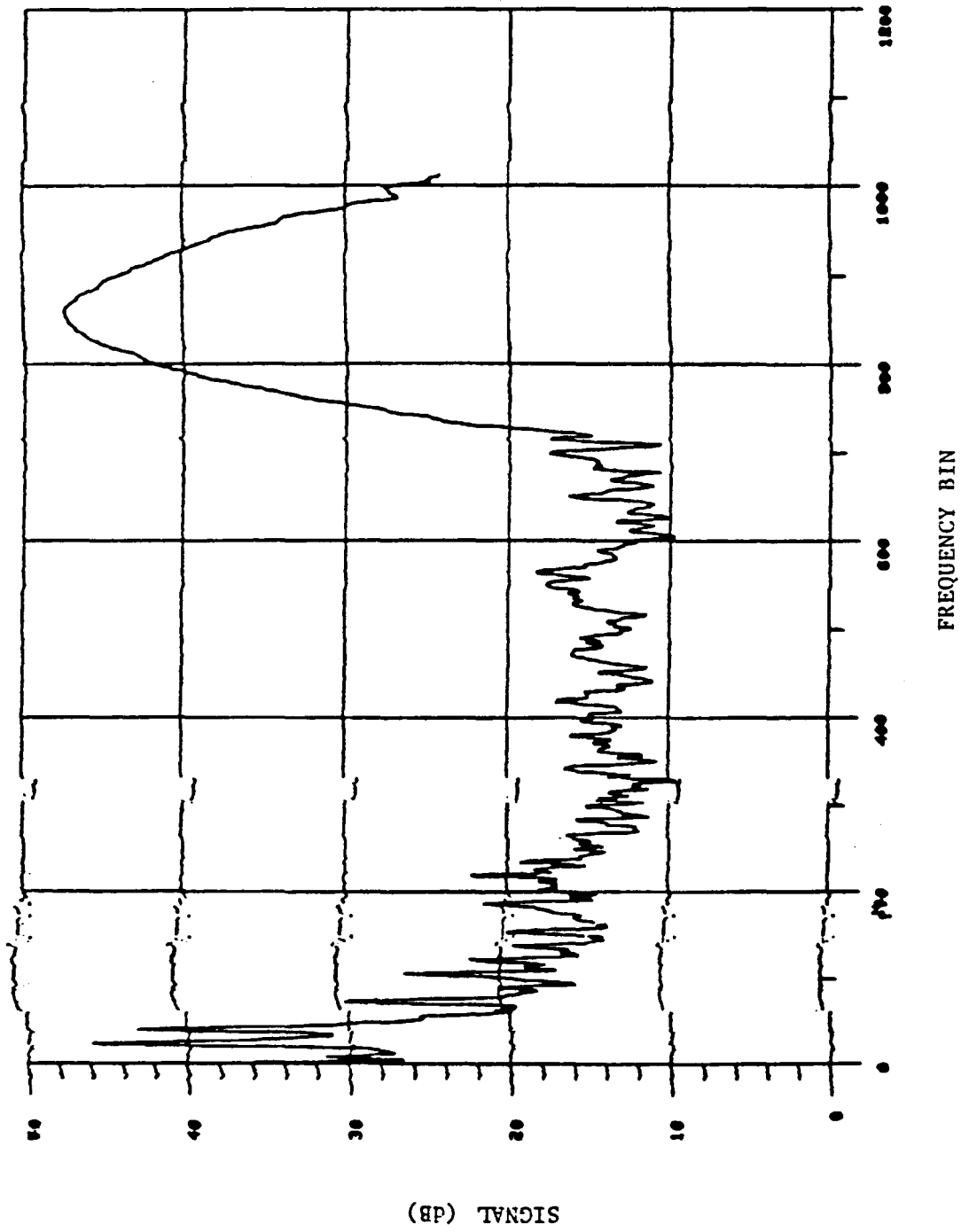


Fig. 9.14 . 1.0 METER BEHIND FOCUS

# 20 METER FOCUS

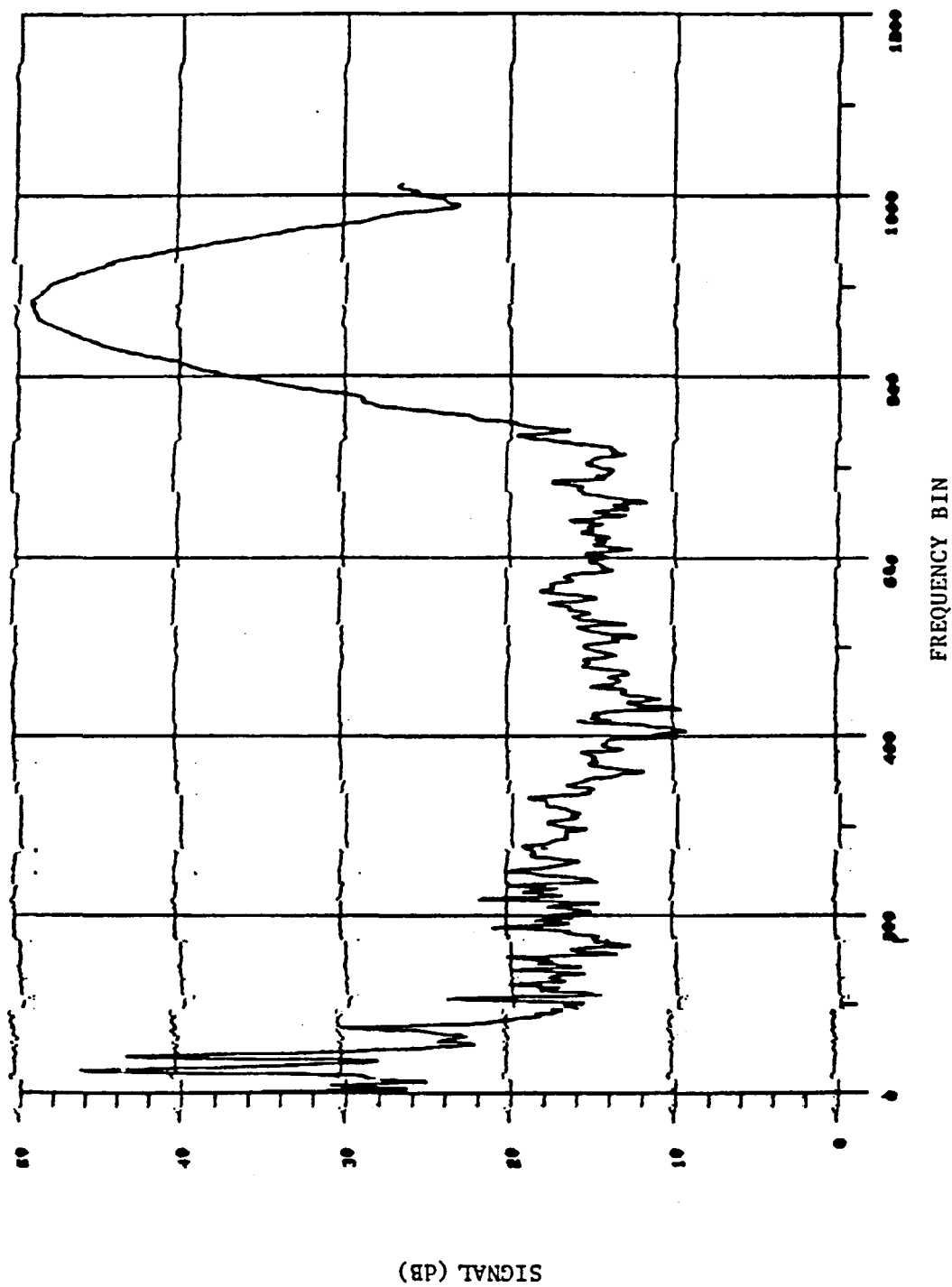
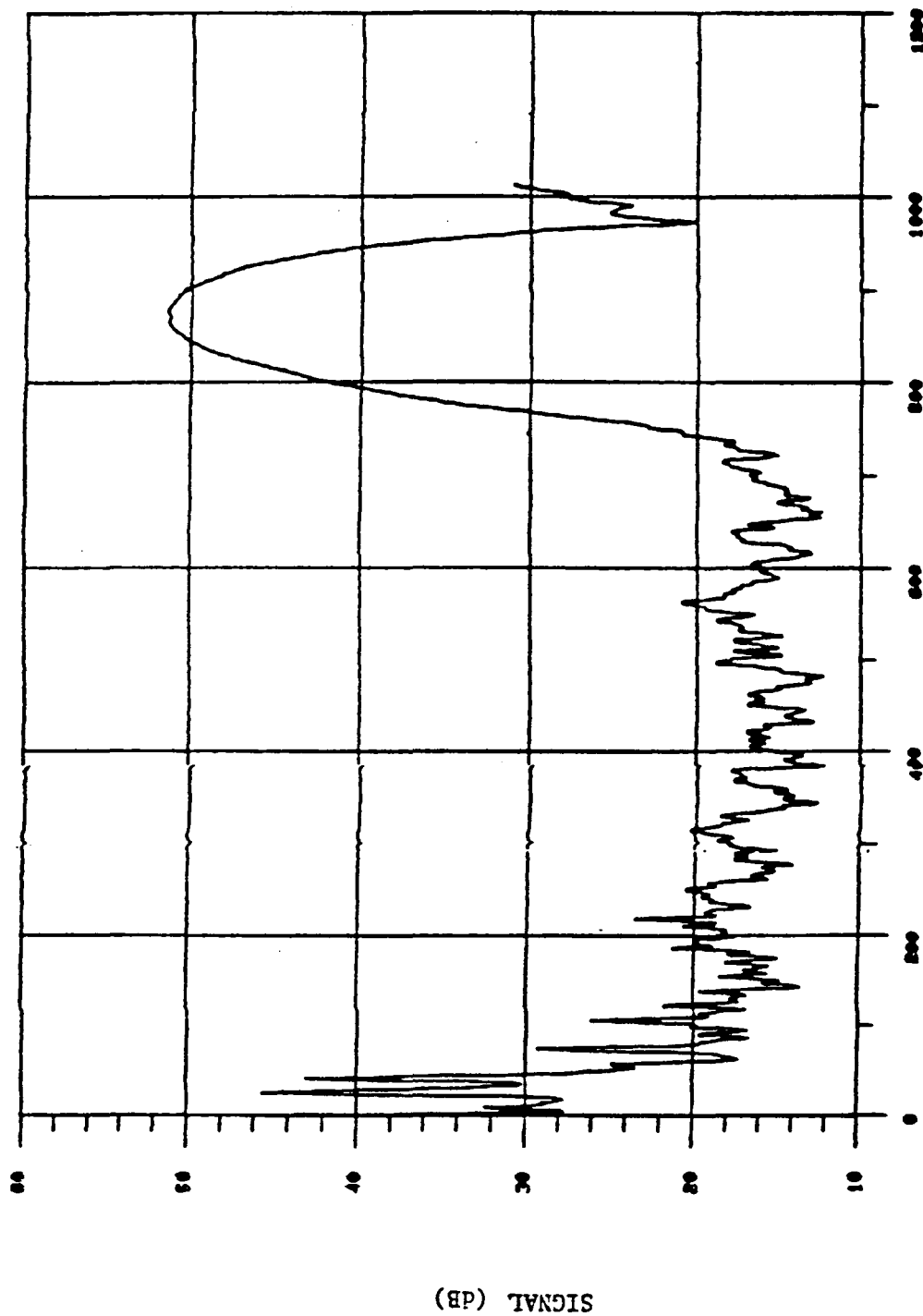


Fig. 9.15. .5 METER BEHIND FOCUS

20 METER FOCUS



FREQUENCY BIN

Fig. 9.16. FOCUS



20 METER FOCUS

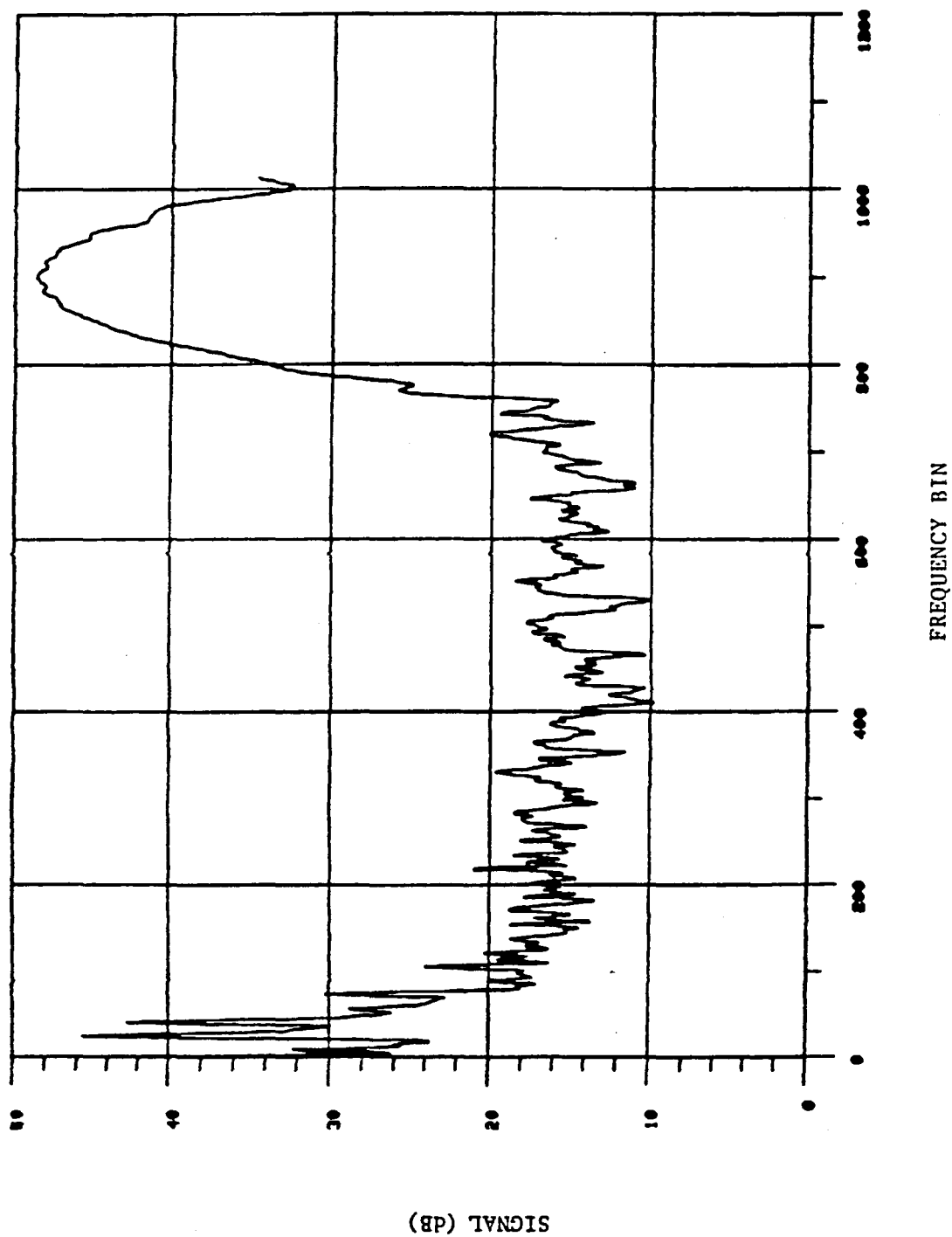


Fig. 9.17. .5 METER IN FRONT OF FOCUS

20 METER FOCUS

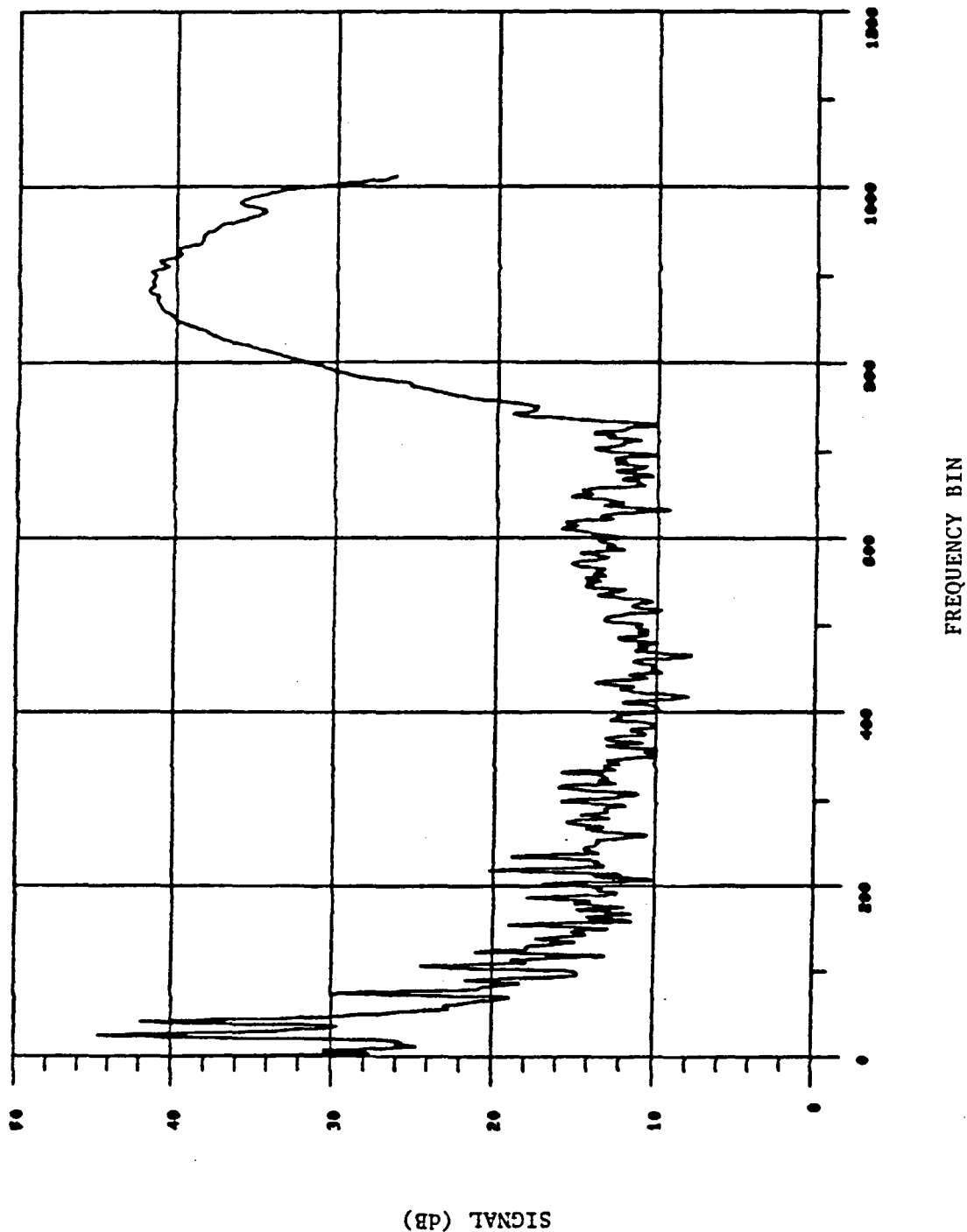
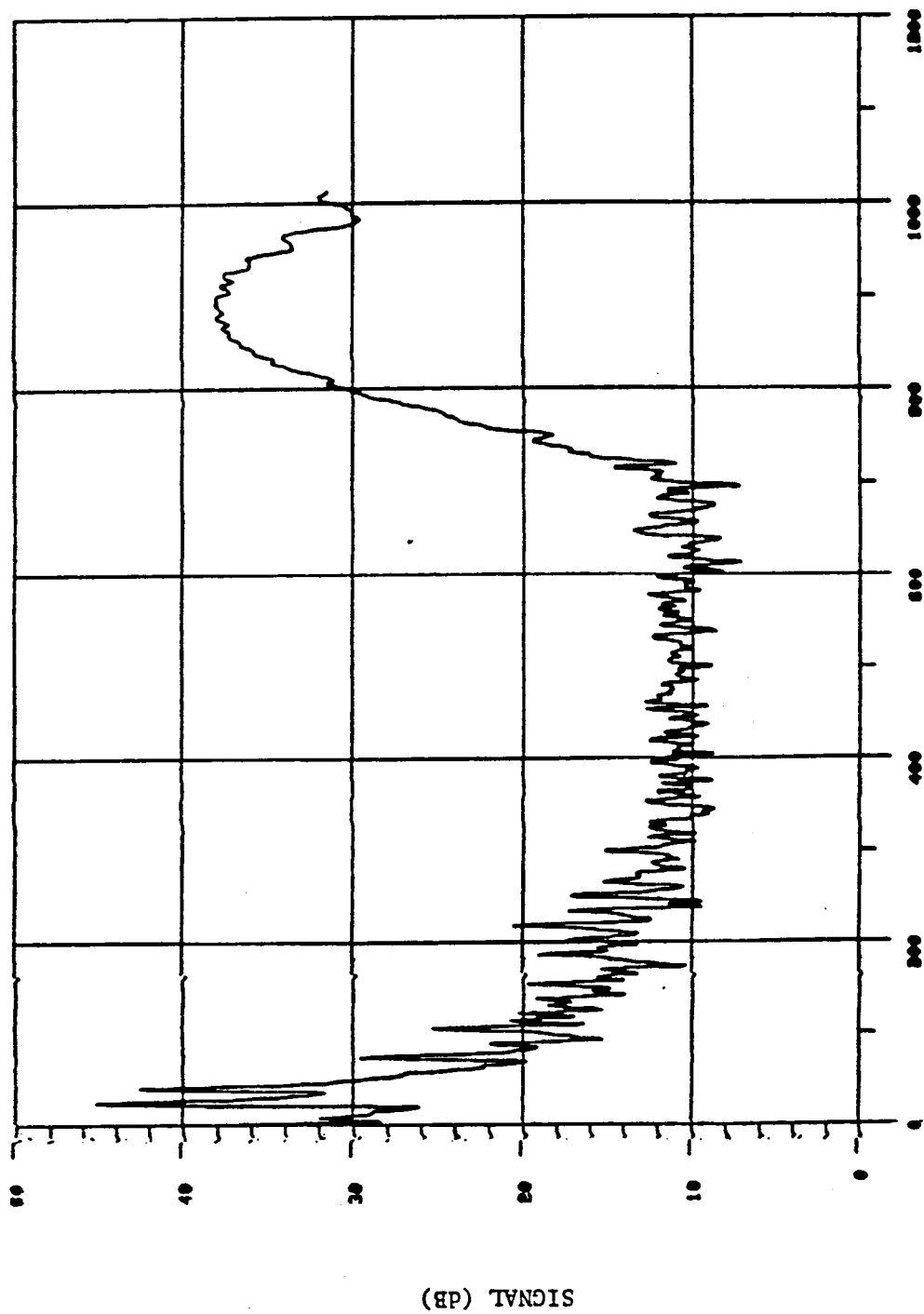


Fig. 9.18. 1.0 METER IN FRONT OF FOCUS

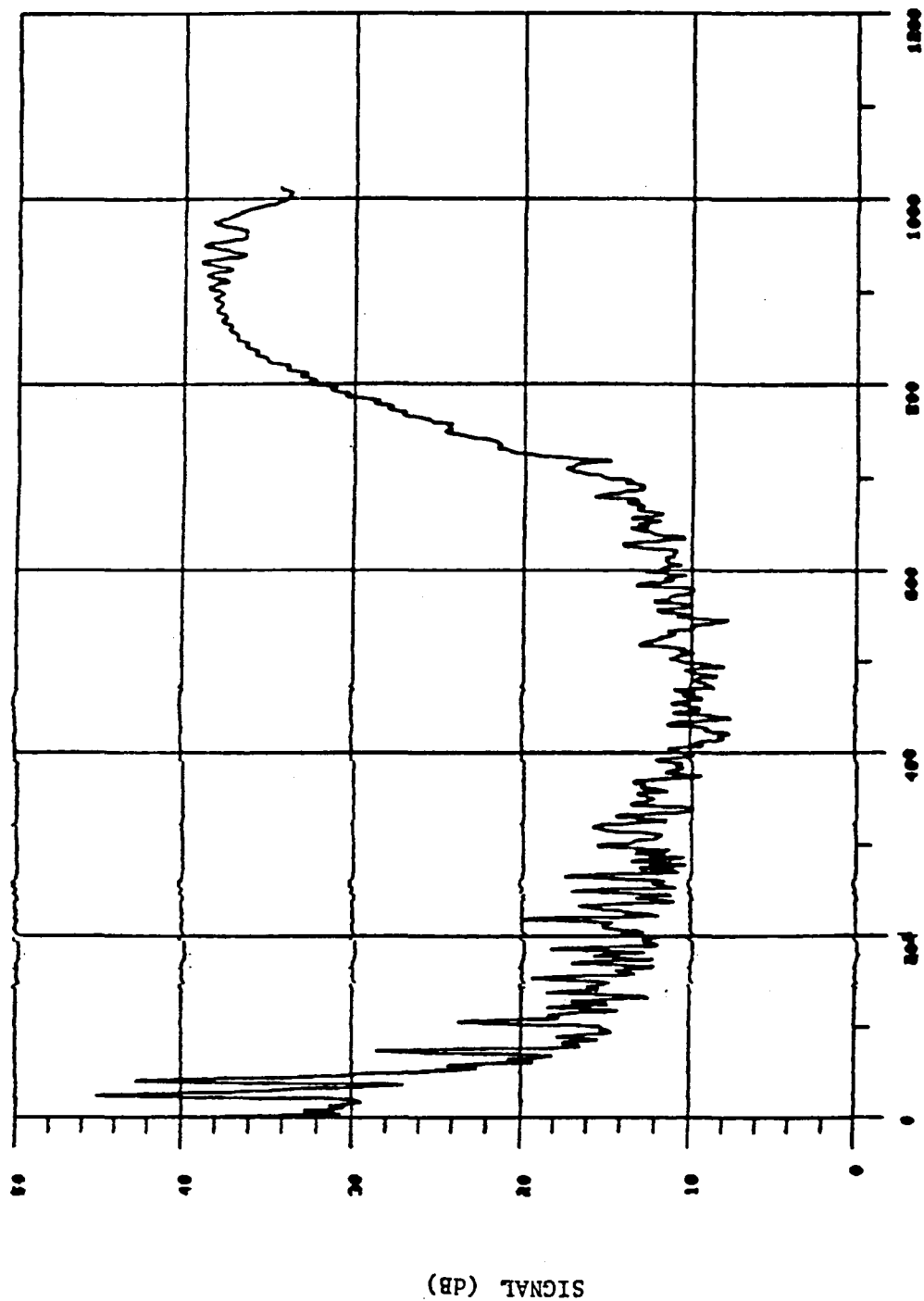
20 METER FOCUS



FREQUENCY BIN

Fig. 9.19. 1.5 METER IN FRONT OF FOCUS

20 METER FOCUS



FREQUENCY BIN

Fig. 9.20. 2.0 METER IN FRONT OF FOCUS

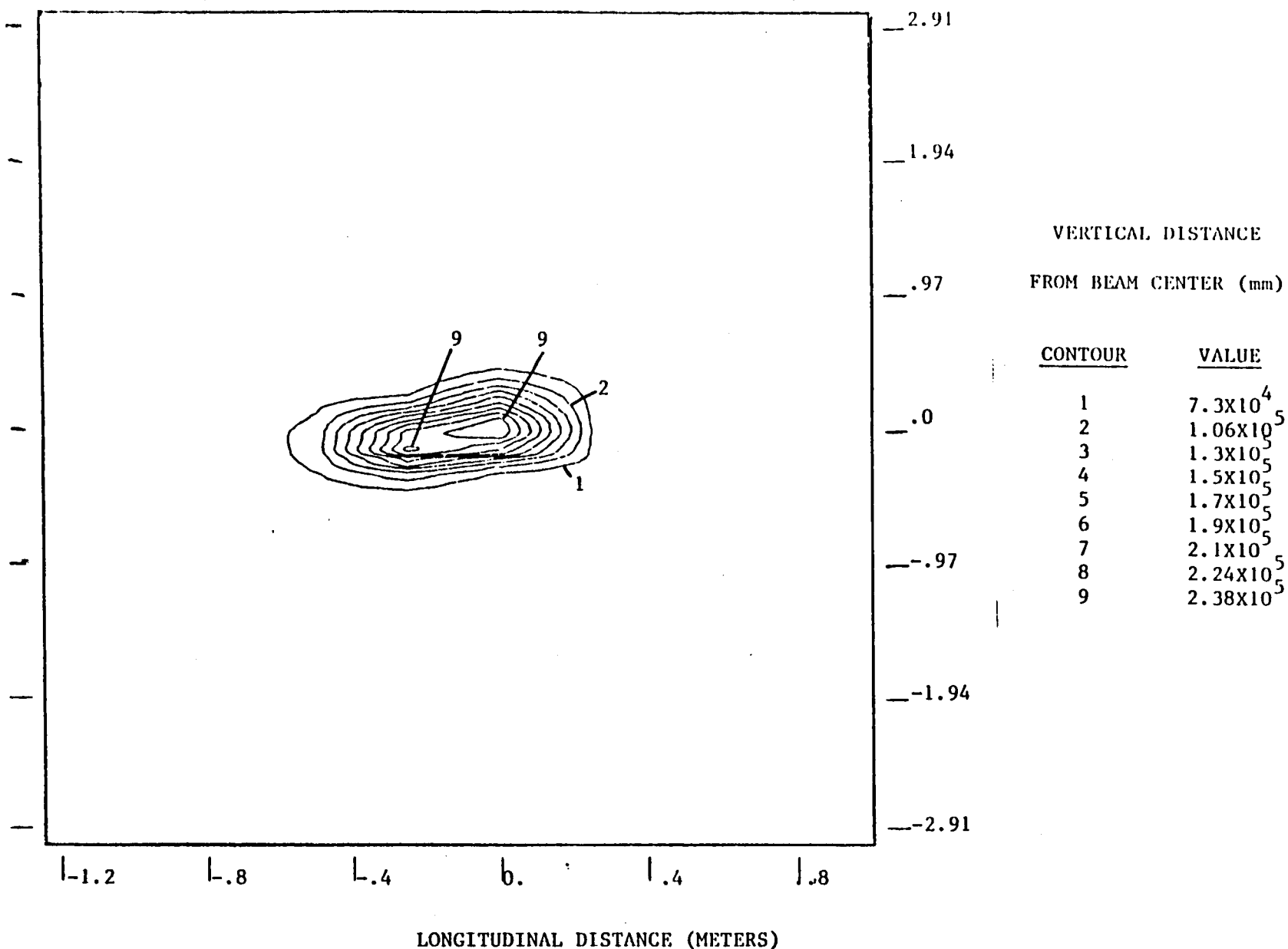


Fig. 9.21. LINEAR CONTOUR PLOT OF 10m DATA

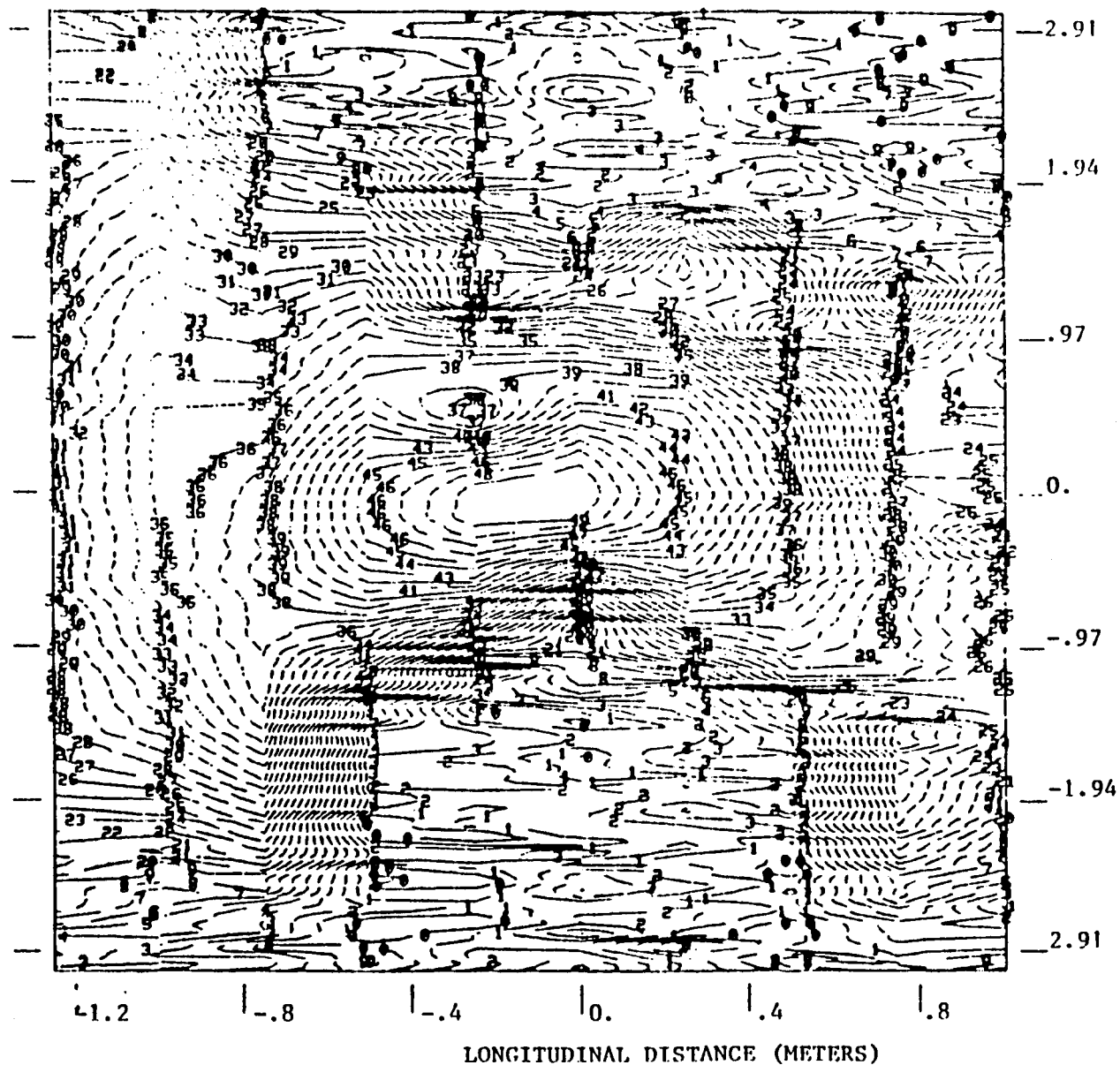


Fig. 9.22. LOGARITHMIC CONTOUR PLOT OF 10 METER DATA

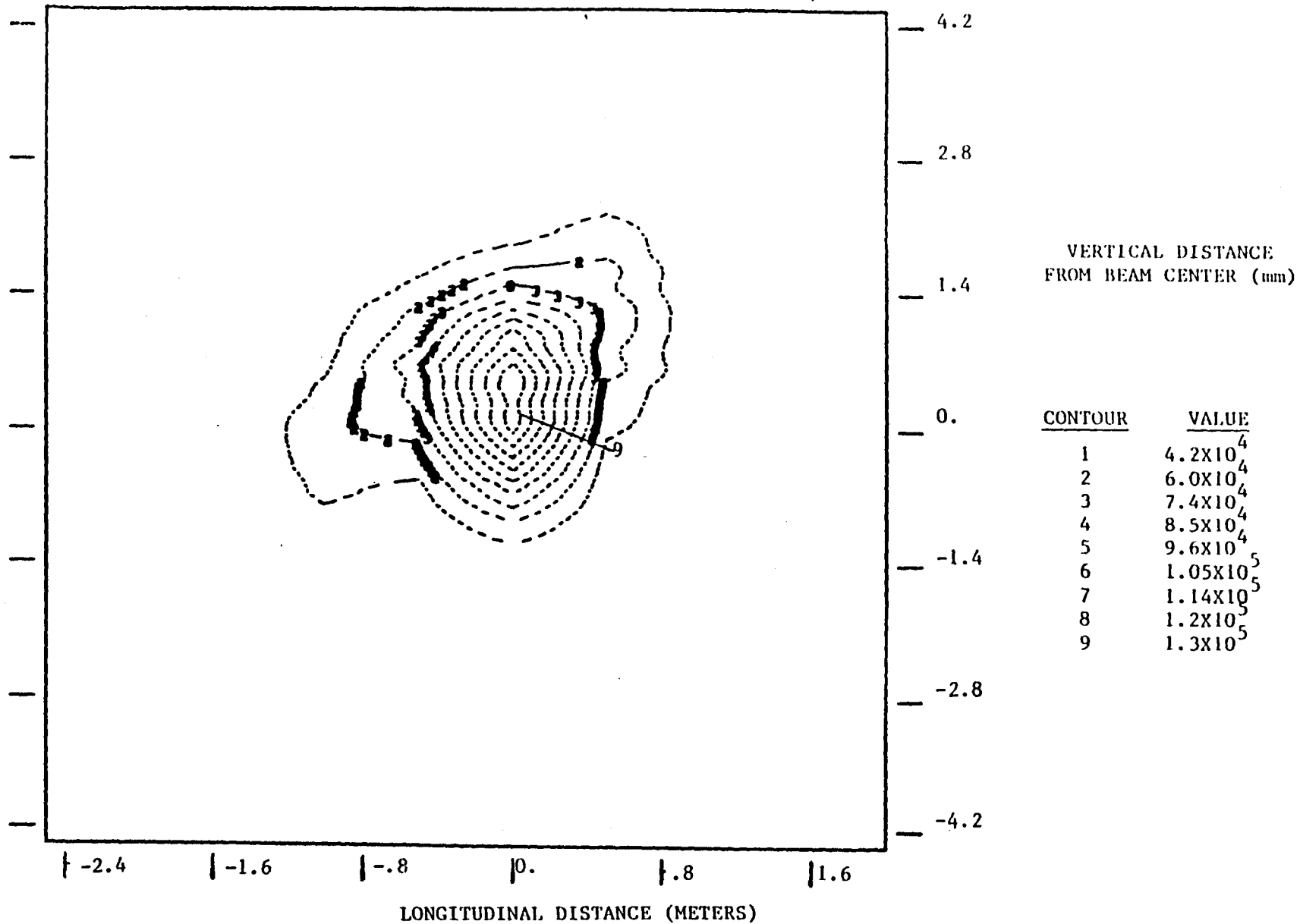


Fig. 9.23. LINEAR CONTOUR PLOT OF 20 METER DATA

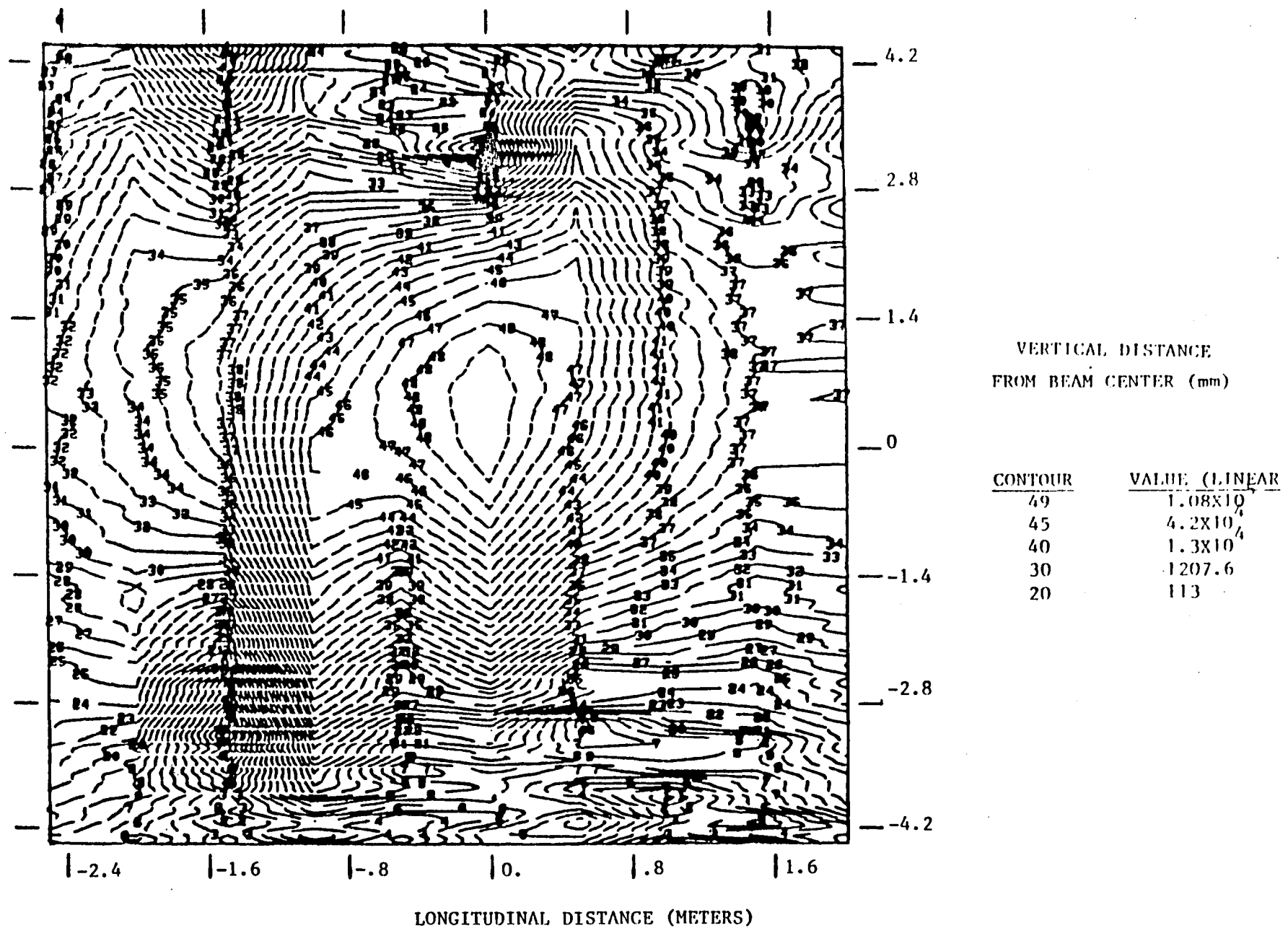


Fig. 9.24. LOGARITHMIC CONTOUR PLOT OF 20 METER DATA



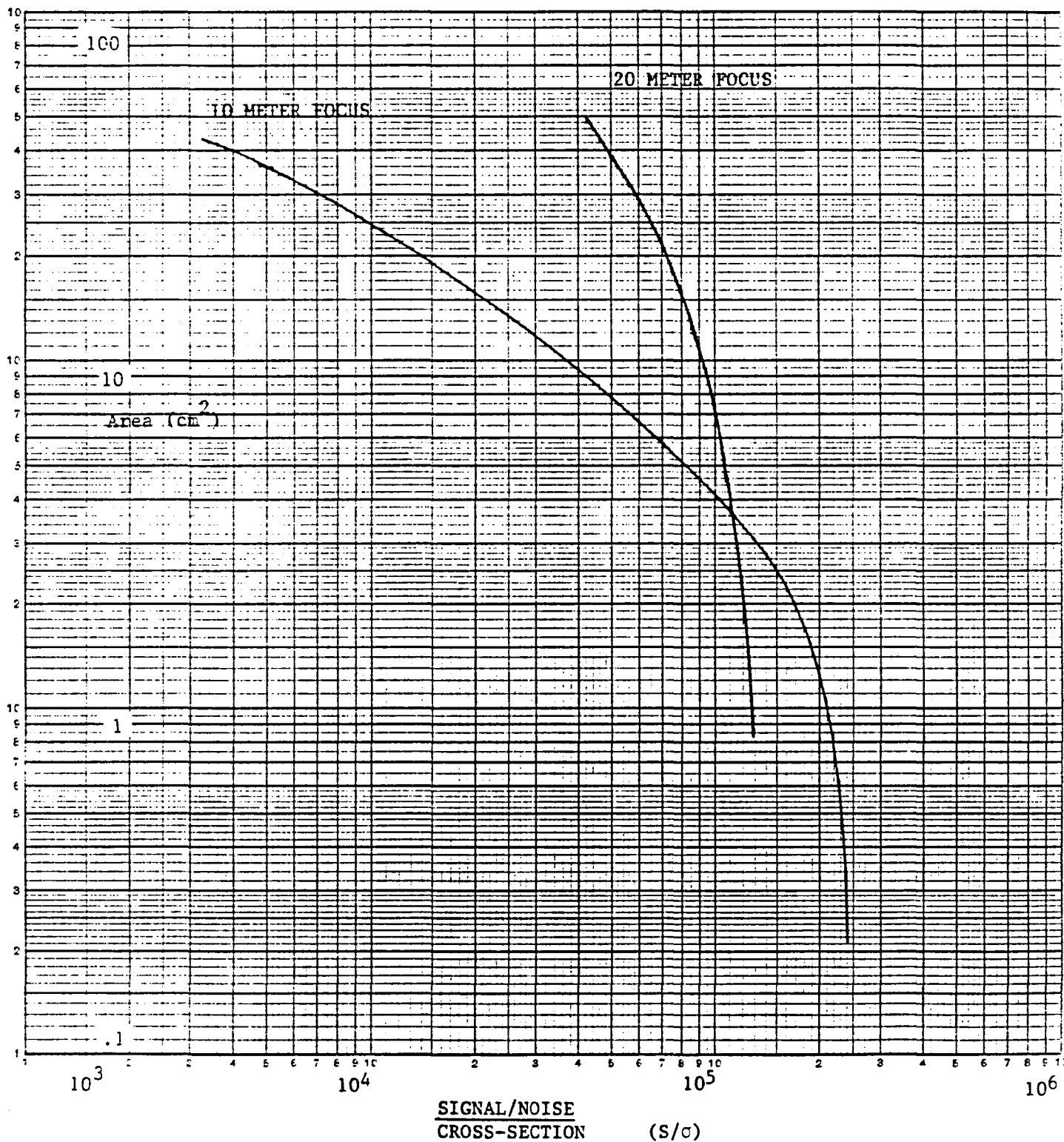


FIGURE 9.25.  $S/\sigma$  VERSUS AREA (RELATIVE SCALE)

115

XX

WRITTEN FOR NASA/MARSHALL  
BY IVAN BURROUGHS/APPLIED RESEARCH INC \*  
131 LONGWOOD AV.  
HUNTSVILLE, AL 35804  
(205) 533-6987

.....

R0 = %0  
 R1 = %1  
 R2 = %2  
 R3 = %3  
 R4 = %4  
 R5 = %5  
 SP = %6  
 R6 = SP  
 PC = %7

## ; SERIAL LINE UNIT

TKS = 177560 ;KB STATUS USES CRT KEYBOARD  
 TKB = TKS+2 ;KB BUFFER  
 TPS = TKS+4 ;PR STATUS CHANNEL 1 SERIAL XMIT TO CRT  
 TPB = TPS+2 ;PR BUFFER  
 KBVEC = 60 ;KB INTERRUPT  
 PRVEC = 64 ;CRT INTERRUPT CHAN 1  
 RSC1 = TKS ;RECIEVER STATUS SERIAL CHANNEL 1 CRT KEYBOARD  
 RDC1 = TKB ; " DATA BUFFER " " " "  
 XSC1 = TPS ;TRANSMITTER STATUS SERIAL CHAN 1 "  
 XDC1 = TPB ; " DATA BUFFER " " " "  
 RSC2 = 176500 ;RECIEVER STATUS SERIAL CHANNEL 2 LP KEYBOARD  
 RDC2 = RSC2+2 ; " DATA BUFFER " " " "  
 XSC2 = 176504 ;TRANSMITTER STATUS SERIAL CHAN 2 FOR LINE PRINTER  
 XDC2 = XSC2+2 ; " DATA BUFFER CHAN 2  
 RSC3 = 176510 ;RECIEVER STATUS SERIAL CHAN 3 FOR SIGMA V  
 RDC3 = RSC3+2 ; " DATA BUFFER " "  
 XSC3 = RSC3+4 ;TRANSMITTER STATUS CHAN 3  
 XDC3 = RSC3+6 ; " DATA BUFFER CHAN 3  
 R2VEC = 300 ;RECIEVER CHAN 2 INTERRUPT VECTOR LP KB  
 X2VEC = 304 ;XMITTER CHAN 2 INTERRUPT VECTOR  
 R3VEC = 310 ;RECIEVER " 3 " "  
 X3VEC = 314 ;XMITTER " " " "  
 DRCSR = 167770 ;DRV11 COMMAND & STATUS REGISTER  
 DROUT = DRCSR+2 ;OUTPUT BUFFER  
 DRIN = DROUT+2 ;INPUT BUFFER

## ; ERROR TRAP VECTORS

ILVEC = 4 ;ILL INSTRUCTION, BUS ERROR  
 RIVEC = 10 ;RESERVED INSTRUCTION  
 TRVEC = 14 ;T BIT TRAP  
 PEVEC = 24 ;POWER FAIL

```

.SBTTL  MACROS, ASSEMBLY CONTROL

.MACRO  CALL      .A,.B
.IF     NB,<.B>
      MOV      '.B',R0
.ENDC
.IF     NB,<.A>
      JSR      PC,'.A'
.IFF
      .PRINT   ;MISSING ARG TO CALL MACRO
.ENDC
.ENDM   CALL

.MACRO  PUSH      .A
.IF     NB,<.A>
      MOV      '.A',--(SP)
.IFF
      .PRINT   ;MISSING ARG TO PUSH MACRO
.ENDC
.ENDM   PUSH

.MACRO  POP      .A
.IF     NB,<.A>
      MOV      (SP)+,'.A'
.IFF
      .PRINT   ;MISSING ARG TO POP MACRO
.ENDC
.ENDM   POP

RETURN  =      RTS+7
CR      =      15
LF      =      12
TAB     =      11
ESC     =      33      ;ESCAPE ASCII CODE

.ASECT
.LIST   MEB      ;EXPAND MACROS
.ENABL  AMA      ;ABSOLUTE CODE
.ENABLE LC      ;LOWER CASE

```

```

      .SBITL  VECTORS
      =      0
IRTRP: HALT
RITRP: HALT

      =      ILVEC
BPTRP: .WORD  IRTRP,200

      =      RIVEC
      .WORD  RITRP,200

      =      TRVEC
      .WORD  BPTRP,200

      =      PFVEC
      .WORD  BPTRP,200

      =      600
DUMY:  CLR    0
      CLR    2
      CLR    4
      MOV    #200,6
      MOV    #2,10
      MOV    #200,12
      MOV    #4,14
      MOV    #200,16
      MOV    #4,24
      MOV    #200,26
      BR     1000

```

```

;LOAD INTERRUPT SECTION

```

```

      .SETTL MAIN
      = 1000
MAIN:  MTPS  #200      ;DISABLE PROCESSOR INTERRUPTS
      MOV   #DHDR-200.,SP ;INITIALIZE STACK
      MOV   #20.,NDSPS   ;SET # DATA SETS/SLICE = 20
      MOV   #2048.,NSAPS ;SET # SAMPLES/DATA SET=2048.
      MOV   #XSC1,R1     ;CHANNEL 1 XMIT TO TERMINAL
      CALL  OUTSTR,#CS00  ;ANNOUNCE PRESENCE
      CALL  OUTSTR,#CS02  ;GIVE FILE NAME
      CALL  OUTSTR,#CS01
      CALL  OUTSTR,#CS03
      CALL  OUTSTR,#CS04  ;PROMPT TO ENTER FILE #
      CALL  NUMBR3        ;ENTER 3 DIGIT FILE START #
      MOV   R2,FILNUM     ;SAVE FILE #
      MOV   #XSC1,R1
      CALL  OUTSTR,#CS05  ;ENTER 2 DIGIT # DATA SETS/BEAM SLICE
      CALL  NUMBR2
      MOV   R2,NDSPS
      INC   NDSPS        ;ADD 1 TO #SETS/SLICE TO MAKE COUNT RIGHT
      ;
      ;***** WAKE UP SIGMA SIGN ON *****
WAKEUP: MOV   #'H,R1
      CALL  STRSV,#CSA6   ;WAKE UP SIGMA
      CALL  CHECK         ;CHECK FOR "H" OF HONEYWELL CP-V
      BNE   WAKEUP        ;TRY AGAIN IF NO GOOD
      MOV   #3.,R3        ;WAIT 3 SECONDS FOR COMPLETION OF SIGMA RESPONSE
W3:     MOV   #1000.,R4    ;MILI SEC COUNTER
W2:     MOV   #238.,R5    ; " " TIMER
W1:     SOB   R5,W1
      SOB   R4,W2
      SOB   R3,W3
SGNON:  MOV   #'!,R1      ;SIGMA RESPONDS WITH "!" AT SIGN ON
      CALL  STRSV,#CSA4   ;SIGN ON
      CALL  CHECK         ;CHECK FOR "!" RESPONSE
      BNE   SGNON        ;TRY AGAIN IF NO GOOD
      ;*****
      ;

```

```

MOV      #XSC1,R1
CALL     OUTSTR,#CS06      ;SIGMA WAKE UP & SIGN ON COMPLETE
CALL     CMETOF            ;COPY ME TO FILE
STRT:    MOV      #1,DSCNTR ;INITIALIZE DATA SET COUNTER
MOV      #DBUF,DTAPTR     ;SET DATA POINTER
MOV      #DHDR,DHPTR      ;SET DATA HEADER POINTER
MOV      #XSC1,R1
CALL     OUTSTR,#CS07      ;ENTER 5 DIGIT RANGE(CM)
CALL     NUMR5
MOV      R2,@DHPTR
ADD      #2,DHPTR
MOV      #XSC1,R1
CALL     OUTSTR,#CS08      ;ENTER 1 DIGIT SLICE #
CALL     NUMR1
MOV      R2,@DHPTR
ADD      #2,DHPTR
MOV      FILNUM,@DHPTR
ADD      #2,DHPTR
MOV      #XSC1,R1
CALL     OUTSTR,#CS09      ;ENTER COMMENTS(57 CHAR MAX)
MOV      DHPTR,R0         ;SET STRING DESTINATION
MOV      #57.,R3          ;SET MAX # CHARS
MOV      #RSC1,R4         ;SET STATUS REG CHAN 1
CALL     INSTR            ;GET COMMENT STRING
DLOOP:   MOV      #XSC1,R1
CALL     OUTSTR,#CS10      ;READY TO TAKE DATA
DWAIT:   CALL     KBIN     ;GET CHAR & ECHO
CMP      R1,#'S
BNE      DWAIT            ;WAIT IF NOT = "S"
CALL     DREAD            ;GET DATA SET
MOV      #XSC1,R1
CALL     OUTSTR,#CS11      ;SAY DONE
CALL     OUTD3,DSCNTR     ;FOR DATA SET # DSCNTR
MOV      #XSC1,R1
CALL     OUTSTR,#PIXL     ;
INC      DSCNTR           ;BUMP DATA SET COUNTER
CMP      DSCNTR,NDSPS     ;CHECK FOR # DATA SETS DONE
BMI      DLOOP            ;LOOP IF DSCNTR<=NDSPS
MOV      #XSC1,R1
CALL     OUTSTR,#CS12      ;SAY DONE FOR ALL DATA SETS
CALL     DTRANS           ;TRANSFER DATA
MOV      #XSC1,R1
CALL     OUTSTR,#CS16      ;WANT TO CLOSE FILE
CALL     KBIN
CMP      R1,#'N

```

```

ESC:  ESC:  ;CLOSE FILE IF NOT "N"
      JMP  STRT  ;CONTINUE TO TAKE DATA OTHER WISE
      MOV  #!,R1
      CALL STRSV,#CSA2  ;SEND SIGMA ESC F TO CLOSE FILE
      CALL CHECK
      BNE  ESCF  ;IF SIGMA DOES'NT GIVE "!" TRY AGAIN
      MOV  #XSC1,R1
      CALL OUTSTR,#CS17  ;SIGMA V
      CALL OUTSTR,#CS01  ;FILE
      CALL OUTD3,FILNUM  ;#
      MOV  #XSC1,R1
      CALL OUTSTR,#PIXL
      CALL OUTSTR,#CS18  ;CLOSED
      INC  FILNUM  ;BUMP FILE COUNTER
      MOV  #XSC1,R1
      CALL OUTSTR,#CS14  ;DO IT AGAIN?
      CALL KBIN
      CMP  R1,#'N
      BEQ  SGNOF
      CALL CMETOF  ;COPY ME TO FILE
      JMP  STRT
      MOV  #'C,R1
      CALL STRSV,#CSA5  ;SIGN OFF
      CALL CHECK
      BNE  SGNOF
      JMP  173000  ;GO TO KEYBOARD OUT (@)

```

SGNOF:

# .SBTTL SUBROUTINES

```

;SUBROUTINE STRSV
;SENDS CHARACTER STRING TO SIGMA V
;STRING ADDRESS SENT OVER IN R0
;USES TRANSMITTER SERIAL CHANNEL 3

```

```

STRSV:  BIT  #200,XSC3  ;TEST BIT 7 IF SET XMITTER READY FOR NEXT CHAR
      BEQ  STRSV  ;BIT 7 CLEAR? WAIT
      TSTB (R0)  ;TEST STRING CHAR
      BEQ  1$  ;EXIT IF NULL
      MOVB (R0)+,XDC3  ;SEND OUT CHAR
      BR   STRSV
1$:  RETURN

```



```

;SUBROUTINE CHECK
;COMPARES CHAR IN R1 TO CHAR ON SERIAL INPUT
;TO SEE IF SIGMA V GIVES CORRECT RESPONSE TO COMMANDS
;CHAR TO BE COMPARED SENT IN R1

```

```

CHECK: MOV     R1,TSTCHR      ;SAVE TEST CHAR
        MOV     #10.,R3      ;10 SECONDS TO WAIT FOR RESPONSE
4$:     MOV     #1000.,R4      ;MILLISEC COUNTER
3$:     MOV     #238.,R5      ;LOAD 1 MS TIMER
        BIT     #200,RSC3      ;CHECK BIT 7 CHAN 3 RECV. DONE
        BNE     1$            ;IF SET CHECK CHAR
2$:     SOB     R5,2$          ;WAIT 1 MS THEN RECHECK RECV. DONE
        SOB     R4,3$          ;COUNT 1000 MS FOR 1 SEC
        SOB     R3,4$          ;COUNT 10 SECS
        CALL    STRNLP,#CSA1   ;PRINT "SIGMA DOES NOT RESPOND"
        MOV     #1,R1          ;SET R1=1 SINCE NO GOOD
        BR      5$
1$:     MOVB    RDC3,R0         ;GET CHAR
        BIC     #177600,R0
        CMP     R0,TSTCHR      ;CHECK FOR CORRECT CHAR
        BNE     3$            ;IF NOT CONTINUE WAIT
        CLR     R1            ;IF GOOD SET R1=0
5$:     RETURN

```

```

;SUBROUTINE STRLP
;SENDS CHARACTER STRING TO LINE PRINTER
;STRING ADDRESS SENT OVER IN R0
;USES TRANSMITTER SERIAL CHANNEL 1

```

```

STRNLP: BIT     #200,XSC1      ;SAME LOGIC AS STRSV
        BEQ     STRNLP
        TSTB    (R0)
        BEQ     1$
        MOVB    (R0)+,XDC1
        BR      STRNLP
1$:     RETURN

```

```

;SUBROUTINE  OUTSTR
;OUTPUTS STRING ON SERIAL LINE
;WHOSE TRANSMITTER STATUS ADDRESS IS IN R1
;STRING ADDRESS IN R0
;USES R0,R1,R2
OUTSTR: -MOV    R1,R2
        ADD     #2,R2          ;PUT ADDRESS OF XMIT DATA BUFFER IN R2
2$:     BIT     #200,(R1)      ;TEST BIT 7 - IF SET XMITTER READY FOR NEXT PULL
        BEQ     2$            ;BIT 7 CLEAR WAIT
        TSTB    (R0)          ;TEST STRING FOR NULL
        BEQ     1$            ;EXIT IF NULL
        MOVB    (R0)+,(R2)     ;SEND CHARACTER
        BR      2$            ;LOOP
1$:     RETURN

```

```

;SUBROUTINE  INSTR
;INPUTS STRING ON SERIAL LINE
;WHOSE RECIEVER STATUS ADDRESS IS IN R4
;STRING DESTINATION ADDRESS IN R0
;MAX # CHARS IN R3
;USES R0,R2,R3,R4
;CALLS KBIN,OUTSTR
INSTR:  MOV     R4,R2
        ADD     #2,R2          ;ADDRESS OF RECIEVER DATA BUFFER IN R2
        MOV     R0,PTR7        ;SAVE R0 IN CASE COMMENTS TOO LONG
        MOV     R3,PTR6        ;SAVE MAX # CHARS
1$:     CALL    KBIN            ;GET & ECHO CHAR
        MOVB    R1,(R0)+       ;SAVE
        DEC     R3              ;COUNT CHARS INPUT
        TST     R3              ;IF = MAX # TRY AGAIN
        BEQ     2$
        CMP     R1,#<CR>        ;CHECK FOR CARRAGE RETURN
        BNE     1$
        MOVB    #0,(R0)+       ;PUT NULL AT END
        BR      3$
2$:     MOV     #XSC1,R1
        CALL    OUTSTR,#CS15    ;COMMENTS TOO LONG
        MOV     PTR7,R0         ;RESTORE R0
        MOV     PTR6,R3         ;      "      R3
        BR      1$             ;GET COMMENTS AGAIN
3$:     RETURN

```

```

;SUBROUTINE CMETOF
;SENDS SIGMA "COPY ME TO FILE FILENAME###"
;USES R1
;CALLS $TRSV,OUTD3,CARRET
CMETOF: MOV     #'. ,R1
        CALL    $TRSV,#CSA0      ;COMMAND SIGMA "COPY ME TO FILE"
        CALL    $TRSV,#CS01      ;SEND FILE NAME
        CALL    OUTD3,FILNUM
        CALL    $TRSV,#PIXL      ;SEND FILE NUMBER
        CALL    CARRET           ;SEND <CR> & CHECK FOR "." RESPONSE
        RETURN

```

```

;SUBROUTINE DTRANS
;TRANSFERS DATA TO SIGMA V
;CALLS $TRSV,OUTD3,OUTD1,OUTD5,CARRET,CHECK,LIST,OUTSTR
;
;   OUTD2

```

```

DTRANS: MOV     #DHDR,DHPTR      ;RESET DATA HEADER POINTER
        CALL    OUTD5,@DHPTR
        CALL    $TRSV,#PIXL      ;SEND RANGE
        ADD     #2.,DHPTR        ;BUMP HEADER POINTER
        CALL    OUTD1,@DHPTR
        CALL    $TRSV,#PIXL      ;SEND SLICE #
        ADD     #2.,DHPTR
        CALL    OUTD3,@DHPTR
        CALL    $TRSV,#PIXL      ;SEND FILE #
        ADD     #2.,DHPTR
        CALL    $TRSV,DHPTR      ;SEND COMMENTS

```

```

CMTS:   MOV     #'. ,R1
        CALL    CHECK            ;CHECK FOR "." FROM SIGMA V
        BNE     CMTS            ;TRY AGAIN IF NO GOOD
        MOV     #1,DSCNTR        ;SET DATA SET COUNTER=1
        MOV     #DBUF,DTAPTR     ;SET DATA POINTER

```

```

TLOOP:  CALL    OUTD2,DSCNTR
        CALL    $TRSV,#PIXL      ;SEND SET#
        CALL    CARRET           ;SEND <CR> & CHECK FOR "."
        MOV     DTAPTR,PTR1
        MOV     NSAPS,PTR3
        CALL    LIST            ;SEND DATA SET
        MOV     PTR1,DTAPTR
        CALL    OUTD3,@DTAPTR
        CALL    $TRSV,#PIXL      ;SEND WIRE SPEED
        CALL    CARRET           ;SEND <CR> & CHECK FOR "."
        ADD     #2,DTAPTR        ;BUMP DATA POINTER
        CALL    OUTD2,DSCNTR
        MOV     #XSC1,R1
        CALL    OUTSTR,#CS10

```

\*TRANSFER DONE FOR DATA SET

CALL	OUTSTR, #PIXL	;#
INC	DSCNTR	;BUMP SET COUNTER
CMP	DSCNTR, NDSPS	
BMI	TLOOP	;LOOP IF DSCNTR<NDSPS
RETURN		

.BLKW	1.
-------	----

;READS BIOMATION DIGITIZER DATA (8 BIT BYTES)  
 ;PACKS 2 BYTES INTO 16 BIT WORD  
 ;USES R0,R1

DREAD:	MOV	NSAPS,R0	;SET BYTE COUNT
	MOV	DTAPTR,R1	;STORAGE ARRAY
1\$:	TST	DRCR	;TEST REQUEST B
	BPL	1\$	;BRANCH IF SIGN BIT CLEAR
2\$:	BIS	#1,DRCR	;TOGGLE 'CMD' LINE
	BIC	#1,DRCR	; LINE
3\$:	TST	DRCR	;TEST FOR REQUEST B
	BPL	3\$	; HIGH AGAIN
	MOVB	DRIN,(R1)+	;STORE DATA
	DEC	R0	;DECREMENT BYTE COUNT
	BNE	1\$	;IF NOT ZERO, DATA REMAINS
	MOV	R1,DTAPTR	;SAVE R1 IN DATA POINTER
	MOV	DRIN,WSPEED	;READ WIRE SPEED IN MOST SIGNIFICANT BYTE
	SWAB	WSPEED	;SWAP BYTES
	BIC	#177400,WSPEED	;AND CLEAR BITS 8 - 15
	MOV	WSPEED,@DTAPTR	;SAVE WIRE SPEED
	ADD	#2,DTAPTR	;BUMP DATA POINTER
	RETURN		

```

;ROUTINE OUT
;SENDS DATA TO SIGMA V IN ASCII
;UNPACKS DATA BUFFER FOR 8 BIT VALUES TO SEND IN 3 DIGIT ASCII
LIST: CLR PTR2 ;ENTER WITH PTR1=DATA ADDRESS
1$: MOV #15.,PTR4 ;AND PTR3=# ITEMS
CALL OUTD4,PTR2 ;PRINT ITEM NUMBER
CALL STRSV,#PIXL ;SEND DATA ITEM #
CLR BYTEF ;CLEAR BYTE FLAG
2$: INC PTR2
INC BYTEF ;SET = 1 SINCE OUTPUTING BYTE
MOVB @PTR1,BYTE
CALL OUTD3,BYTE
CALL STRSV,#PIXL ;SEND DATA ITEM
CLR BYTEF ;CLEAR BYTE FLAG
ADD #1,PTR1
CMP PTR2,PTR3 ;ENUF ITEMS?
BPL 4$
DEC PTR4
BPL 2$
CALL CARRET ;SEND CARRAGE RETURN CHECK FOR "."
BR 1$
4$: CALL CARRET
RETURN

```

```

;SUBROUTINE CARRET
;SENDS CARRAGE RETURN TO SIGMA CHECKS FOR RESPONSE "."
;NO ARGS PASSED

```

```

CARRET: MOV #'. ,R1
CALL STRSV,#CSA7 ;SEND CR
CALL CHECK ;CHECK FOR "."
BNE CARRET ;TRY AGAIN IF NO GOOD
RETURN

```

```

.BLKW 10.

```

```

.SBTL  TERMINAL I/O ROUTINES
;      N-DIGIT DECIMAL OUTPUT ROUTINES FOR INTERRUPT USE

OUTD1: MOV    #1,R5          ;1-DIGIT DECIMAL OUTPUT
      MOV    #K1,R4
      BR     DIGIT

OUTD2: MOV    #2,R5          ;2-DIGIT DECIMAL OUTPUT
      MOV    #K10,R4
      BR     DIGIT

OUTD3: MOV    #3,R5          ;3-DIGIT DECIMAL OUTPUT
      MOV    #K100,R4
      BR     DIGIT

OUTD4: MOV    #4,R5          ;4-DIGIT DECIMAL OUTPUT
      MOV    #K1K,R4
      BR     DIGIT

OUTD5P: MOV    #5,R5          ;5-DIGIT POSITIVE OUTPUT
      MOV    #K10K,R4
      BR     DIGITP

OUTD5: MOV    #5,R5          ;5-DIGIT DECIMAL OUTPUT
      MOV    #K10K,R4
      ;SUBROUTINE DIGIT
      ;TESTS BYTEF FOR BYTE OR WORD PUTS "-" IN PIXL IF NEG
DIGIT: MOV    #PXL,R3
      TST    BYTEF          ;TEST BYTE FLAG 1=BYTE 0=WORD
      BEQ    WORD          ;WORD IF 0
      TSTB   R0             ;TEST BYTE
      BPL    DIGITP         ;BRANCH IF +
      NEGB   R0
      MOVB   #'-(R3)+       ;PUT "-" IN PIXL
      BR     DIGITP
WORD:  TST    R0             ;TEST WORD
      BPL    DIGITP         ;BRANCH IF +
      NEG    R0
      MOVB   #'-(R3)+       ;PUT "-" IN PIXL

```

```

2$: MOV R0,R1
    BLO 3$
    INC R2
    SUB R1,R0
    BR 2$
3$: ADD #10,R2
    MOVB R2,(R3)+
    SOB R5,DIGITP
    MOVB #1,(R3)+
    CLRB (R3)+
    RETURN

```

```

PIXL: .BLKW 3
      0000
K10K: 10000.
K1K: 1000.
K100: 100.
K10: 10.
K1: 1.

```

; N-DIGIT DECIMAL INPUT FOR INTERRUPT HANDLERS

```

NUMBR1: MOV #1,R3
        BR INUMBR
NUMBR2: MOV #2,R3
        BR INUMBR
NUMBR3: MOV #3,R3
        BR INUMBR
NUMBR4: MOV #4,R3
        BR INUMBR
NUMBR5: MOV #5,R3

```

```

INUMBR: CLR R2
1$: MOV R2,R1 ;ENTER W/R3=# DIGITS
    MUL #10.,R1
    MOV R1,R2
    CALL NUMBR1 ;GET A DIGIT
    ADD R1,R2 ;AND ADD IT.
    SOB R3,1$
    RETURN ;RETURN W/# IN R2
      .BLKW 1.

```

```

.SBTTL  UTILITY INPUT ROUTINES

CHAR:   CALL  KBIN          ;GET A CHAR FROM USER
        RETURN

NMBR1:  CALL  KBIN          ;GET A DIGIT FROM USER
        ADD   #-60,R1
        BMI   NMBR1        ;LESS THAN ZERO
        CMP   #11,R1       ;IS IT REALLY A DIGIT?
        BLO   NMBR1        ;NO IGNORE
        RETURN

LETR:   CALL  KBIN          ;GET A CHAR A-Z ONLY
        CMP   #172,R1
        BMI   LETR
        CMP   #100,R1
        BPL   LETR
        RETURN            ;RETURN VALUE IN R1

;      GET A CHAR FROM USER (KB INTERRUPT DISABLED)

KBIN:   MOVW  TKB,R1        ;EMPTY BUFFER
2$:     TSTB  TKS          ;WAIT FOR FLAG
        BPL   2$
KBIN1:  MOVW  TKB,R1        ;CHAR NOW IN R1
        BIC   #177600,R1
1$:     TSTB  TPS          ;ECHO IT
        BPL   1$
        MOVW  R1,TPB
        RETURN

.BLKW   1.

```



.SBTTL COUNTERS , POINTERS & VARIABLES

:COUNTERS

NDSPS: 0	;# DATA SETS/SLICE IN BEAM
NSAPS: 0	;#SAMPLES/DATA SET
FILNUM: 0	;FILE # FOR SIGMA V (3 DIGITS)
DSCNTR: 0	;DATA SET COUNTER

.BLKW 20.

:POINTERS

DHPTR: 0	;DATA HEADER POINTER
DTAPTR: 0	;DATA BUFFER POINTER
PTR1: 0	;GENERAL-PURPOSE POINTERS FOR LIST
PTR2: 0	
PTR3: 0	
PTR4: 0	
PTR5: 0	
PTR6: 0	
PTR7: 0	

:VARIABLES

BYTE: 0	;TEMPORARY STORAGE FOR LIST
TSTCHR: 0	;TEST CHARACTER FOR SUB. CHECK
BYTEF: 0	;BYTE FLAG FOR BINARY TO ASCII ROUTINES
WSPEED: 0	;WIRE SPEED 8 BITS

```

CS00: .ASCIIZ <CR><LF>"WIRE WHEEL DATA COLLECTION AND TRANSFER PROGRAM READY"
CS01: .ASCIIZ "WIREWHEEL"
CS02: .ASCIIZ <CR><LF>"FILE NAMES ON SIGMA WILL BE"<CR><LF>
CS03: .ASCIIZ " FOLLOWED BY 3 DIGIT DECIMAL #"
CS04: .ASCIIZ <CR><LF>"PLEASE ENTER 3 DIGIT FILE START #"<CR><LF>"# "
CS05: .ASCIIZ <CR><LF>"ENTER 2 DIGIT # OF DATA SETS/HEAM SLICE - "
CS06: .ASCIIZ <CR><LF>"SIGMA V AVAILABLE FOR DATA TRANSFER"
CS07: .ASCIIZ <CR><LF>"ENTER 5 DIGIT (32767 MAX) RANGE (LM)-- "
CS08: .ASCIIZ <CR><LF>"ENTER 1 DIGIT SLICE # -- "
CS09: .ASCIIZ <CR><LF>"ENTER FILE COMMENTS (57 CHARS MAX)"<CR><LF>
CS10: .ASCIIZ <CR><LF>"READY TO TAKE DATA ENTER - S - "
CS11: .ASCIIZ <CR><LF>"FINISHED TAKING DATA FOR DATA SET # "
CS12: .ASCIIZ <CR><LF>"FINISHED FOR ALL DATA SETS - TRANSFERING TO SIGMA V"
CS13: .ASCIIZ <CR><LF>"FINISHED TRANSMISSION FOR DATA SET # "
CS14: .ASCIIZ <CR><LF>"DO IT AGAIN (Y)ES OR (N)O "
CS15: .ASCIIZ <CR><LF>"COMMENTS TOO LONG TRY AGAIN"<CR><LF>"* "
CS16: .ASCIIZ <CR><LF>"WANT TO CLOSE SIGMA V FILE (Y)ES OR (N)O? "
CS17: .ASCIIZ <CR><LF>"SIGMA V FILE "
CS18: .ASCIIZ " CLOSED!"
CSA0: .ASCIIZ "C ME TO "
CSFILE: .ASCIIZ "SIGMA FILE NAME *****"<CR>
CSA1: .ASCIIZ <CR><LF>"SIGMA V DOES NOT RESPOND"
CSA2: .ASCIIZ <ESC>"F"
CSA3: .ASCIIZ <CR><LF>
CSA4: .ASCIIZ "BILBRO,EC32505"<CR>
CSA5: .ASCIIZ "OFF"<CR>
CSA6: .ASCIIZ <ESC><ESC> ;EQUIVALENTE TO BRAKE
CSA7: .ASCIIZ <CR>
CSA9: .ASCIIZ <CR><LF>"ENTER SIGMA V FILE NAME (11 CHARS MAX) THEN CR"<CR><LF>
CSB2: .ASCIIZ <CR><LF>"USING SIGMA COMMAND"<CR><LF>
CSB3: .ASCIIZ <CR><LF>"FILE NAME TOO LONG TRY AGAIN PLEASE"<CR><LF>
CSB5: .ASCIIZ <CR><LF>"WANT TO RUN AGAIN? Y(ES) OR N(O)"
CSB6: .ASCIIZ <CR><LF>"FILE NAME OK? Y(ES) OR N(O)"<CR><LF>
CSB7: .ASCIIZ <CR><LF>"ENTER AGAIN"<CR><LF>

```

.SBTTL STORAGE ALLOCATION

.EVEN

LASTW

=

LASTW+400

=

DHDR:  
DBUF:

.BLKW  
.BLKW

40.  
1.

PTEND

=

.END

DUMY

.TITLE DUMBT V 1.0 1/21/82

.SBTTL IDENTIFICATION

\*\*\*\*\*

DUMBT: DUMB TERMINAL ROUTINE TO TALK TO SIGMA V  
TRANSFERS TO SIGMA V

WRITEN FOR NASA/MARSHALL  
BY IVAN BURROUGHS/APPLIED RESEARCH INC #  
131 LONGWOOD AV.  
HUNTSVILLE, AL 35804  
(205) 538-6987

\*\*\*\*\*

.SBTTL DEFINITIONS  
;PROCESSOR DEFINITIONS

R0 = %0  
R1 = %1  
R2 = %2  
R3 = %3  
R4 = %4  
R5 = %5  
SP = %6  
R6 = SP  
PC = %7

; SERIAL LINE UNIT

TKS = 177560 ;KB STATUS USES CRT KEYBOARD  
TKB = TKS+2 ;KB BUFFER  
TPS = TKS+4 ;PR STATUS CHANNEL 1 SERIAL XMIT TO CRT  
TPB = TPS+2 ;PR BUFFER  
KBVEC = 60 ;KB INTERRUPT  
PRVEC = 64 ;CRT INTERRUPT CHAN 1  
RSC1 = TKS ;RECIEVER STATUS SERIAL CHANNEL 1 CRT KEYBOARD  
RDC1 = TKB ; " DATA BUFFER " " " "  
XSC1 = TPS ;TRANSMITTER STATUS SERIAL CHAN 1 "  
XDC1 = TPB ; " DATA BUFFER " " "  
RSC2 = 176500 ;RECIEVER STATUS SERIAL CHANNEL 2 LP KEYBOARD  
RDC2 = RSC2+2 ; " DATA BUFFER " " " "  
XSC2 = 176504 ;TRANSMITTER STATUS SERIAL CHAN 2 FOR LINE PRINTER  
XDC2 = XSC2+2 ; " DATA BUFFER CHAN 2  
RSC3 = 176510 ;RECIEVER STATUS SERIAL CHAN 3 FOR SIGMA V  
RDC3 = RSC3+2 ; " DATA BUFFER " "  
XSC3 = RSC3+4 ;TRANSMITTER STATUS CHAN 3  
XDC3 = RSC3+6 ; " DATA BUFFER CHAN 3  
R2VEC = 300 ;RECIEVER CHAN 2 INTERRUPT VECTOR LP KB  
X2VEC = 304 ;XMITTER CHAN 2 INTERRUPT VECTOR  
R3VEC = 310 ;RECIEVER " " "  
X3VEC = 314 ;XMITTER " " "  
DRC5R = 167770 ;DRV11 COMMAND & STATUS REGISTER  
DROUT = DRC5R+2 ;OUTPUT BUFFER  
DRIN = DROUT+2 ;INPUT BUFFER

**This Page Intentionally Left Blank**

```

        .SBTTL VECTORS
        = 0
IRTRP:  HALT
RITRP:  HALT

        = ILVEC
BPTRP:  .WORD IRTRP,200

        = RIVEC
        .WORD RITRP,200

        = TRVEC
        .WORD BPTRP,200

        = PFVEC
        .WORD BPTRP,200

        = 600
DUMY:   CLR 0 ;LOAD INTERRUPT SECTION
        CLR 2
        CLR 4
        MOV #200,6
        MOV #2,10
        MOV #200,12
        MOV #4,14
        MOV #200,16
        MOV #4,24
        MOV #200,26
        BR 1000

        .SBTTL MAIN
        ;SIGMA V ON SERIAL CHANNEL 3
        ;CRT " " " 1
        = 1000
MAIN:   MTPS #200 ;DISABLE PROCESSOR INTERRUPTS
        MOV #XSC1,R1 ;CHANNEL 1 XMIT TO TERMINAL
        CALL OUTSTR,#C$00 ;ANNOUNCE PRESENCE
LOOP:   CALL KBIN ;GET CHAR,SEND TO SIGMA & ECHO
        CALL SVIN ;GET SIGMA CHAR & PRINT
        BR 1000

```

```

;SUBROUTINE SVIN
;GETS CHAR FROM SIGMA V IF PRESENT & PUTS TO CRT
SVIN:  TSTB    RSC3                ;TEST IF CHAR PRESENT
      BPL     1$                  ;EXIT IF NOT
      MOVB    RDC3,R1
      BIC     #177600,R1          ;CHAR IN R1
2$:    TSTB    TPS                ;TEST CRT STATUS
      BPL     2$
      MOVB    R1,TPB              ;SEND TO CRT
1$:    RETURN

;SUBROUTINE KBIN
;GETS A CHAR FROM CRT IF PRESENT & PUTS ON CRT
KBIN:  TSTB    TKS                ;IF NO CHAR IN BUFFER EXIT
      BPL     EX
KBIN1: MOVB    TKB,R1              ;CHAR NOW IN R1
      BIC     #177600,R1
4$:    TSTB    XSC3                ;TEST STATUS ON SERIAL CHAN 3
      BPL     4$                  ;WAIT IF NOT READY
      MOVB    R1,XDC3              ;SEND TO SIGMA V
1$:    TSTB    TPS                ;ECHO IT
      BPL     1$
      MOVB    R1,TPB
EX:    RETURN

;OUTPUTS STRING ON SERIAL LINE
;WHOSE TRANSMITTER STATUS ADDRESS IS IN R1
;STRING ADDRESS IN R0
;USES R0,R1,R2
OUTSTR: MOV     R1,R2
      ADD     #2.,R2                ;PUT ADDRESS OF XMIT DATA BUFFER IN R2
2$:    BIT     #200,(R1)            ;TEST BIT 7 - IF SET XMITTER READY FOR NEXT BYTE
      BEQ     2$                  ;BIT 7 CLEAR WAIT
      TSTB    (R0)                ;TEST STRING FOR NULL
      BEQ     1$                  ;EXIT IF NULL
      MOVB    (R0)+,(R2)           ;SEND CHARACTER
      BR      2$                  ;LOOP
1$:    RETURN

CS00:  .ASCIZ  <CR><LF>"DUMB TERMINAL READY!!"<CR><LF>
      .END      DUMY

```



Contour Routine and Sample

```

COMMON/FIR/TR(2048),TI(2048)
COMMON/SER/P(1012)
DIMENSION X(9),Y(101),S(9,101)
CALL INITI(9600)
REWIND 5
DX=.4953
NY=101
NS=9
NX=NS
ND=2024
NDP=2048
NU=11
FS=20.E+06
TW=.0035
ND2=ND/2
DO 7 L=1,NDP
  TR(L)=0.
7  TI(L)=0.
  LS=NS/2+1
  DO 1 I=1,LS
1  READ(5,1000) (TR(L),L=1,2024)
    CALL FFT(NDP,NU)
    DO 4 L=1,ND2
4  P(L)=(TR(L)*TR(L)+TI(L)*TI(L))/(FS*FS)
C  WRITE(6,5000) (P(L),L=1,1012)
    I=0
    CALL SERCH(NM1,ND2,I,PT1)
    WRITE(101,2000) NM1
    OUTPUT PT1
    LL=1-ND
    LU=0
    REWIND 5
    DO 6 I=1,NS
    DO 9 L=1,NDP
      TR(L)=0.
9  TI(L)=0.
    OUTPUT I
    READ(5,1000) (TR(L),L=1,2024)
    WRITE(6,4000) (TR(L),L=1,2024)
1000 FORMAT(20G)
4000 FORMAT(20F4.0)
    CALL FFT(NDP,NU)
    DO 5 L=1,ND2
5  P(L)=(TR(L)*TR(L)+TI(L)*TI(L))/(FS*FS)
    IF(I.EQ.4) P(424)=0.
C  WRITE(6,5000) (P(L),L=1,1012)
5000 FORMAT(10E7.1)
    CALL SERCH(NM,ND2,I,PT)
    WRITE(101,3000) NM
    OUTPUT PT

```

```

      DO 2 J=1,101
2    S(I,J)=P*(N1-50+J)/(0.01*PT1)
      WRITE(6,1000) (S(I,J),J=1,NY)
6    CONTINUE
      DF=FS/10
      W=2.*3.14159/TA
      DV=(10.6E-03)*DF/2.
      DY=DV/W
      OUTPUT DF,DV,DY
      NX2=N/2
      NY2=N/2
      DO 10 I=1,NX
10   X(I)=(I-NX2-1)*DX
      DO 11 I=1,NY
11   Y(I)=(I-NY2-1)*DY
      OUTPUT *
      PAUSE " HIT RETURN TO GO"
      CALL INITT(9600)
      CALL DRINDO(0.,780.,0.,780.)
      CALL TRINDO(0,780,0,780)
      CALL CONTOUR(X,Y,S,NX,50,NX)
      CALL FINITT(0,780)
2000 FORMAT($BEAM MIDPOINT ISS,16)
3000 FORMAT($STREAK MIDPOINT ISS,16)
8    CONTINUE
      END
      SUBROUTINE FFT(N,NU)
      COMMON/FTR/XR(2024),XI(2024)
      N2=N/2
      NU1=NU-1
      K=0
      DO 100 L=1,NU
102  DO 101 I=1,N2
      P=IBITR(K/2**NU1,NU)
      ARG=6.283185*P/FLOAT(N)
      C=COS(ARG)
      S=SIN(ARG)
      K1=K+1
      K1N2=K1+N2
      TR=XR(K1N2)*C+XI(K1N2)*S
      TI=XI(K1N2)*C-XR(K1N2)*S
      XR(K1N2)=XR(K1)-TR
      XI(K1N2)=XI(K1)-TI
      XR(K1)=XR(K1)+TR
      XI(K1)=XI(K1)+TI
101  K=K+1
      K=K+N2
      IF(K,LT,N) GO TO 102
      K=0
      NU1=NU1-1
100  N2=N2/2
      DO 103 K=1,N

```

```

      I=IBITR(K-1,NU)+1
      IF(I.LE.K) GO TO 103
      T=XR(K)
      TI=XI(K)
      XR(K)=XR(I)
      XI(K)=XI(I)
      XR(I)=T
      XI(I)=TI
103  CONTINUE
      RETURN
      END
      FUNCTION IBITR(J,NU)
      J1=J
      IBITR=0
      DO 200 I=1,NU
      J2=J1/2
      IBITR=IBITR*2+(J1-2*J2)
200  J1=J2
      RETURN
      END
      SUBROUTINE SERCH(NM,ND2,J,PT)
      COMMON/SEP/P(1012)
      PT=.5E-09
      DO 1 I=1,1012
      P1=P(ND2-I)
      IF(P1.GT.PT) PT=P1;NM=ND2-I
1  CONTINUE
      PTT=.5E-09
      IF(PT.LE.PTT) WRITE(101,9) J
9  FORMAT(3NO MAX FOUND$,2I6)
      RETURN
      END
      SUBROUTINE CONTOUR ( X,Y,Z,NXX,NYY,NZDIM )
C
C  IMPLICIT DOUBLE PRECISION (A-H,O-Z)
      REAL IMIN,IMAX
C
C  CONTOUR PLOT OF Z=F(X,Y)
C
C
      DIMENSION CV(51),IN(51),LABEL(51),
      *  XP(4),YP(4),XV(5),YV(5),ZV(5)
      COMMON /PLTCOM/ NPLTF,IPLTC,IPFLG,IPPEN
C
      DIMENSION X(NXX),Y(NYY),Z(NZDIM,NYY),
      CCONTAB(30),INTNSTY(30),LABL(30),ICONOPS(5)
      DATA (LABL(I),I=1,20) /2H1 ,2H2 ,2H3 ,2H4 ,2H5 ,2H6 ,2H7 ,2H8 ,
      * 2H9 ,2H10,2H11,2H12,2H13,2H14,2H15,2H16,2H17,2H18,2H19,2H20/
C
C  OPTIONS IN ICONOPS(I)
C  I=1, 0 = COMPUTE CONTOUR TABLE
C  I=2, 1 = ABSOLUTE VALUE SPECIFIED IN CONTAB

```

```

C          2 = RELATIVE VALUE SPECIFIED IN CONTAB
C          I=2, 0 = COMPUTE INTENSITIES
C          1 = INTENSITY VALUES SPECIFIED IN INTENSITY
C          I=3, 0 = DO NOT PRINT CONTOUR TABLE,
C          1 = PRINT CONTOUR TABLE
C          I=4, 0 = OMIT SCALES AND BORDER
C          1 = INCLUDE BORDER
C          2 = INCLUDE SCALE DIVISIONS
C          3 = INCLUDE SCALE NUMBERS
C          I=5, 0 = OMIT CONTOUR LABELS
C          1 = CONTOUR LABELS SPECIFIED
C          2 = SETUP CONTOUR LABELS
C

```

```
DATA ICSIZ2, ICSIZ3 /3H 01,3H 02/
```

```
DATA XPMX, YPMX, XPMN, YPMN /50.,50.,750.,750./
```

```
DATA IXB0, IYB0, IMIN, IMAX, NCVS, ICONGPS
```

```
* /3,3,12.,16.,20,1,0,0,3,0/
```

```

C
C
C      OUTPUT NXX, NYY
C      DO 10 I=1,20
C      CONTAB(I)=5.*I
10  IN(I)=16
C      ERROR CHECKS
100  NX      = NXX
      NY      = NYY
      IF ( NX .LT. 2 ) GO TO 950
      IF ( NY .LT. 2 ) GO TO 950
      IF ( NZDIM .LT. NX ) GO TO 950
      IF ( XPMX .GT. 1700. ) XPMX=1700.
      IF ( YPMX .GT. 1000. ) YPMX=1000.
      NZ      = NCVS + 1
      IF ( NZ .GT. 50 ) NZ=50
      IF ( NZ .LT. 2 ) NZ= 2
      NZ2     = NZ/2 + 1
      NZ4     = NZ/4

```

```

C
C      COMPUTE MIN AND MAX
120  XMIN     = X(1)
      XMAX     = X(NX)
      YMIN     = Y(1)
      YMAX     = Y(NY)
      ZMIN     = 1.E30
      ZMAX     = -ZMIN
      DO 130 I=1, NX
      DO 130 J=1, NY
      ZMIN     = MIN1 ( ZMIN, Z(I,J) )
130  ZMAX     = DMAX1 ( ZMAX, Z(I,J) )
      DLAB     = ( ((XPMX-XPMN)/(NX-1))**2
*      +      ((YPMX-YPMN)/(NY-1))**2 ) * .5

```

```

C
C      CONTOUR OPTION SETUP

```

```

140 I      = ICONOPS(1)
    IF ( I .NE. 1 ) GO TO 150
    DO 144 I=1,NZ
144 CV(I) = CONTAB(I)
    CV(NZ) = 2.*CV(NZ-1) - CV(NZ-2)
    I      = 1
145 I      = I + 1
    IF ( CV(I-1) .GT. CV(I) ) GO TO 955
    IF ( I .LI. NCYS ) GO TO 145
    GO TO 170
150 IF ( I .NE. 2 ) GO TO 160
    DZ      = (ZMAX-ZMIN)/100.
    DO 155 I=1,NZ
155 CV(I) = CONTAB(I)*DZ + ZMIN
    I      = 1
    GO TO 145
160 C      = NZ - 1
    DZ      = (ZMAX-ZMIN)/C
    I      = INT(LOG10(DZ)+1000.)-1001.
    C      = 10.**I
    DZ      = INT ( DZ/C ) * C
    ZPMN    = INT ( ZMIN/DZ ) * DZ
    IF ( ZMIN .LT. 0. ) ZPMN = ZPMN-DZ
    C      = ZPMN
    CV(1)   = ZPMN
    DO 165 I=1,NZ
    C      = C + DZ
165 CV(I+1) = C
170 ZF      = 100./((CV(NZ)-CV(1)))
    ZB      = - CV(1)*ZF
    DO 172 I=1,NZ
172 LABEL(I) = LABEL(I)
    I      = ICONOPS(5)
    IF ( I .NE. 2 ) GO TO 180
    I      = 0
174 I      = I + 1
    C      = CV(I)*ZF + ZB
    ENCODE ( 4, 984, LABEL(I) ) C
    IF ( I .LT. NZ ) GO TO 174
180 I      = ICONOPS(2)
    IF ( I .NE. 0 ) GO TO 190
    ZF      = (IMAX-IMIN)/(CV(NZ)-CV(1))
    ZB      = IMIN - ZF*CV(1)
    DO 184 I=1,NZ
184 IN(I)   = ZB + ZF*CV(I)
    DO 186 I=1,NZ,5
186 IN(I)   = IN(I) + 3
    GO TO 195
190 DO 192 I=1,NZ
    K      = INTNSTY(I)
    IF ( K.GT.28 .OR. K.LT.2 ) K=16
192 IN(I)   = K

```

```

195 I = ICC,PS(3)
IF ( I .EQ. 0 ) GO TO 200
PRINT,PS(3), (LABEL(I),CV(I),I=1,NZ)

```

C

C CONTOUR GENERATION

```

200 XF = (XPMX-XPMN)/(XMAX-XMIN)
YF = (YPMX-YPMN)/(YMAX-YMIN)
XB = XPMN - YF*XMIN
YB = YPMN - YF*YMIN
IX = 1
X2 = X(IX)*XF + XB
IXB = -IXB0
I = ICONCP(5)
IF ( I .EQ. 0 ) IXB = 20
DO 205 I=1,NY

```

```

205 Y(I) = Y(I)*YF + YB

```

C

C LOOP ON X-VALUES

```

210 IF ( IX .EQ. NX ) GO TO 270
C OUTPUT X2

```

C

```

X1 = X2
IX = IX + 1
X2 = X(IX)*XF + XB
XV(1) = X1
XV(2) = X1
XV(3) = X2
XV(4) = X2
XV(5) = X1
IYB = -IYB0
IXB = IXB + 1
IF ( IXB .EQ. 1 ) IXB = -IXB0
IY = 1
Y2 = Y(IY)
ZV(2) = Z(IX-1,IY)
ZV(3) = Z(IX,IY)

```

C

C LOOP ON Y-VALUES

```

220 IF ( IY .EQ. NY ) GO TO 210
Y1 = Y2
IYB = IYB + 1
IF ( IYB .GT. 0 ) IYB = -IYB0
IY = IY + 1
Y2 = Y(IY)
YV(1) = Y1
YV(2) = Y2
YV(3) = Y2
YV(4) = Y1
YV(5) = Y1
ZV(4) = ZV(3)
ZV(5) = ZV(2)
ZV(1) = ZV(2)
ZV(2) = Z(IX-1,IY)

```

```

ZV(3) = Z(IX ,IY)
ZM = MIN ( ZV(1),ZV(2),ZV(3),ZV(4) )
ZX = MAX ( ZV(1),ZV(2),ZV(3),ZV(4) )

```

```

C
C SEARCH FOR CONTOURS BETWEEN ZM AND ZX
IC = 1
I = NZ2
IF ( CV(I) .LT. ZM ) IC = 1
I = IC + NZ4
IF ( CV(I) .LT. ZM ) IC = 1
IC = IC - 1

```

```

C
230 IC = IC + 1
C = CV(IC)
IF ( C .LT. ZM ) GO TO 230
IF ( C .GT. ZX ) GO TO 220

```

```

C
C INTERPOLATE FOR CONTOUR INTERSECTIONS

```

```

I = 1
N = 1
235 I = I + 1
IF ( (C-ZV(I-1))*(ZV(I)-C) .LE. 0. ) GO TO 240
XP(N) = XV(I-1)
YP(N) = YV(I-1) + (YV(I)-YV(I-1))
* (C-ZV(I-1))/(ZV(I)-ZV(I-1))
N = N + 1
240 I = I + 1
IF ( (C-ZV(I-1))*(ZV(I)-C) .LE. 0. ) GO TO 245
YP(N) = YV(I-1)
XP(N) = XV(I-1) + (XV(I)-XV(I-1))
* (C-ZV(I-1))/(ZV(I)-ZV(I-1))
N = N + 1
245 IF ( I .EQ. 3 ) GO TO 235
IF ( N .NE. 3 ) GO TO 230

```

```

C
C PLOT THE CONTOUR SEGMENT
250 IF ( IXB .EQ. 0 ) GO TO 260
C CALL UPEN
255 CALL MOVEA ( XP(1),YP(1) )

```

```

C
C ** NOTE: THE VARIABLE INTENSITY FEATURE
C ** HAS BEEN DISABLED.

```

```

C CALL DWPEN (IN(IC))
C
C CALL DWPEN ( IPPEN )
CALL DRAWA ( XP(2),YP(2) )
GO TO 230

```

```

C
C ANNOTATE THE CONTOUR
260 IF ( IYB .NE. 0 ) GO TO 255
IYB = -IYB0

```



```

V      = (XP(1)-XP(2))*+2+(YP(1)-YP(2))*+2
IF ( V .LT. DLAB ) GO TO 255
I      = LABEL(IC)
C      CALL UPPEN
Z1     = (XP(1)+XP(2))*+5-5.
Z2     = (YP(1)+YP(2))*+5-5.
C      CALL MOVEA ( Z1, Z2 )
C      CALL DWPEN ( IPPEN )
C      CALL PDCM ( I, 2, ICSIZ2 )
GO TO 220

C
C      PUT SCALES ON THE CONTOUR BORDER
270 N    = ICONOPS(4)
C      OUTPUT N
IF ( N .LE. 0 ) GO TO 300
C      CALL UPPEN
C      CALL MOVEA ( XPMN, YPMN )
C      CALL DWPEN ( IPPEN )
C      CALL DRAWA ( XPMN, YPMX )
C      CALL DRAWA ( XPMX, YPMX )
C      CALL DRAWA ( XPMX, YPMN )
C      CALL DRAWA ( XPMN, YPMN )
C
IF ( N .LT. 2 ) GO TO 300
DX     = (XMAX-XMIN)/(XPMX-XPMN)*100.
IC     = INT(LOG10(DX)+999.9999999) - 1000.
C      = 10.**IC
DX     = INT( DX/C+.99999999 ) * C
X1     = INT(XMIN/DX)*DX + DX
IF ( XMIN .LT. 0. ) X1 = X1-DX
Y1     = YPMN - 10.
Y2     = YPMN - 30.
Z1     = YPMN + YPMX - Y1
Z2     = YPMN + YPMX - Y2
X2     = XMAX
C      = 1. / C
278 C    = .1 * C
IC     = IC + 1
IF ( ABS(X1*C) .GE. 10. ) GO TO 278
IF ( ABS(X2*C) .GE. 10. ) GO TO 278
280 X2  = XF*X1 + XB
C      CALL UPPEN
C      CALL MOVEA ( X2, Z1 )
C      CALL DWPEN ( IPPEN )
C      CALL DRAWA ( X2, Z2 )
C      CALL UPPEN
C      CALL MOVEA ( X2, Y1 )
C      CALL DWPEN ( IPPEN )
C      CALL DRAWA ( X2, Y2 )
IF ( N .NE. 3 ) GO TO 285
S      = X1*C
ENCODE (4,984,V) S

```

```

C      CALL UPPEL
      CALL MOVEA ( X2-25., Y2-30. )
      CALL PBCH (V,5,ICSIZ3)
285    X1      = X1 + DX
      IF ( X1 .LT. XMAX ) GO TO 260
      X2      = Y2 + 60.
      I = 6Z40F1F040

```

```

C      CALL UPPEL
      CALL MOVEA ( X2, Y2-30. )
      CALL PBCH (I,3,ICSIZ2)
      ENCODE (3,986,I) IC

```

```

C      CALL UPPEL
      CALL MOVEA ( X2+25., Y2-15. )
      CALL PBCH (I,3,ICSIZ2)

```

```

C
      DY      = (YMAX-YMIN)/(YPMX-YPMN)*100.
      IC      = INT(LOG10(DY)+999.9999999) - 1000.
      C      = 10.**IC
      DY      = INT( DY/C+.99999999 ) * C
      Y1      = INT(YMIN/DY)*DY + DY
      IF ( YMIN .LT. 0. ) Y1 = Y1-DY
      X1      = XPMN - 10.
      X2      = XPMN - 30.
      Z1      = XPMN + XPMX - X1
      Z2      = XPMN + XPMX - X2
      Y2      = YMAX
      C      = 1. / C
288    C      = .1 * C
      IC      = IC + 1
      IF ( ABS(Y1*C) .GE. 10. ) GO TO 288
      IF ( ABS(Y2*C) .GE. 10. ) GO TO 288

```

```

290    Y2      = YF*Y1 + YB
      CALL UPPEL
      CALL MOVEA ( X1, Y2 )
      CALL DWPEN ( IPPEN )
      CALL DRAWA ( X2, Y2 )
      CALL UPPEL
      CALL MOVEA ( Z1, Y2 )
      CALL DWPEN ( IPPEN )
      CALL DRAWA ( Z2, Y2 )
      IF ( N .NE. 3 ) GO TO 295

```

```

      S      = Y1*C
      ENCODE (4,984,V) S
      CALL UPPEL
      CALL MOVEA ( X2-70., Y2-5. )
      CALL PBCH (V,5,ICSIZ3)
295    Y1      = Y1 + DY
      IF ( Y1 .LT. YMAX ) GO TO 290
      Y2      = Y2 + 50.

```

```

      I = 6Z40F1F040
      CALL UPPEL
      CALL MOVEA ( X2-55., Y2 )

```

```

CALL PBCH (1,3,ICS123)
ENCODE (3,986,1) IC
CALL JPFED
CALL MOVEA (X2-30., Y2+15.)
CALL PBCH (1,3,ICS122)

```

```

300 YF = 1./YF
DO 305 I=1,NY
305 Y(I) = (Y(I)-YB)*YF

```

```

RETURN

```

```

ERROR MESSAGE

```

```

950 PRINT 987, AX,AY,AZDIM
GO TO 980
955 PRINT 988, (CONTAB(I),I=1,AZ)
980 STOP

```

```

983 FORMAT ( 1H1//T110,20HSYMBOL CONTOUR VALUE
* // (T110,A2,E19.5) )
984 FORMAT ( F4.1 )
985 FORMAT ( F5.2 )
986 FORMAT ( I3 )
987 FORMAT ( 1H1,20X22HERPUP IN CONTOUR USAGE /
* 10X3HAX=,I4,10X3HAY=,I4,10X5HVDIMZ,I4// )
988 FORMAT ( 20X32HCONTOUR VALUES NOT MONOTONICALLY
* 11H INCREASING //(5X,5E20.6) )

```

```

END
SUBROUTINE PBCH (L,N,K)

```

```

DIMENSION L(40),KV(3),ID(9),IA(4)
DATA ID /1H1,1H2,1H3,1H4,1H5,1H6,1H7,1H8,1H9/
DATA IA /1H0,1H1,1H2,1H3/

```

```

CALL ANMODE
IF (N.LE.0) RETURN
IF (N.GT.4) NN=4
GO TO (10,20,30,40) NN
10 WRITE (102,15) L(1)
15 FORMAT (A1)
RETURN
20 WRITE (102,25) L(1)
25 FORMAT (A2)
RETURN
30 WRITE (102,35) L(1)
35 FORMAT (A3)
RETURN
40 WRITE (102,45) L(1)
45 FORMAT (A4)

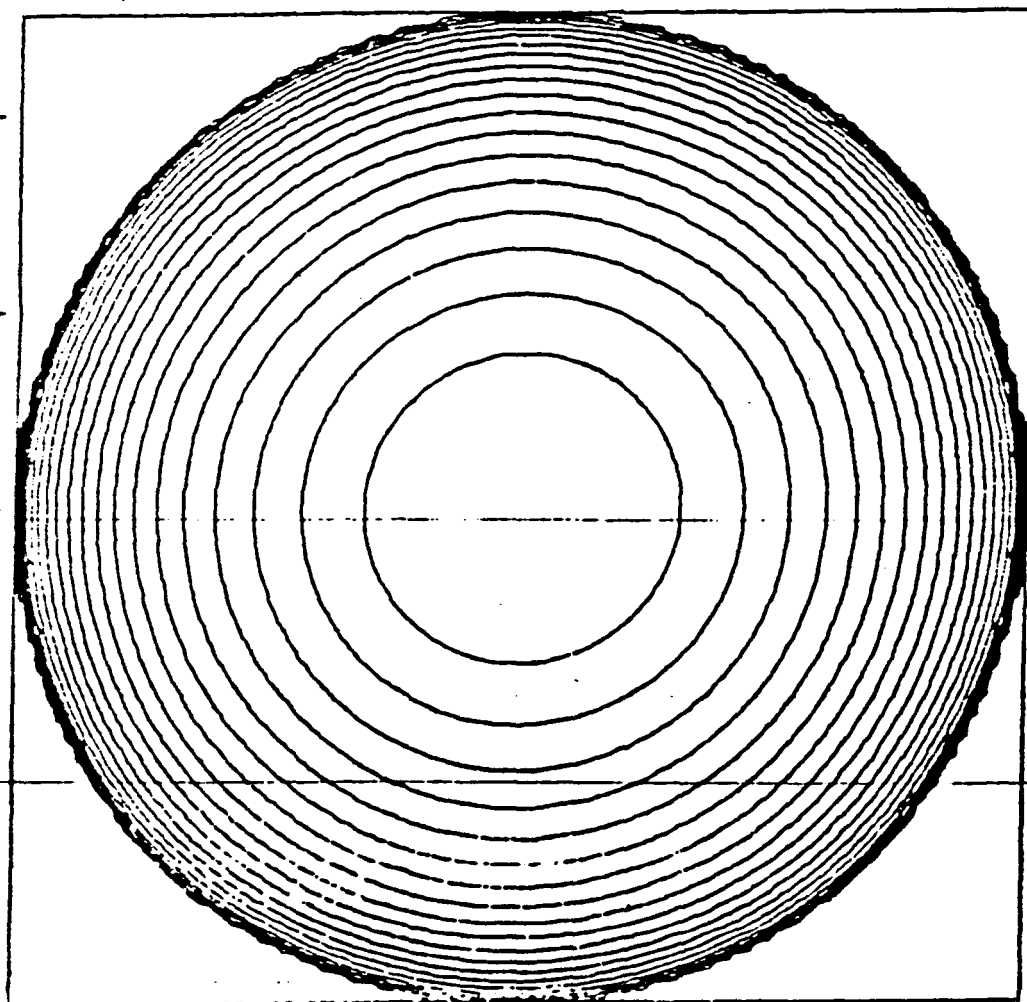
```

```

RETURN
END

```

STOP 2



## 11. Task 10: Single Aerosol Response

The design and fabrication of an apparatus for generating and propelling single aerosols through the lidar beam in order to determine the lidar response has been previously described. The technique for measuring this response requires only that the lidar response to a particle crossing a region of the beam of known relative calibration be determined. When this is known, each relatively determined contour in the focal volume map can be absolutely determined.

This response can be ascertained from an ensemble of time domain single particle responses obtained from particles near the beam response maximum. A display mode which simply accumulates these responses in superposition can then be read to determine the maximum response, from a group of identically backscattering particles. Care must be taken to assure that only single particle returns are used. If in doubt, a histogram display of pulse heights should indicate any multiple responses.

The state of calibration of the lidar system must be known during these measurements in order that, under different calibrations, the single particle response can be determined from the measured value by scaling. That is, when the system is recalibrated with a waist measurement, the new

single particle response is just the ratio of the waist calibrations times the old single particle response.

Single particle signals from the single particle generator have been obtained and are seen in Figure 10.1 showing a spectrum analyzer trace. Heights of these peaks are proportional to the particle scattering cross-section and are also dependent on where the particle crosses the focal volume. If all particles have the same backscatter cross-section, the highest peaks indicate the single particle response of the system as each particle crosses the center of the beam waist.

Single Particle Algorithm: An algorithm for measurement of Beta under conditions such that only single particles give significant scattering from the focal volume has been developed. It can be shown that, utilizing ordinary volume mode processing techniques, much smaller backscatter values can be determined in the single particle mode. Under the assumption that the response of the system at each point of the focal volume is known, the following equation yields Beta per unit flight path from the distribution of peak signals collected over some time interval (and therefore over some spatial region):

$$\beta = N \sum \omega_i \sigma_i / \sum \omega_i a_i$$

Here  $N$  = number of particles seen

$\sigma_i$  = backscatter cross-section

$\omega_i$  = probability of  $\sigma_i$

$a_i$  = focal area sensitive to  $\sigma_i$

The  $a_i$  are found by calibration and mapping of the focal volume, while  $\omega_i$  are determined by fitting the following equation for the peak signal distribution,  $S_j$ , to the measured peak signal distribution using a least squares fit:

$$S_j = \sum A_{ji} n_i$$

$A_{ji}$  = Cross-sectional area of focal volume sensitive to  $\sigma_i$  and yielding a peak signal  $S_j$

$$n_i = N \omega_i / \sum \omega_j a_j$$

= number of particles with cross-section  $\sigma_i$  per unit area.

The distribution  $\omega_i$  is assumed to be parameterized by

$$\omega_i = B/\sigma_i^b$$

where  $0 < B < 3$ . Hence the single particle algorithm

- 1) assumes  $N$  determined by real time measurement
- 2) assumes  $a_i$  and  $A_{ji}$  are determined by system calibration
- 3) loops over the parameter  $B$  until  $S_j$  fits the measured values in a least square sense
- 4) takes the successful  $B$  parameter and calculates  $\beta$ .

Simulated data from a system with an ideal Gaussian beam focussed at 5 meters with a 10 centimeter diameter mirror were used to test the algorithm. Random parameters in the simulation were the actual distribution, and the particle positions.

Table 10.1 shows the effect of the number of integration steps on the algorithm for three different simulated power law densities ( $B$  values). It is generally noted that as few as 5 integration steps gives reasonable results.

Table 10.2 shows the effect of "signals seen" on the Beta algorithm. These results show that no noticeable deterioration is evident until the # of particles seen drops to between 10,000 and 5,000.

Tables 10.3 and 10.4 show the effect of varying the # of signal and sigma bins. The general conclusion reached here is that the important variable is the "# of signals over the threshold." When this number becomes a large fraction of



the total # of signals then the results may not be realistic.

#### Procedure Required to Run the Single Particle Inversion Algorithm:

In order to run the  $\beta$  inversion algorithm the following steps should be followed:

- 1) establish correspondence between signal bin number and linear signal value
- 2) establish noise value, since algorithm uses s/n
- 3) determine s/n threshold and set SIGL = threshold s/n
- 4) set number of signal bins (M) and number of sigma bins (MS) - in general, number of sigma bins should be larger than number of signal bins - say M = 4 and MS = 7
- 5) set SIGH = highest linear S/N value
- 6) input a signal histogram that corresponds to the number of bins desired and the size of each bin in array NP; also as an N + 1 element include the number of particles above the maximum s/n.

Other parameters of interest are:

NI - number of integration steps

ETA - system efficiency

BW - bandwidth

FSI - sigma bin size relative to preceding bin size,  
i.e., FSI = 2 means that each bin doubles in  
size from the first bin interval to the last  
bin interval.

The algorithm as currently coded uses a theoretical Area  
versus  $s/\sigma$  table. The experimental determined Area versus  
 $a/\sigma$  curve can be used to replace this "Area table."

Subroutine AREA does the theoretical calculation and should  
be removed. Array AR (101) is used to store the "Area  
table."

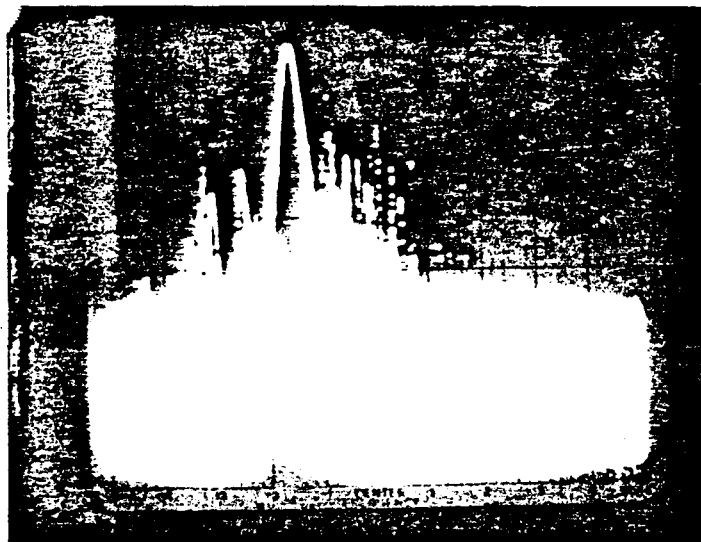


Fig. 10.1. SINGLE PARTICLE SIGNALS

Table 10.1

Effect of # of Integration steps on Beta algorithm

<u># Steps</u>	<u><math>\beta</math> (<math>\times 10^{-2}</math>)</u>	<u>B Value</u>
30	2.459949	2.5
20	2.459994	2.5
10	2.460194	2.5
5	2.461007	2.5
30	2.180584	1.5
20	2.180605	1.5
10	2.180709	1.5
5	2.181125	1.5
30	2.108201	.5
20	2.108227	.5
10	2.108355	.5
5	2.108887	.5

Fixed ParametersParticle Size ( $\mu$ ) - (1. - 1.316228)Cross section (geometric) - ( $\pi \cdot 10^7$ )

Focal length - 5.0

# Sigma bins - 7

# Signal bins - 3

# Signals seen - 25,000

Table 10.2  
Effect of "# signals seen" on  $\beta$  algorithm

<u># signals</u>	<u>Selected B</u>	<u>(<math>\beta</math>/#signals) <math>\times 10^{-7}</math></u>
30,000	1.5	8.7223366
25,000	1.5	8.722336
20,000	1.5	8.722335
15,000	1.5	8.72234
10,000	1.5	8.722335
5,000	1.4	8.663662
2,000	1.3	8.613045
1,000	1.3	8.613041
500	1.5	8.72233

Fixed parameters

No. of integration steps	- 30
Particle size ( $\mu$ )	- (1 - 3.16228)
Cross section (geometric)	-( $\pi$ - 10 $\pi$ )
Simulated B	- 1.5
Focal length	- 5.0
#sigma bins	- 7
#signal bins	- 3

Table 10.3

Effect of varying # signal bins, MS = 10 (# sigma bins)

<u># signal bins</u>	<u><math>\bar{E}</math> (<math>\times 10^{-2}</math>)</u>	<u>Selected B</u>	<u># signals over threshold</u>
2	2.197394	1.6	24,218
3	2.197394	1.6	23,237
4	2.180583	1.5	21,538
5	2.180583	1.5	18,554
6	2.180583	1.5	14,325
7	2.180583	1.5	9,057
8	2.180583	1.5	4,224
9	2.180583	1.5	1,011
10	2.180583	1.5	1,011

Total # Signals - 25,000  
                   B - 1.5  
 # Integration steps - 30  
 Particle size ( $\mu$ ) - (1 - 3.16228)  
 Cross section (geometric) - ( $\pi$  - 10  $\pi$ )  
 Focal length - 5.0

Table 10.4

Effect of varying # of sigma bins

M=3 (# signal bins)

<u># sigma bins</u>	<u><math>\beta</math> (<math>\times 10^{-2}</math>)</u>	<u>Selected B</u>	<u># signals over threshold</u>
10	2.197394	1.6	23287
9	2.180582	1.5	21744
8	2.180585	1.5	19054
7	2.180584	1.5	15058
6	2.180592	1.5	9839
5	2.180606	1.5	4830
4	2.180649	1.5	1243

Total # signals - 25,000  
 B - 1.5  
 # integration steps - 30  
 Particle size ( $\mu$ ) - (1.-3.16228)  
 Cross section (geometric) - ( $\pi$  -10  $\pi$ )  
 Focal length - 5.0

12. Task 11: Software for Transfer to Sigma V Computer

Software was developed to transfer backscatter data which was collected and stored on disk files on the Beta signal processor. The LSI-11 processor was interfaced with the Sigma V Computer and the following functions automatically performed: sign-on, opening of the data file on the Sigma, transfer of data, close data file, and sign-off. The transfer of more than one data disc is also possible.



13. Task 12: Interface of HP 1000L Computer with  
Peripheral Devices

ARI has developed necessary software to interface a Hewlett-Packard 1000L computer with peripheral devices for the purpose of transferring, processing, displaying, and storage of recorded data. Three routines have been written for the project.

- A listing routine to provide Source code listings using the system plotter. This routine is fully operational. A list of this code follows.
- A routine to read LeCroy Digitizer data and transfer to the hard disk.
- A routine to read data from the hard disk and make plots. A digitizer routine is designed to facilitate data collection in the field. Data is transferred from the digitizer in a block whose starting point and length is within the total sample frame and is user defined for each frame. This may be as much or as little as desired. The data is packed two data points per computer memory word and transferred to hard disk on a track and sector basis. This design bypasses the operating systems file management but is an order of magnitude faster with a typical data transfer taking 4 to 6 seconds.

The disk read and plot routine is intended only for data verification and as an example of how the user should read data from the disk to any processing program which becomes necessary.

#### 14. Conclusion

For this contract Applied Research, Inc. has accomplished a broad range of tasks in support of the NASA/MSFC Laser Doppler Velocimeter project. These tasks involved hardware procurement and fabrication for the laser system, software development, system calibration, flight support, and data analysis. A two color LDV system design analysis was accomplished and an adaptative filtering signal processing technique was evaluated, both in support of future systems. Notable in the area of hardware development were the design and fabrication of a single particle generator and a spinning wire target, both used for coherent focal volume calibration. Coherent focal volume mapping was accomplished for the first time on LDV systems. A mathematically formulated definition of the relationship between hard target calibration and atmospheric return was formulated in  $L_{eff}$ . Many of these efforts serve to enhance the validity of backscatter measurements in the volume mode (high return case). New in this effort was the implementation of the single particle mode of backscatter measurement for the case of low backscatter, which, in addition, yields the backscatter cross-section distribution. This mode may be capable of providing backscatter measurements when the volume mode is not sufficiently sensitive.

**End of Document**